

# **Climatic Stability of Polymer Optical Fibers (POF)**

**Dissertation**  
zur Erlangung des akademischen Grades  
"doctor rerum naturalium"  
(Dr. rer. nat.)  
in der Wissenschaftsdisziplin "Physikalische Chemie"

eingereicht an der  
**Mathematisch-Naturwissenschaftlichen Fakultät**  
der **Universität Potsdam**

von  
**Anilkumar Appajaiah**

**Potsdam, den 16 August 2004**

## **Acknowledgments**

I am beholden to the 'Federal Institute for Materials Research and Testing (BAM)' and the 'University of Potsdam' (both of in Germany) for creating me an opportunity to carry out my dissertation.

With a sense of profound gratitude I would like to express my heartfelt thanks to Prof. W. Daum and Dr. W. Czepluch of BAM for their inspiration, support, advice, encouragement, recommendations and fruitful guidance in bringing out this project to a successful end.

I would like to express my sincere gratefulness to Prof. H-G. Löhmannsröben of the university of Potsdam and Prof. H. Poisel of the university of Applied Sciences, Nürnberg, as reviewers of my work. Also for their guidance, cooperation and advice in improving the thesis.

I like to express my deep gratitude to Dr. H.G. Kretzschmar and Dr. V. Wachtendorf of BAM for their constant support in setting-up of the experimental work and precious discussion of the results particularly of infrared and chemiluminescence measurements.

I am very thankful to all other colleagues of the 'Department of Measurements and Testing Technology; Sensors (BAM-S.1)' for their nice cooperation. Especially I want to express many thanks to my laboratory colleagues: Dr. Witt, Dr. Döring, Mr. Kadoke, Mr. Jankowski, Mr. Gründer, Mr. Hammer, Mr. Günther, Mr. Otto and Dr. Steckert for their general assistance, cooperation and their kindness, which all made a pleasant environment during the completion of my dissertation.

I am very grateful to co-workers of the 'Department of Performance of Polymeric Materials (BAM-VI)' especially to Mrs. Klein, Mrs. Bistriz, Mrs. Bertus, Mr. Neubert and Mrs. Dr. Krüger for their collaboration and assistance in carrying out the measurements.

I would like to express my gratitude to Indian colleagues: Prof. Selvarajan, Dr. Srinivas and Dr. Siddaramaiah for their constant encouragement and discussion in doing this dissertation work. My thanks also to Indian friends: Mr. Murthy, Mr. Jeevananda, Mr. Mahaveer, Mr. Prasanna, Mr. Lawrence and others who extended their friendship, even across the distances, filled me with pleasure.

I must express my profound gratitude to my beloved parents: Mr. Appajiah and Mrs. Kempajamma, and to my brothers: Mr. Ashok and Mr. Arun Kumar for their continuous inspiration and moral support in carrying my doctoral work for the past few years. I am deeply indebted to my wife Mrs. Savitha for her constant support and patience during the shaping up of the thesis.

Finally, I express my thanks to the people who helped me directly or indirectly in my doctoral work and/or for my pleasant stay in Berlin.

## List of Publications

- [1] *Aging behavior of polymer optical fibers: Characterization of thermo-oxidative stability by chemiluminescence*, Anilkumar Appajaiah and Volker Wachtendorf, Proceedings of the Polymer Optical Fibers (POF) International Conference, Germany, September 28-30, 2004, pp. 166-173.
- [2] *Chemiluminescence investigation of high temperature and humidity aging of PMMA Based polymer optical fibres (POF)*, Anilkumar Appajaiah, Volker Wachtendorf, and Lukasz Jankowski, Proceedings of the (POF) Conference, U.S.A., 2003, pp. 152-155.
- [3] *Climatic aging of PMMA based polymer optical fibers (POF): Analysis of polymer degradation*, Anilkumar Appajaiah and Hans-Juergen Kretzschmar, 3<sup>rd</sup> International IEEE Conference on Polymers and Adhesives in Microelectronics and Photonics, Polytronic 2003, Montreux, Switzerland, 2003, pp. 57-62.
- [4] *Modelling the light propagation through aged and unaged POFs*, Lukasz Jankowski, Anilkumar Appajaiah, Christian-Alexander Bunge and Joseba Zubia, Proceedings of the POF Conference, U.S.A., 2003, pp. 148-151.
- [5] *Climatic aging or degradation of plastic optical fibers (POFs): Chemical analyses*, Anilkumar Appajaiah and Hans-Juergen Kretzschmar, Proceedings of the POF Conference, Japan, 2002, pp. 213-216.
- [6] *A review on aging or degradation of polymer optical fibers (POFs): Polymer chemistry and mathematical approach*, Anilkumar Appajaiah and Lukasz Jankowski, Proceedings of the POF Conference, The Netherlands, 2001, pp. 317-324.
- [7] *Photosensitive sol-gel waveguides on silicon substrates as MOEM devices*, A. Selvarajan, A. Anil Kumar, D. Anil Kumar, G.M. Hegde and T. Srinivas, SPIE 7<sup>th</sup> Intl. Symposium on Smart Structures and Materials, U.S.A., Vol. 3990, 2000.
- [8] *Bragg Grating on Ce<sup>3+</sup> doped sol-gel waveguides for sensor applications*, G.M. Hegde, A. Anil Kumar, T. Kiran Kumar and A. Selvarajan, Proceedings of the International Conference on Smart Materials, Structures and Systems, July 1999, Indian Institute of Science, India, 1999.

## List of Symbols

$\alpha_a$	Absorption co-efficient
$\theta_1, \theta_2$	Angle of incidence and refraction
$\chi$	Anharmonicity constant
$\alpha$	Attenuation or optical loss
$\delta$	Bending vibrations
$k$	Boltzmann constant
$C_u(90)$	Cabbens factor
$\phi_{CL}$	Chemiluminescence quantum yield
$\theta_C$	Critical angle
$\rho$	Density
$\epsilon$	Dielectric constant
$D_c$	Diffusion co-efficient
$\Delta S$	Entropy of reaction
$\Delta H$	Enthalpy of reaction
$\Delta H_R$	Enthalpy of reaction
$\phi_{Flu}$	Fluorescence quantum yield
$T_f$	Fictive temperature
$\Delta G$	Free energy change
$\nu_1$	Fundamental vibration frequency
$R$	Gas constant
$T_g$	Glass transition temperature
$\kappa$	Interatomic force constant
$\beta_T$	Isothermal compressibility
$L$	Length of the fiber
$\theta_{max}$	Maximum acceptance angle
$\epsilon_a$	Molar absorption co-efficient
$T_m$	Melting temperature
$M_n$	Number average molecular weight
$h$	Planck's constant
$\nu$	Quantum number
$r$	Radius
$n$	Refractive index
$n_1, n_2$	Refractive indices of two media
$n_{core}$	Refractive index of the core
$n_{clad}$	Refractive index of the cladding
$n_a$	Refractive index of air

$\mu$	Reduced mass
$\tau$	Turbidity
$\alpha_T$	Thermal expansion co-efficient
$C$	Velocity of light
$\lambda$	Wavelength of light
$M_w$	Weight average molecular weight

### List of Abbreviations

ATR	Attenuated total reflection
CCD	Charge coupled device
CL	Chemiluminescence
CYTOP	Cyclic transparent optical polymer
D	Deuterium
D2B	Digital domestic bus
DSC	Differential scanning calorimetry
FTIR	Fourier transform infrared
GI	Graded-index
GPC	Gel permeation chromatography
IR	Infrared
MMA	Methyl methacrylate
MOST	Media oriented system transport
LAN	Local area network
LED	Light emitting diode
NA	Numerical aperture
PMT	Photomultiplier tube
PD	Polydispersity
PA 12	Polyamide 12
PC	Polycarbonate
PE	Polyethylene
PMMA	Poly(methyl methacrylate)
PFA	Poly(fluoroalkyl acrylate)
PFMA	Poly(fluoroalkyl methacrylate)
POF	Polymer Optical Fiber
PS	Polystyrene
PTFE	Polytetrafluoroethylene
RH	Relative humidity
SEM	Scanning electron microscope
SI	Step-index
TG	Thermogravimetry
UV	Ultra-violet

# CONTENTS

<b>SUMMARY .....</b>	<b>I</b>
<b>ZUSAMMENFASSUNG.....</b>	<b>A</b>
<b>1 INTRODUCTION.....</b>	<b>1</b>
<b>2 BASICS OF FIBER OPTIC .....</b>	<b>5</b>
2.1 SNELL'S LAW AND TOTAL INTERNAL REFLECTION.....	5
2.2 OPTICAL FIBERS .....	6
2.3 TYPES OF OPTICAL FIBER.....	7
2.4 REFRACTIVE INDEX DISTRIBUTION .....	8
2.4.1 Step-index (SI).....	9
2.4.2 Graded-index (GI).....	10
2.5 NUMERICAL APERTURE .....	10
2.6 OPTICAL ATTENUATION OR OPTICAL LOSS .....	11
<b>3 POLYMER OPTICAL FIBERS (POFS) – TECHNOLOGICAL ASPECTS</b>	<b>13</b>
3.1 MOTIVATION.....	13
3.1.1 Technical background.....	14
3.2 ADVANTAGES AND APPLICATIONS .....	15
3.3 POF MATERIALS .....	16
3.3.1 Materials of the core .....	16
3.3.1.1 Poly (methyl methacrylate) (PMMA).....	16
3.3.1.2 Deuterated polymers.....	17
3.3.1.3 Fluoropolymers.....	18
3.3.2 Materials of the cladding .....	19
3.3.3 Materials of the jacket.....	21
<b>4 OPTICAL LOSS MECHANISM AND RELIABILITY OF POFS.....</b>	<b>22</b>
4.1 OPTICAL LOSS MECHANISM IN POFS.....	22
4.2 INTRINSIC LOSS FACTOR.....	23
4.2.1 Absorption overtones .....	24
4.2.2 Electronic transitions .....	26
4.2.3 Rayleigh scattering.....	27
4.3 EXTRINSIC LOSS FACTOR.....	28
4.3.1 Absorption by contaminants .....	28
4.3.2 Scattering due to physical imperfections .....	28
4.4 RELIABILITY OF POFS.....	29
4.4.1 Environmental effects .....	29
4.4.2 Industrial environmental stress factors of POFS .....	30
4.4.3 Climatic stability of POFS – State of the art .....	31

<b>5</b>	<b>THERMAL OXIDATIVE DEGRADATION OF POLYMERS .....</b>	<b>32</b>
5.1	INTRODUCTION - POLYMER DEGRADATION .....	32
5.2	THERMAL OXIDATIVE DEGRADATION PROCESSES IN POLYMERS.....	33
5.2.1	Maximum rate of oxygen consumption or induction time.....	35
5.2.2	Oxygen diffusion control in polymers .....	35
5.3	THE ROLE OF MOISTURE IN OXIDATIVE DEGRADATION OF POLYMERS .....	36
5.3.1	Dual mechanism of water transportation .....	37
5.3.2	Reversible and irreversible physical influences of water .....	38
5.3.3	Chemical interaction of water in polymers .....	39
<b>6</b>	<b>CHEMILUMINESCENCE METHOD OF INVESTIGATION OF THERMAL OXIDATIVE STABILITY/DEGRADATION.....</b>	<b>40</b>
6.1	CHEMILUMINESCENCE (CL) – GENERAL REMARKS .....	40
6.2	PHYSICAL CHEMISTRY BACKGROUND .....	41
6.2.1	Electronic excitation and bonding .....	41
6.2.2	Excitation by chemical reactions .....	43
6.2.3	Chemiluminescence and quantum yield .....	44
6.3	EVALUATION OF POLYMER OXIDATION PROCESSES .....	46
6.3.1	Polymer oxidation scheme for chemiluminescence.....	46
6.4	TYPES OF MEASUREMENTS.....	49
<b>7</b>	<b>EXPERIMENTAL DETAILS.....</b>	<b>51</b>
7.1	MATERIALS AND SAMPLE PREPARATION .....	51
7.1.1	POFs and bulk material selection .....	51
7.1.2	POF sample preparation.....	53
7.2	CLIMATIC EXPOSURES OR AGING.....	54
7.2.1	Exposure conditions.....	54
7.2.2	Exposure tests .....	55
7.3	OPTICAL TRANSMISSION MEASUREMENTS .....	57
7.3.1	Measurements by using multiplexer .....	57
7.3.2	Measurements by using miniature spectrometer.....	58
7.4	POF CLADDING EXTRACTION.....	58
7.5	CHEMILUMINESCENCE EXPERIMENTS.....	59
7.5.1	Instrumentation .....	60
7.5.2	Sampling .....	62
7.5.3	Measurements .....	62
7.6	FTIR MEASUREMENTS .....	63
7.6.1	Attenuated total reflection (ATR) - FTIR.....	64
7.6.1.1	<i>Practical aspects</i> .....	64
7.6.1.2	<i>Measurements</i> .....	65
7.7	SUPPLEMENTARY MEASUREMENTS .....	66

<b>8</b>	<b>RESULTS AND DISCUSSION.....</b>	<b>67</b>
8.1	CHARACTERIZATION OF THE UNEXPOSED POFs.....	67
8.1.1	Glass transition ( $T_g$ ) and melting temperature ( $T_m$ ) by DSC .....	67
8.1.2	Molecular weights by GPC .....	71
8.1.3	Chemical compositions analysis by FTIR .....	72
8.2	CLIMATIC EXPOSURE OF POF CABLES .....	77
8.2.1	Online optical transmission measurements.....	77
8.2.2	Investigation of thermo-oxidative stability/degradation using CL .....	79
8.2.2.1	<i>Initial peak and plateau behavior</i> .....	80
8.2.2.2	<i>CL of the unexposed bare POFs</i> .....	82
8.2.2.3	<i>CL of the unexposed claddings</i> .....	84
8.2.2.4	<i>CL of the exposed bare POFs and claddings</i> .....	85
8.2.3	Investigation of climatic exposure influences using FTIR .....	90
8.2.4	Investigation of climatic exposure effects using supplementary methods.....	95
8.2.4.1	<i>Thermal stability analysis by thermogravimetry (TG)</i> .....	95
8.2.4.2	<i>UV/visible transmittance</i> .....	98
8.2.4.3	<i>Molecular weight analysis</i> .....	99
8.2.5	Spectral transmission measurements .....	100
8.2.6	Optical transmission loss - possible explanation .....	101
8.3	CLIMATIC EXPOSURES OF BARE POFs.....	103
8.3.1	Online optical transmission measurements.....	103
8.3.1.1	<i>Exposure to temperature-humid climates</i> .....	103
8.3.1.2	<i>Exposure to temperature with very low humid climates</i> .....	115
8.3.2	Investigation of thermo-oxidative stability/degradation using CL .....	120
8.3.2.1	<i>Comparison of the unexposed bare POF with, core and cladding</i> .....	120
8.3.2.2	<i>Comparison of the unexposed bare POFs</i> .....	123
8.3.2.3	<i>CL peak emission behavior versus initial transmission loss</i> .....	125
8.3.2.4	<i>CL of samples exposed to 92 °C / 50 %RH</i> .....	126
8.3.2.5	<i>CL of samples exposed to 100 °C / low humidity</i> .....	130
8.3.2.6	<i>CL of samples exposed to 90 °C / low humidity</i> .....	134
8.3.2.7	<i>Summary</i> .....	137
8.4	SHORT-TERM CLIMATIC EXPOSURES OF BARE POFs.....	138
<b>9</b>	<b>CONCLUSIONS AND OUTLOOK .....</b>	<b>143</b>
	<b>REFERENCES.....</b>	<b>148</b>

## Summary

Polymer optical fibers (POFs) are a rather new tool for high-speed data transfer by modulated light. They allow the transport of high amounts of data over distances up to about 100 m without be influenced by external electromagnetic fields. Due to organic chemical nature of POFs, they are sensitive to the climate of their environment and therefore the optical fiber properties are as well. Hence, the optical stability is a key issue for long-term applications of POFs.

The causes for a loss of optical transmission due to climatic exposures (aging/degradation) are researched by means of chemical analytical tools such as chemiluminescence (CL) and Fourier transform infrared (FTIR) spectroscopy for five different (with respect to manufacturers) step-index multimode PMMA based POFs and for seven different climatic conditions. Three of the five POF samples are studied more in detail to realize the effects of individual parameters and for forecasting long-term optical stability by short-term exposure tests.

At first, the unexposed POF components (core, cladding, and bare POF as combination of core and cladding) are characterized with respect to important physical and chemical properties. The glass transition temperature  $T_g$ , and the melting temperature  $T_m$  are in the region of 120 °C to 140 °C, the molecular weight ( $M_w$ ) of cores is in the order of  $10^5$  g mol<sup>-1</sup>. POFs are found to have different chemical compositions of their claddings as could be detected by FTIR, but identical compositions of their cores.

Two of the POFs are exposed as cables (core, cladding and jacket) for about 3300 hours to the climate 92 °C / 95 % relative humidity (RH) resulting in a different transmission decrease. Investigating the related unexposed and exposed bare POFs for degradation using CL, FTIR, thermogravimetry (TG), UV/visible transmittance and gel permeation chromatography (GPC) suggest that claddings of POFs are more affected than cores. Probably the observed loss of transmission is mainly due to increased light absorption and imperfections at the core-cladding boundary caused by a large degradation of claddings. Hence, it is highly possible that the optical transmission stability of POFs is governed mainly by the thermo-oxidative stability of the cladding and minor of the core.

Three bare POFs (core and cladding only) are exposed for different duration of exposure time (30 hours to 4500 hours) to 92 °C / 95 %RH, 92 °C / 50 %RH, 50 °C / 95 %RH, 90 °C / low humidity, 100 °C / low humidity, 110 °C / low humidity and 120 °C / low humidity. In these climates their transmission variations are found to be different from each other, too.

The outcomes strongly inform that under high temperature and high humid climates physical changes such as volume expansion, are the main sources for the loss of optical transmission. Also, the optical transmission stability of POFs is found to be dependent on chemical compositions of claddings.

Under high temperature and low humid conditions, a loss of transmission at the early stages of the exposure is mainly caused by physical changes, presumable by core-cladding interface imperfections. For the later stages of exposures it is proposed to an additional increase of light absorption by core and cladding owes to degradation. Optical simulation results obtained parallel by Mr. L. Jankowski (a PhD student of BAM) are found to confirm these results. For bare POFs, too, the optical stability of POFs seems to depend on their thermo-oxidative stability.

Some short-term exposure tests are conducted to realize influences of individual climatic parameters on the transmission property of POFs. It is found that at stationary high temperature and variable humidity conditions POFs display to a certain amount a reversible transmission loss due to physically absorbed water. But in the case of varying temperature and constant high humidity such reversibility is hardly

noticeable. However, at room temperature and varying humidity, POFs display fully reversible transmission loss.

The whole research described above has to be regarded as a starting point for further investigations. The restricted distribution of fundamental POF data by the manufacturers and the time consuming aging by climatic exposures restrict the results more or less to the samples, investigated here. Significant general statements require for example additional information concerning the variation of POF properties due to production. Nevertheless the tests, described here, have the capability for approximating and forecasting the long-term optical transmission stability of POFs.

## Zusammenfassung

Optische Polymerfasern stellen ein relativ neues Medium zur Hochgeschwindigkeitsdatenübertragung mittels moduliertem Licht dar. Sie gestatten die Verbreitung großer Datenmengen über Entfernungen bis zu ca. 100 m, ohne eine Beeinflussung durch externe elektromagnetischen Feldern. Jedoch reagieren die Fasern und somit auch ihre optischen Eigenschaften aufgrund des organisch-chemischen Faseraufbaus empfindlich auf das Klima ihrer Umgebung.

Die Ursachen für die Abnahme der optischen Transmission aufgrund von klimatischen Einflüssen (Alterung, Degradation) werden mittels chemisch analytischer Verfahren wie Chemilumineszenz (CL) und Fourier Transform Infrarot (FTIR) Spektroskopie untersucht. Dabei kommen fünf, von verschiedenen Herstellern bezogene, Multimode- POFs aus PMMA in sieben verschiedenen Klimaten zum Einsatz. Drei dieser fünf POFs werden genauer untersucht, um den Einfluss einzelner Parameter festzustellen und optische Langzeitstabilität aufgrund von Kurzzeittests vorherzusagen.

Als erstes erfolgt eine Kennzeichnung unbeanspruchter POF Komponenten (Kern, Mantel und nackte POF als Kombination von Kern und Mantel) über ihre physikalischen und chemischen Eigenschaften. Die Glas- und die Schmelztemperaturen liegen im Bereich von 120 °C bis 140 °C, das Molekulargewicht des Kerns bei größenordnungsmäßig  $10^5 \text{ g mol}^{-1}$ . FTIR-

Messungen zeigen zwar Unterschiede in der chemischen Zusammensetzung der Mäntel aber keine Unterschiede bei den Kernen.

Bei zwei der POF Proben, die als Kabel (Kern, Mantel und Schutzhülle) für 3300 Stunden einem Klima aus 92 °C und 95 % relativer Feuchte (r.F.) ausgesetzt waren, verringern sich daraufhin die optische Transmissionen in unterschiedlicher Weise. Die Untersuchung der zugehörigen nackten POFs mittels CL, FTIR, Thermogravimetrie (TG), UV/VIS und Gel Permeation Chromatographie (GPC) lässt eine stärkere Schädigung der Mäntel als der Kerne vermuten. Wahrscheinlich führt eine starke Manteldegradation zu einer erhöhten Absorption und Fehlstellen im Mantel und damit zu einer Transmissionsabnahme. Daher scheint die optische Stabilität der POF stärker durch die thermo-oxidative Stabilität des Mantels bestimmt zu sein als durch die des Kernes.

Drei nackte POFs (Kern und Mantel) sind unterschiedlich lang (30 Stunden bis 3000 Stunden) folgenden Klimaten ausgesetzt: 92 °C / 95 % r.F., 92 °C / 50 % r.F., 50 °C / 95 % r.F., 90 °C / geringe Feuchte, 100 °C / geringe Feuchte, 110 °C / geringe Feuchte und 120 °C / geringe Feuchte. Auch in diesen Klimaten ergaben sich probenbedingte unterschiedliche Transmissionsänderungen.

Die Ergebnisse deuten stark darauf hin, dass bei gleichzeitig hoher Temperatur und hoher Feuchte physikalische Änderungen wie die Volumenausdehnung die Hauptursachen für die Abnahme der optischen Transmission bilden. Ein weiterer Einflussfaktor ist die chemische Zusammensetzung der Mäntel.

Bei Kombination von hoher Temperatur und geringer Feuchte erzeugen in den Anfangsstadien der Alterung physikalische Änderungen Transmissionsabnahmen, vermutlich entstehen Fehlstellen in der Kern-Mantel-Grenzschicht. Hinzukommen in den späteren Stadien wahrscheinlich zunehmende Lichtabsorption in Kern und Mantel. L. Jankowski (Doktorand in der BAM) bestätigt diese Annahme durch parallel ausgeführte optische Simulationsrechnungen. Auch für nackte POFs scheint also die thermo-oxidative Stabilität die optische Stabilität zu bestimmen.

Kurzzeitalterungstests sollen Aufschluss über den Einfluss individueller Klimaparameter auf die POF Eigenschaften geben. Es zeigt sich bei dauerhaft hoher Temperatur und variabler Feuchte aufgrund des physikalisch absorbierten Wassers bis zu einem gewissen Grad ein reversibles Verhalten des Transmissionsverlustes. Dieses

Verhalten tritt aber nur kaum merkbar auf, wenn bei konstanter hoher Feuchte die Temperatur variiert wird. Bei Raumtemperatur und variabler Feuchte stellt sich jedoch ein voll reversibles Verhalten des Transmissionsverlustes ein.

Die hier beschriebenen Untersuchungen sind als Ausgangspunkt für weitergehende Forschungen zu verstehen. Die begrenzte Zurverfügungstellung von POF Basisdaten durch die Hersteller und der zeitaufwendige klimabedingte Alterungsprozess beschränken die Ergebnisse mehr oder weniger auf die untersuchten Proben. Signifikante allgemeine Aussagen erfordern aber beispielsweise zusätzliche statistische Daten der Produktionsschwankungen von POF Eigenschaften. Dennoch besitzen die hier beschriebenen Tests das Potential für eine Annäherung an die optische Langzeitstabilität und deren Vorhersage.

# 1 Introduction

The present era is often called as “information age”. One of the basic requirements for information is the speed at which data can be transferred or gathered through cables. Copper cables were the main medium for data transmission before glass and polymer fiber cables have arrived to the market. But they have the disadvantage of increasing inductive loss with the increasing data rate. Additionally, they are very sensitive to electromagnetic radiation generated by neighboring cables and on the other hand sources of radiations themselves, causing large errors in the data transmission (so called the *cross-talk*). Nevertheless, these problems can be solved by means of optical fibers made out of inorganic glasses and organic polymers. Besides the data transmission, optical fibers have found a wide range of applications from sensors to decorative elements.

It is no doubt that inorganic glass optical fibers are superior to polymer optical fibers (POFs) with respect to high rate data communication over long-distances. However, with the glass fibers, technical difficulties such as small core diameter and small numerical aperture (NA) make the installation uneasy and expensive. The larger diameter and NA of POFs facilitates and reduces the cost of installation, but because of their high attenuation, restricts their usage in the present to a length in the order of 100 m. Nevertheless, the recent breakthrough in large-scale manufacturing graded-index POF promises much lower attenuation. From the viewpoint of the functional

property, the core and cladding are the major parts that influence the optical quality of the POF [1,2,3].

POFs have found many application areas out of which the area of automobile field is a major consumer. Nevertheless, depending on ultimate applications, POFs are employed under various environmental stresses such as climatic (e.g.: temperature and humidity), mechanical (e.g.: repeated bending and impact) and biological (e.g.: microorganisms) ones. For all long-term applications under these environmental stress factors the optical reliability is a key issue [3].

It is well established that changes in physical and chemical properties of polymer materials take place due to degradation as a result of outdoor exposures, influenced by temperature and humidity. In outdoor use, the oxidation is known to take place in many organic substances including polymers [56].

The utility of conventional methods such as Fourier transform infrared spectroscopy (FTIR) coupled with thermogravimetry (TG) and differential scanning calorimetry (DSC) etc. is limited by their lacking sensitivity to monitor thermo-oxidative degradation of polymers. In contrast, the chemiluminescence (CL) technique has been known for many years for monitoring the thermal oxidation in many organic compounds and organic polymers [65-76]. Since the development of single photon counting technique, CL has been demonstrated to be a powerful tool to investigate the thermo-oxidative stability of a number of polymers including poly(methyl methacrylate) (PMMA) based POFs [51,52].

The present PhD thesis will focus mainly on three issues.

- Influences of climatic stress factors temperature and humidity on the optical transmission stability of PMMA based different POFs (with respect to manufacturers) in view of their long-term reliability.
- Investigation of the thermo-oxidative degradation/stability of the unexposed and exposed POFs. This mainly uses CL because of its large selectivity and high sensitivity.
- It proposes possible mechanisms for optical transmission altering due to climatic exposures.

At the same time, another PhD work is prepared by Mr. Jankowski (of BAM), modeling the optical transmission through the unexposed and exposed POFs with respect to their optical characteristics such as scattering/attenuation. Some of the results from this work will utilize for comparing the chemical analysis results of the present study.

The thesis comprises seven chapters.

Chapter 2 will introduce the basics of fiber optics that are applicable to POFs. Here, the main emphasis is paid to review the optical fiber structure and optical terms that are often used in this thesis.

Chapter 3 will focus on technological aspects of POFs. Here, the recent developments in bandwidth achievement, polymerization and fabrication techniques, advantages over glass optical fibers and application areas of POFs are provided. However, much attention is paid to materials that are used for core, cladding and jacket. Special interest is given to cladding materials as its chemical nature was not disclosed by manufacturers.

In Chapter 4, the loss mechanism and reliability of POFs are reviewed. The prominence is given to understand intrinsic and extrinsic loss factors of POFs. The industrial environmental stress factors are classified and state of the art of reliability testing and understanding of the transmission loss mechanism in stressed POFs are reviewed.

Chapter 5 and 6 will focus on chemical aspects of thermo-oxidative degradation of polymers and its detection by employing CL. These are studied in detail in view of fact that climatic exposures lead to oxidative degradation of POFs and its detection needs sensitive methods like CL. As CL is a new technique for the analysis of POFs it is reviewed in little more detail. Also, physical and chemical effects of water (humidity or moisture) in polymers and on their thermo-oxidative degradation are extensively reviewed in the direction of humidity substantially affect the optical stability of POFs.

Chapter 7 is the experimental part. It provides details of materials, sample preparation, exposure tests, exposure conditions, optical measurements, CL, DSC, attenuated total reflection (ATR) FTIR, UV/visible transmittance, TG, GPC (gel permeation

chromatography) and SEM (scanning electron microscopy) measurements are employed in the present work. Some components of the instruments used here (e.g.: CL) are prototypes and therefore described in more detail. Also, a method of the separation of the cladding/core by using solvents is described.

Chapter 8 is the results and discussion part. It is structured mainly into four sections.

- In the first section, individual components (bare POF, core and cladding) of the unexposed POFs are characterized for their important physical constants (glass transition  $T_g$ , glass melting temperature  $T_m$  and molecular weights) and chemical compositions by using DSC, GPC and FTIR.
- In the second section, the optical transmission stability of two POF cables (having core, cladding and jacket) exposed to the climate 92 °C / 95 % relative humidity (RH) is investigated. The transmission loss behavior is tried to be correlated with physical and chemical changes of POFs. The relative thermo-oxidative stability of the unexposed bare POFs and claddings is investigated by using CL. The exposed samples (bare POF, cladding and core) are investigated in relation to degradation by using CL, FTIR, TG, UV/visible transmittance and GPC. Finally, the possible mechanisms for the loss of transmission of POFs are proposed.
- In the third section, the optical transmission stability under seven different temperature and humid climates is investigated for three bare POF samples (core with cladding only). The possible mechanisms for the observed loss of transmission at the early stages of exposures are researched to some extent. For the first time, the relative thermo-oxidative stability of the individual components bare POF, cladding and core is investigated as a model by using CL. CL is explored to detect degradation of the exposed bare POFs and claddings. The probable causes for the loss of transmission are discussed.
- In the fourth section, three short-term exposure tests are carried out for three bare POF samples to realize influences of temperature and humidity on the optical transmission of POFs. Using these measurements, possibilities for approximating the optical transmission stability under long-term exposures are explored.

## 2 Basics of Fiber Optic

### 2.1 Snell's law and total internal reflection

The ratio of the velocity of a light wave in vacuum ( $C_v$ ) to the velocity of a light wave in a medium ( $C_m$ ) is defined as the refractive index ( $n$ ) of that medium and it can be expressed as:

$$n = \frac{C_v}{C_m} . \quad (2-1)$$

Let us consider two semi-infinite media (medium 1 and medium 2) having refractive indices  $n_1$  and  $n_2$ , respectively, with  $n_2 > n_1$ . It is assumed that a light ray passes from the optically thin medium 1 under an angle  $\theta_1$  (with respect to normal to the interface) to the optically thick medium 2 through an interface between these two media. Then a part of the incident energy is reflected back into the medium 1 under the same angle  $\theta_1$  and a part of it refracted into the medium 2 under the angle  $\theta_2$ . This refracted ray is bent towards the normal to the interface (Fig. 2.1a). The refraction can be expressed by:

$$\frac{\sin \theta_1}{\sin \theta_2} = \frac{n_2}{n_1} . \quad (2-2)$$

Equation (2-2) represents the Snell's law of refraction. Fig. 2.1 shows the schematic of optical layout of the Snell's law.

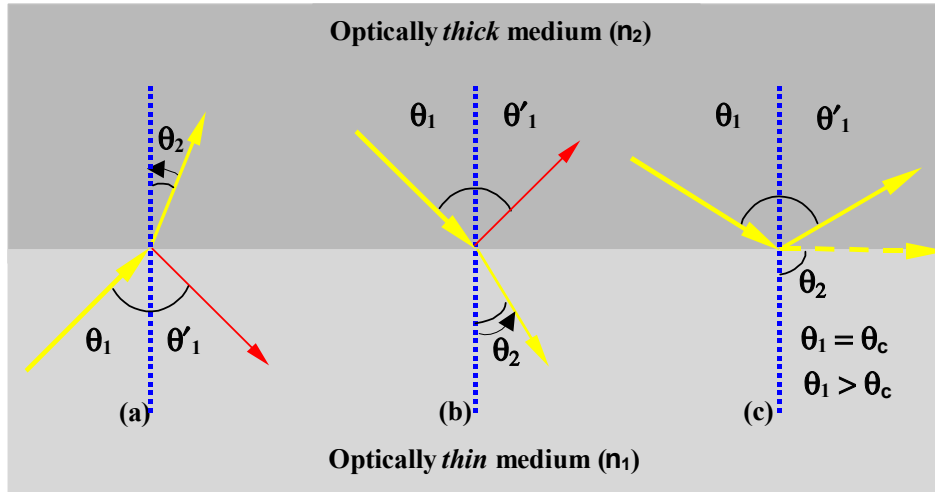


**Figure 2.1:** Schematic representation of the Snell's law of refraction and total internal reflection.

The same phenomenon is observed when a light ray passes from the medium 2 of  $n_2$  to the medium 1 of  $n_1$  but here the refracted ray is bent away from the normal to the interface (Fig. 2.1b). But at a particular angle of incidence - called as *critical angle* ( $\theta_1 = \theta_c$ ) - refracted light beam passes perpendicular to the normal ( $\theta_2 = 90^\circ$ ), i.e. grazes along the interface (Fig. 2.1c). When the angle of incidence is increased beyond  $\theta_c$ , all incident light is totally reflected back, nothing is transmitted (Fig. 2.1c). This phenomenon is called as *total internal reflection*. It is the fundamental optical effect for light propagation through optical fibers. The critical angle ( $\theta_c$ ) is given by:

$$\theta_c = \sin^{-1}\left(\frac{n_2}{n_1}\right). \quad (2-3)$$

## 2.2 Optical fibers

An *optical fiber* is a special form of an *optical waveguide* and consists mainly of a cylindrical core and a cladding (see Fig. 2.2), both made out of highly transparent materials. The core refractive index  $n_{core}$  is slightly higher than that of the cladding  $n_{clad}$ . Depending on ultimate applications, there are few layers coated followed by the cladding, acting as additional claddings or protective layers. Light is coupled into the core in one end-face under the critical angle (or larger) condition. According to Snell's law it is totally reflected at the border to the cladding or in the case of several

claddings exist within the outermost cladding – guided in this way through the whole fiber and leaves the fiber at the other end-face. So far the theory, in practice there are problems, which will be discussed later.

The core is made up of either inorganic or organic (polymer) materials or combination of both. The well-known inorganic material is glass ( $\text{SiO}_2$ ), and poly(methyl methacrylate) (PMMA) is the known organic polymer material. But other polymers such as polystyrene and polycarbonate are also known core materials. CYTOP<sup>®</sup> and Teflon<sup>®</sup> AF are the recently developed perfluoropolymers as core materials. A few attempts have been made to use of elastomers based on silicon with organic entities as core materials (see Section 3.3).

The core diameter for instance in silica based optical fibers typically varies from 5  $\mu\text{m}$  up to about 100  $\mu\text{m}$  and in polymer optical fibers (POFs) from 200  $\mu\text{m}$  up to about 1000  $\mu\text{m}$ . The cladding diameter of POFs typically is in the range from 20  $\mu\text{m}$  up to 50  $\mu\text{m}$  higher than the core, in glass fibers even more. Fig. 2.2 shows the geometry of an optical fiber.

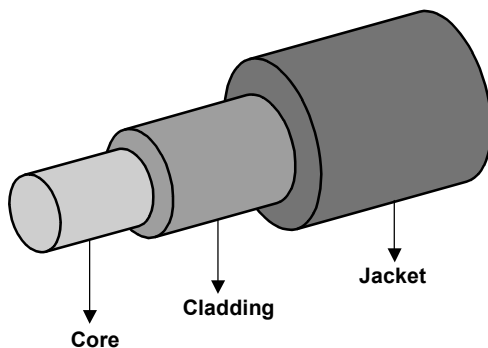


**Figure 2.2:** *Geometry of an optical fiber.*

### 2.3 Types of optical fiber

Optical fibers are characterized by their physical structure (refractive index distribution of the core) and transmission properties. With respect to data transmission they can be classified into two types based on the number of light modes that supports by an optical fiber. The types are:

- Single-mode.
- Multimode.

According to mode theory, sets of guided electromagnetic waves are used to call *modes* of an optical fiber. An optical fiber is always being able to propagate at least one mode, which is referred as the fundamental mode of the fiber.

In *single mode* optical fibers, the core size (diameter) is small and it is typically around 8  $\mu\text{m}$  to 10  $\mu\text{m}$ . This type of fibers allows only lowest order or the fundamental mode and is suitable for the applications preferably at 1300 nm wavelength. Single mode optical fibers have lower signal loss and higher information capacity (i.e. bandwidth) than multimode optical fibers. These fibers are capable of transferring higher amounts of optical data due to lower fiber dispersion.

*Multimode* (describes the number of different light intensity distributions of light within the fiber) optical fibers support over 100 modes depending on the core diameter and numerical aperture NA, describing the angular region of light coupled into the fiber. As the core size and NA increase, the number of mode increases. The main disadvantage of multimode optical fibers is high modal dispersion, which directly reduces the bandwidth of the fibers because the information transport (bandwidth) is mode dependent. Multimode optical fibers have some advantages compared to single mode ones, e.g.: ease of light launch, ease of connection and the use of cheap light emitting diodes LEDs (normally for single mode optical fibers, laser diodes are used). However, optimization of core diameter, NA and refractive index of the fiber can lead to an increase in bandwidth. For instance, a polymer optical fiber with a NA of 0.5, and a core radius of 0.5 mm, at a  $\lambda$  of 650 nm can support up to 3 million modes.

## 2.4 Refractive index distribution

In optical waveguides the light guidance takes place through the phenomenon *total internal reflection* (see Fig. 2.1). The light propagation in an optical fiber is mainly dependent on the refractive index distribution or profile of the core. Based on this optical fibers are categorized into *step-index* (SI) and *graded-index* (GI) fibers.

### 2.4.1 Step-index (SI)

In SI type optical fibers the core refractive index distribution is constant through out its radius  $r$ , it can be schematically represented as shown in the Fig. 2.3A. Mathematically it may be expressed as:

$$n(r) = \begin{cases} n_{core} & 0 < r < a & \text{Core} \\ n_{clad} & r > a & \text{Cladding} \end{cases} \quad (2-4)$$

where  $n_{core}$  and  $n_{clad}$  are refractive indices of the core and cladding respectively, and 'a' is the core radius.

In the SI fiber, since the core has a constant refractive index distribution the light rays will experience several bounces at the core-cladding interface and then travels along the fiber. A guided mode in a SI fiber corresponds to a superposition of many rays propagating at a particular angle ( $\theta$ ) with respect to the direction of the fiber axis. Fig. 2.3A shows the propagation of light rays in the SI type fiber. Depending on this reflection angle rays may travel different distances and therefore a considerable time difference is observed between each ray at the end of propagation leading to mode dispersion.

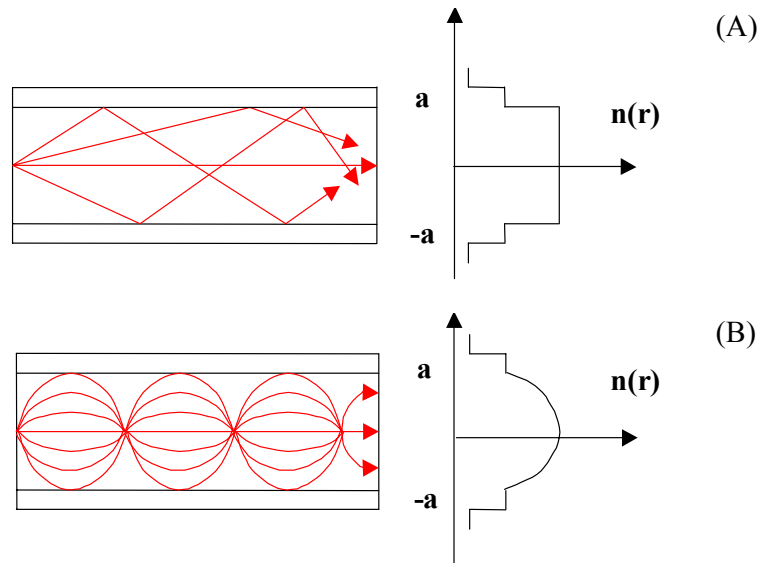


**Figure 2.3:** Scheme of the refractive index profile: (A) step-index optical fiber; (B) graded-index fiber.

### 2.4.2 Graded-index (GI)

In GI type optical fibers the core refractive index is of the parabolic profile. In other words, the core refractive index decreases from the center to periphery. The schematic representation of the parabolic profile of the refractive index of the core is as shown in Fig. 2.3B. The mathematical expression is as follows:

$$n^2(r) = \begin{cases} n_{core}^2 \left[ 1 - 2\Delta \left( \frac{r}{a} \right)^2 \right]; & 0 < r < a \\ n_{core}^2 [1 - 2\Delta] = n_{clad}^2; & r > a \end{cases} \quad (2-5)$$

where  $\Delta = \frac{n_{core}^2 - n_{clad}^2}{2n_{core}^2}$ .

In the graded-index fiber, light rays will experience both the refraction and total internal reflection. Because of the parabolic index distribution of the core light rays are refracted at each point of incidence and it increases gradually as a result light rays become curved shape (Fig. 2.3B). When the angle of incidence becomes larger than the critical angle, light will suffer total internal reflection.

According to (1.1), light travels faster in a material with a lower refractive index. Therefore, light rays that travel the longer distance in the lower refractive index region travel at a greater average velocity. This means that rays travel farther from the fiber axis will arrive at the fiber axis in the ideal case at the same time as rays travel along the fiber axis and therefore generate only one mode. This lack of time difference between light rays reduces the modal dispersion drastically compared to multimode SI fibers.

## 2.5 Numerical aperture

Numerical aperture (NA) determines the light gathering power of an optical fiber. A light ray (with an incidence angle  $\theta$ ) to be guided through the fiber is given by:

$$n_a \cdot \sin \theta \leq \sin \theta_{\max} = NA = \sqrt{(n_{core}^2 - n_{clad}^2)} \quad (2-6)$$

where  $n_a$  is the refractive index of air and  $\sin \theta_{max}$  the maximum incidence acceptance angle. It can be schematically represented as shown in Fig. 2.4.

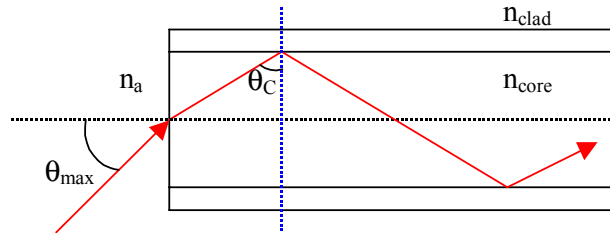


**Figure 2.4:** Representation of maximum acceptance angle ( $\theta_{max}$ ) of light in a multimode step-index optical fiber.

The quantity  $\sin \theta_{max}$  is commonly known as *numerical aperture* (NA) of an optical fiber. Therefore, generally, NA is related to the difference of refractive indices of the core and cladding. A large NA generates more modes and eases the problems of installation. Usually, NA of polymer fibers is larger as compared to glass fibers.

## 2.6 Optical attenuation or optical loss

Attenuation or power loss of an optical fiber is the loss of optical power as light rays travel along its length. It is defined as the ratio of the optical power input ( $P_i$ ) to the optical power output ( $P_o$ ). The following equation characterizes the attenuation as a unit of length.

$$attenuation = \alpha = \frac{10}{L} \cdot \log_{10} \left( \frac{P_i}{P_o} \right) \quad (2-7)$$

where  $L$  is the fiber length in kilometers and  $\alpha$  is expressed in dB/km.

Currently available POFs have the attenuation between 30 and 200 dB/km. The attenuation is mainly caused by absorption and scattering of light. These are influenced by fiber material properties, fiber structure and wavelength of use. The preferred windows of operation for (commercially available) POFs are in the expanse of 500 nm to 650nm falling in the visible region of the spectrum.

The optical loss mechanism in polymer and silica optical fibers is comparable, for POFs it will be discussed in Chapter 4. Basically, in silica fibers, the optical loss is

separated into intrinsic and extrinsic losses, which are mainly due to absorption and scattering, respectively.

Light scattering processes in an optical fiber can be broadly divided into microscopic and macroscopic scattering. In the microscopic type, two kinds of scattering i.e. *Rayleigh scattering* and *Mie scattering* are observed. Rayleigh scattering takes place when the size of the defect (density fluctuation in the fiber) is less than about one-tenth of the wavelength of light under operation. When it is equivalent or greater than one-tenth of the wavelength, then is called Mie scattering. Macroscopic or bulk scattering is mainly caused by imperfections such as micro bends and micro cracks and voids in the fiber.

References for Chapter 2 are [1,2,3].

## 3 Polymer Optical Fibers (POFs) – Technological Aspects

### 3.1 Motivation

The present era is often called as “information age”. Since the invention of “computer technology”, it has almost become that our present everyday business (i.e. education, job, banking, entertainment, collection and distribution of information etc.) cannot proceed without the computer. One of the requirements for the computer-based business is how fast the data can be transmitted to another computer through the cables. Indeed, the advent of “internet technology”, the computer has to meet high rate data transformation and gather. Copper cables were the main source of data transmission before glass and polymer fiber cables have arrived to the market. But copper cables are not able meet the high rate data transmission because of high loss. Moreover, they are very sensitive to electromagnetic radiations and on the other hand sources of radiations causing large errors in data transmission (so called the *cross-talk*). These problems can be solved by means of optical fibers made out of glass and polymers [2,3,4]. Moreover, the development of laser technology has strengthened their use especially in the telecommunication industry. Because polymer optical fibers (POFs) have some great advantages (see Section 3.2) over glass optical fibers as well as copper fibers, they are largely preferred for optical data communication particularly over shorter distances.

### 3.1.1 Technical background

A polymer optical fiber (POF) consists mainly of the (polymer) core and cladding. Therefore the basic principles of fiber optics hold also for POFs, too. Poly (methyl methacrylate) (PMMA), polystyrene (PS) and polycarbonate (PC) are the most used polymers as core materials in commercially available multimode step-/graded-index POFs.

POFs are having the history since 1960 and they were first commercialized in 1970's [3,4]. DuPont from the United States and Mitsubishi Rayon from Japan were the two main competitors of the POF market in 1970's. The first commercialized PMMA based POF exhibited an optical loss of more than 1000 dB/km [3,4]. The reduction of optical loss of POFs is a major challenge for materials scientists as well as for optical engineers in the area optical data communication.

One of the main causes of high optical loss of PMMA, PS and PC based POFs is the C-H vibrations absorption, which can be substantially reduced by replacing hydrogen atoms with heavier atoms such as fluorine, chlorine and deuterium [5,6].

By means of molecular engineering such as perfluorination and deuteration of polymers, it has become possible to reduce the attenuation  $< 50$  dB/km at the visible and near infrared region of the spectrum [7,8]. Although it is still higher compared to glass fibers, due to a few major advantages of POFs (see Section 3.2) increased their use in the area of optical data communication, remarkably in the last two decades. POFs are now replacing copper cables and glass fibers in the short-distance optical data communication field.

Since the advantage of GI over SI optical fibers in achieving high rate optical data transmission led the researchers to develop GI POFs. Recently, there are a few GI-POFs based on perfluoropolymers have been developed specially to meet high bandwidth and low attenuation. LUCINA™ based on CYTOP®, is a recently introduced GI POF for high optical performance [9]. Using this POF it is possible to achieve the transmission speed of  $\sim 1.2$  Gb/s/km with an attenuation of 30 dB/km [7,9].

The most important property of POFs is the optical transmission, which mainly depends on core materials, drawing process and conditions employed in the manufacturing process.

For producing polymers (core materials) of SI POFs, *bulk polymerization* technique is preferred because of the purity advantage of an obtainable polymer [4,10]. *Continuous-*, *batch- extrusion* and *melt spinning* are the most used drawing techniques for POF manufacturing [3,4,5,11].

Since last three decades the following polymerization techniques have been proposed to produce the preform for GI POFs [12,13,14,15,16,17]:

- Two-step copolymerization technique.
- Photo copolymerization technique.
- Interface-gel copolymerization technique.
- Dopant diffusion technique.
- Centrifugal field technique.

Fabrication of GI POFs mainly uses the *preform hot-drawing* technique [3,4,11,17,18].

## 3.2 Advantages and applications

The main advantages of POFs over glass multi mode optical fibers are [3,4,7]:

- Easy installation owing to large diameter (typically 0.25 mm – 1 mm).
- Efficient light coupling owing to large numerical aperture (NA) (typically 0.5 i.e. 60°).
- High ductility (or low modulus) and resistance to impact and vibrations.
- Low cost of production (also their connectors).

The major applications fields of POFs are [3,7,11,19,20,21]:

- Data communication field (e.g.: local area network LAN and home networks).
- Automotive field (e.g.: entertainment networks, navigation systems, systems, digital domestic bus D2B and media oriented system transport MOST).

- Lighting technology (e.g.: traffic signal-, airport signal-, street lighting and for decorative purposes).
- Sensor technology (e.g.: temperature, humidity, methanol, inorganic acids and Bragg grating sensors).
- Specialty POFs (e.g.: fiber light amplifiers and scintillating fibers).

### 3.3 POF materials

#### 3.3.1 Materials of the core

The important criteria for core or cladding materials are high transparency and fiber or film forming ability. Until recently, thermoplastics are proven to be best suitable for the core fiber fabrication. Among the thermoplastics PMMA, PS, and PC are the well-known polymers for the use in POF industries as core materials [3,4,5,7,11]. Fig. 3.1 shows the molecular structure of these polymers. In the last three decades, some perfluoropolymers are also developed for high optical performance [9,15,22,23,24,25]. Recently, thermosetplastics and elastomers based POFs have been researched [26,27].

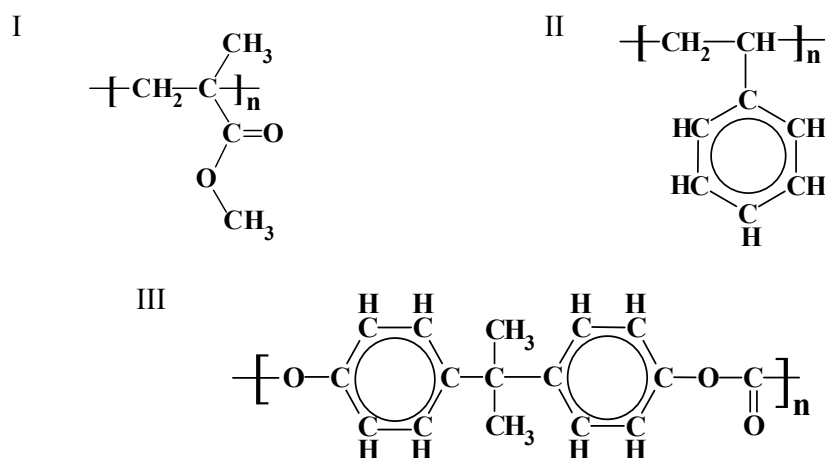


**Figure 3.1:** Molecular structure: (I) PMMA; (II) PS and (III) PC.

##### 3.3.1.1 Poly (methyl methacrylate) (PMMA)

Polymers from *methacrylate* family are well known to exhibit high transparency [28,29]. Poly(methyl methacrylate) (PMMA) is the first member of the homologous

series. It may be called as ‘high-tech polymer’. It is commercially better known as Plexiglass<sup>®</sup>. PMMA has a wide range of applications from building material up to data communication medium [28]. The research area of POFs is one of the promising fields for a large consumption of extremely pure PMMA as a core material. Beside PMMA, there are other methacrylate polymers exhibit very good optical properties [28,29].

PMMA is building blocks of monomer methyl methacrylate (MMA). MMA is produced from acetone. PMMA is manufactured by free radical polymerization using bulk or suspension technique [30].

While the PMMA and PS core POFs are developed as typical SI POFs for the normal conditional use, PC core POF is developed specially for high temperature applications ( $T_g \approx 145$  °C of PC is higher than that of PMMA and PS). However, the optical loss of all these is quite high especially of PC and PS based POFs [3,5,7,11].

**Table 3-1:** Physical and mechanical constants of PMMA [28].

Properties	Value	Units	Test procedure
Refractive index	1.491	$n_D^{20}$	DIN 53491
Density	1.18	g/cm <sup>3</sup>	DIN 53479
Tensile strength	80 (72)	MPa	DIN 53455
Charpy impact strength	15	kJ/m <sup>2</sup>	ISO 179/1D
Flexural strength	115 (105)	MPa	DIN 53452
Modulus of elasticity	3300	MPa	DIN 53457
Glass transition temperature ( $T_g$ )	105	°C	[31]
Co-efficient of thermal expansion		K <sup>-1</sup>	DIN 53752-A
-Linear	$7 \cdot 10^{-5}$ (0-50 °C)		
-Volume	$2.72 \cdot 10^{-4}$ (< $T_g$ ) $5.80 \cdot 10^{-4}$ (> $T_g$ )		[31]
Shrinkage onset temperature	> 80	°C	[28]
Water absorption	30	mg	DIN 53495

### 3.3.1.2 Deuterated polymers

Since the conventional polymers (PMMA, PS and PC) based POFs show high optical loss, the research on low loss POFs resulted in deuterated (D) polymer core POFs. These POFs exhibit a reduced loss (~ 20 dB/km in the red region by PMMA-D8 POFs) as compared to the conventional POFs [3,4,5,32]. DuPont developed the first deuterated PMMA POF in 1977 [3,4,5]. Kaino [5,32] has done a significant work in developing deuterated PMMA (PMMA-D5 and PMMA-D8) and PS (PS-D5 and

PS-D8) POFs. Although these POFs have registered a reduced optical loss, they are commercially less significant due to their large water absorption and high cost of production.

### 3.3.1.3 Fluoropolymers

The fully halogenated homo- and copolymers or perfluoropolymers (e.g.: polytetrafluoroethylene PTFE, polytetrafluoroethylene-co-hexafluoropropylene FEP) are known to be highly crystalline in chemical nature, which gives rise to a high optical loss owing to Rayleigh scattering [3,4]. In addition, their monomers are unsuitable for the bulk polymerization and they have high melt viscosity, which brings difficulty in fiber drawing. Therefore perfluoropolymers are unsuitable for the core fiber of POFs.

Partially halogenated polymers (e.g.: fluorinated acrylate polymers) would compromise all the problems of crystallinity, polymerization and processing. Yet, the main drawback of this type of polymers as core materials is a lower refractive index, which yields difficulty in finding cladding materials of the refractive index close to the core [3,4,15]. Therefore most of them are best suitable as cladding materials for SI POFs.

Nevertheless, since the development of GI POFs, perfluoropolymers as well as partially fluorinated polymers can be used as core materials but blended with other polymers (e.g.: PMMA), copolymerized with other monomers or adding low molecular weight dopants [3,4,7,14,33]. Duijnhoven has reported the possible uses of blends of PMMA and poly(2,2,2-trifluoroethyl methacrylate) (PTFEMA) and blends of PMMA and poly(2,2,3,3-tetrafluoropropyl methacrylate) (PTFPMA) as core materials [17].

Still, perfluorocopolymers and partially fluorinated polymers show considerable crystallinity and hence increase the scattering loss. On the other hand, further research has focused on cyclic perfluoropolymers resulted in poly(perfluorobutenyl vinyl ether) (CYTOP<sup>®</sup>: Cyclic Transparent Optical Polymer) [9,25]. It is the first perfluorocyclopolymer developed as a core material by Asahi Glass Company (AGC). It is highly amorphous and transparent polymer, and has excellent thermal and chemical properties. The optical fiber made out of CYTOP<sup>®</sup> is commercially known

as LUCINA™ introduced by AGC. Following CYTOP®, 2,2-bis(trifluoro-methyl)-4,5-difluoro-1,3-dioxole (Teflon® AF) has been introduced by DuPont [23,25]. Most of POFs based on perfluoropolymers show excellent optical properties in the far visible and near infrared region of the spectrum.

### 3.3.2 Materials of the cladding

Two of the main requirements for cladding materials are low refractive index (but close to the index of the core material) and good film forming ability. In addition, the application of claddings can provide a good mechanical and thermal resistance to the core.

A variety of cladding polymers have been developed since the invention of glass as well as polymer optical fibers. As discussed above that perfluoropolymers and partially fluorinated polymers alone are unsuitable for the fiber core, the research centered on the possible use of them as cladding materials.

Actually, there are two classes of fluoropolymers, which are widely used as cladding materials: *copolymers of fluoroolefins* and *poly(fluoroalkyl acrylates)* (PFAs) [22,34]. Out of these, PFAs are preferred because of their amorphous nature, high transparency and good adhesion properties etc. As a result durable optical properties can be obtained. Another main advantage of PFAs is their monomers easily coating (by solution) on the core and can be easily photopolymerized.

In general, there are already a number of monomers of PFAs mainly for fiber optic applications especially as cladding materials available in the market. Some monomers of poly(fluoroalkyl methacrylates) are listed in Table 3-2 along with glass transition temperature ( $T_g$ ) and refractive index ( $n$ ) of their corresponding homopolymers.

However, the formulation of cladding materials depends on individual optical fiber producers. Some of them are presented here. Schleinitz et al. [36] have proposed copolymers of fluorinated methyl and ethyl esters of acrylic and methacrylic acids as cladding materials for the PMMA core. They also have proposed a few homo- and copolymers of fluoroolefins. Kaino et al. [37] have claimed the following materials for the cladding: 1H,1H,3H-tetrafluoropropyl methacrylate polymer blended with a copolymer of vinylidene fluoride and tetrafluoroethylene, a copolymer of 1H,1H,5H-octafluoropentyl methacrylate and 1H,1H-trifluoroethyl methacrylate, and

1H,1H,5H-octafluoropentyl methacrylate polymer blended with a copolymer of vinylidene fluoride and tetrafluoroethylene. Hulme-Lowe et al. [38] have disclosed different compositions of the cladding, which is mainly comprised of fluorinated monoacrylate and a polyfunctional crosslinking acrylate with a number of additives. Baran et al. [34] and Savu et al. [39] have investigated the cladding materials, which are some homo- and copolymers of different fluoroalkyl esters: methacrylic and acrylic and  $\alpha$ -fluoromethacrylic acids. Recently, Nakumura et al. [40] have reported the PMMA POF with three-layer structure that is core, cladding and a protective layer. The cladding material is mainly composed of a copolymer of long chain fluoroalkyl methacrylate, methyl methacrylate and methacrylic acid. The protective layer material is composed of a copolymer of vinylidene fluoride and tetrafluoroethylene. More recently, Ballato et al. [41] have studied the possible use of a copolymer of 2,2,3,3,4,4-heptafluoro-butyl-methacrylate (HFBMA) and methyl methacrylate as a cladding for the PMMA core fiber.

**Table 3-2:** The commercially available monomers of poly(fluoroalkyl methacrylates), and  $T_g$  and  $n_D$  of their homopolymers [35]. 'R' represents the alkyl group of the monomer methacrylate (see Fig. 3.11).

Monomer	—R <sub>F, H</sub>	T <sub>g</sub> [°C]	n <sub>D</sub>
Methyl methacrylate	—CH <sub>3</sub>	105	1.489
2,2,2-trifluoroethyl methacrylate	—CH <sub>2</sub> —CF <sub>3</sub>	69	1.418
2,2,3,3-tetrafluoropropyl methacrylate	—CH <sub>2</sub> —CF <sub>2</sub> —CHF <sub>2</sub>	68	1.417– 1.422
2,2,3,3,3-pentafluoropropyl methacrylate	—CH <sub>2</sub> —CF <sub>2</sub> —CF <sub>3</sub>	70– 77	1.1395
1,1,1,3,3,3-hexafluoroisopropyl methacrylate	$\begin{array}{c} \text{CF}_3 \\ \diagup \\ \text{—CH}_2 \\ \diagdown \\ \text{CF}_3 \end{array}$	56	1.390
2,2,3,4,4,4-hexafluorobutyl methacrylate	—CH <sub>2</sub> —CHF—CF <sub>2</sub> —CF <sub>3</sub>	-	-
2,2,3,3,4,4,4-heptafluorobutyl methacrylate	—CH <sub>2</sub> —CF <sub>2</sub> —CF <sub>2</sub> —CF <sub>3</sub>	65	1.383

### 3.3.3 Materials of the jacket

The application and choice of a jacket or a sheath determine the ultimate properties of POFs. The ultimate properties such as thermal and mechanical properties are of very importance from the viewpoint of long-term reliability of POFs. The possible jacket materials for POFs are listed with their density and temperature of operation, in Table 3-3 [3].

**Table 3-3:** *Polymers for the use as jacket materials in POFs.*

<b>Polymer</b>	<b>Allowed operation temperature [°C]</b>	<b>Density [g/cm<sup>3</sup>]</b>
Polyvinylchloride (PVC)	70	1.20-1.50
Polyethylene (PE)		
-Low density	70	1.30-1.60
-High density	80	0.95-0.98
Polypropylene	90	0.91
Polyamide 6 (PA 6)	80-90	1.10-1.15
Polyurethane (PU)	90-100	1.15-1.20
Copolymer of Ethylene-Vinylacetate (EVA)	120	1.30-1.50
Perfluoroethylenepropylene (PFEP)	180	2.00-2.30
Polytetrafluoroethylene (PTFE)	260	2.00-2.30

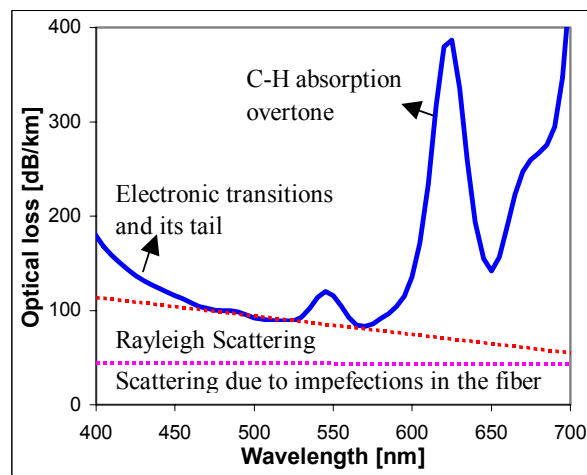
## 4 Optical Loss Mechanism and Reliability of POFs

### 4.1 Optical loss mechanism in POFs

Since the development of polymer optical fibers, the primary importance has been given to understand and to reduce their optical transmission loss. Likewise in glass optical fibers, the optical loss factor of commercially available POFs can be divided into *intrinsic* and *extrinsic* loss factors (see Chapter 1) [3-5,7,42]. Table 4-1 shows the sources of loss factors, that is the optical loss mechanism of POFs. It can be schematically spectrally represented as shown in Fig. 4.1 [3-5,20,32,43], which uses PMMA based POFs as an example.

**Table 4-1:** Optical loss factors of POFs.

Intrinsic	Absorption	<ul style="list-style-type: none"> <li>▪ Higher harmonics of C-H absorption</li> <li>▪ Electronic transitions</li> </ul>
	Rayleigh Scattering	<ul style="list-style-type: none"> <li>▪ Density or refractive index fluctuations</li> <li>▪ Orientation fluctuations</li> <li>▪ Composition fluctuations</li> </ul>
Extrinsic	Absorption	<ul style="list-style-type: none"> <li>▪ Transition metals</li> <li>▪ Organic contaminants</li> <li>▪ Absorbed water</li> </ul>
	Scattering	<ul style="list-style-type: none"> <li>▪ Dust, micro voids and fractures</li> <li>▪ Fluctuations in core diameter</li> <li>▪ Orientation birefringence</li> <li>▪ Core-cladding boundary imperfections</li> <li>▪ Micro and macro voids</li> </ul>

**Figure 4.1:** Schematic spectral representation of optical loss factors in (PMMA) POFs.

## 4.2 Intrinsic loss factor

It is mainly caused by basic fiber-material properties. Materials properties such as *absorption* and *scattering (Rayleigh)* are the main impulses of the intrinsic loss factor (see Table 4-1). The contribution of intrinsic loss factor to the total attenuation is higher than that of the extrinsic loss factor and therefore it can be a major source of the optical loss in POFs.

### 4.2.1 Absorption overtones

In POFs, the primary sources of absorption are vibrations and electronic transitions of molecular groups. These are the inherent property and can vary with types of materials. In view of the fact that POFs core is made of organic materials (polymers), vibrations of molecular groups such as carbon-hydrogen (C–H), carbon-deuterium (C–D), carbon-fluorine (C–F), carbon-chlorine (C–Cl), carbon-bromine (C–Br), oxygen-hydrogen (O–H), carbon double-bond oxygen (C=O), carbon-oxygen (C–O), and carbon-carbon (C–C) are the fundamental origin of the absorption loss. Molecular groups such as carbon double-bond carbon (C=C), and C=O are the origin of the optical loss by light absorption owing to electronic transitions [5,6,43].

According to the classical theory, the fundamental vibration frequency of any molecular bonds can be approximated by the expression:

$$\nu_1 = \frac{1}{2\pi C} \sqrt{\frac{\kappa}{\mu}} \quad \text{cm}^{-1} \quad (4-1)$$

where  $\mu$  is the reduced mass,  $\kappa$  the force constant, and  $C$  the velocity of light in vacuum.

Since the molecular bonds are approximated as anharmonic oscillators, their vibration absorption overtone bands (higher harmonics) are positioned at nearly multiples of the fundamental frequency. The wavelength region of  $n^{\text{th}}$  overtone of a molecular bond vibration may be calculated by [6,43]

$$\nu_v = \frac{\nu_1 v - \nu_1 \chi v(v+1)}{1 - 2\chi} \quad (4-2)$$

where  $v = 2, 3, 4, \dots$ , and  $\chi$  is anharmonicity constant.

The fundamental vibration absorption of the molecular bonds mentioned above falls in the infrared region but has absorption overtones extending up to the visible region causing high optical loss of POFs. In Table 4-2, positions of the fundamental vibration absorption of some important molecular groups are provided. Therefore, in organic polymer optical fibers vibrational absorption appears as a major source compared to inorganic glass optical fibers.

**Table 4-2:** Positions of the fundamental vibration absorption of molecular bonds.

<b>Molecular group</b>	<b>Vibration absorption [<math>\mu\text{m}</math>]</b>
C–H	3.3 – 3.5
C–D	4.4
C–F	8.0
C=O	5.3 – 6.5
C–C	7.9 – 10.0
C–O	7.9 – 10.0
C–Cl	11.7 – 18.2
O–H	2.8

In commercially available POFs based on PMMA, PS and PC the absorption loss is caused mainly by vibrations absorption of C–H bonds. With PMMA and PS based POFs, it has been found that the C–H stretching and bending vibrations absorption overtones  $\nu_5^{\text{CH}}$ ,  $\nu_5^{\text{CH}} + \delta$ ,  $\nu_6^{\text{CH}}$ ,  $\nu_6^{\text{CH}} + \delta$ , and  $\nu_7^{\text{CH}}$  are the main contributing bands for the loss due to absorption in the region between 500 nm and 750 nm [5].  $\nu$  and  $\delta$  represent the stretching and bending vibrations, respectively.

The absorption loss can arise always from molecular vibrations of C=O, C–C, C–O, and C=C because these groups are the fundamental constitution of organic molecules. These vibrations have a low anharmonicity constant and therefore their overtones band strength influence is very low for contribution to the absorption loss. However, the overlapping of these vibrations overtones with the other molecular vibrations (C–X, where X is H, D, F, Cl, and Br) may have a large contribution to the absorption loss of POFs [6,43].

It is well established in POF technology that the replacement of H atoms by halogen atoms F, Cl and Br will significantly reduces the absorption loss by shifting the fundamental vibration absorption to a relatively longer wavelength region as compared to both C–H and C–D bonds (see Table 4-2). Since the fundamental absorption fall at a longer wavelength region and a low anharmonicity constant of C–F vibrations, their overtones band strength decreases as a result a very low absorption loss can be achieved in the spectral region of POF data communication [3-7,43].

## 4.2.2 Electronic transitions

Electronic transitions occur by exciting electrons from a lower energy level to a higher due to absorption of light. Transitions can occur between any filled orbital and any empty orbital (subject to selection rules) [6,44]. The molar absorption coefficient of an electronic absorption is given by the equation:

$$\varepsilon_a = \frac{1}{cl} \log_{10} \frac{I_0}{I} \quad (4-3)$$

where  $c$  and  $l$  are the concentration and path length of the sample.  $I_0$  and  $I$  are the intensity of light falling on the sample and transmitted by the sample, respectively.

In general, the saturated molecules (single bond) can only undergo  $\sigma \rightarrow \sigma^*$  transitions, which give rise to spectra in far UV region with less analytical interest. On the other hand, unsaturated molecules having multiple bonds, undergo  $\pi \rightarrow \pi^*$ ,  $n \rightarrow \sigma^*$ , and  $n \rightarrow \pi^*$  transitions, which give rise to spectra in the near UV and visible region with more analytical interest. Within a molecule, the isolated multiple bonds such as C=C, C≡C, C=O, C=N and C=S give rise to a strong absorption band due to  $\pi \rightarrow \pi^*$  transition in the far UV region, and a weak absorption band due to  $n \rightarrow \pi^*$  transition in the near UV and visible region. However, the position of absorption maximum significantly varies when multiple bonds are conjugated with another multiple bonds via a single bond.

Generally, strong absorption peaks due to electronic transitions appear in the UV region have the absorption tail stretching into the visible region, which has a significant influence on the transmission loss of optical materials. It is in accordance with the Urbach's rule that in non-metallic solids the absorption coefficient at the band edge is an exponential function of the photon energy at a certain temperature [45]. Then the absorption coefficient  $\alpha_a$  (dB/km) at an arbitrary wavelength  $\lambda$  is shown as:

$$\alpha_a = Q \cdot \exp\left(\frac{R}{\lambda}\right) \quad (4-4)$$

where  $Q$  and  $R$  are the material constants and can be determined from the absorption spectrum. For instance, the values of  $Q$  and  $R$  for PMMA are  $1.58 \cdot 10^{-12}$  dBkm<sup>-1</sup> and

$1.15 \cdot 10^4$  nm respectively at 500 nm. For PS,  $1.10 \cdot 10^{-5}$  dBkm<sup>-1</sup> and  $8.0 \cdot 10^3$  nm, respectively at 500 nm and 600 nm [4,7].

### 4.2.3 Rayleigh scattering

It is caused mainly by fluctuations in density and composition and molecular orientation of the polymer material.

Since POF core polymers are highly amorphous in material nature, they can be considered as super cooled liquids. Thus the turbidity ( $\tau$ ) or scattering due to density fluctuations in amorphous polymers can be calculated using Clausius-Mossotti's equation [4,17,46]:

$$\tau = \frac{8\pi^3}{3\lambda^4} \left[ \rho \left( \frac{\partial \epsilon}{\partial \rho} \right)_T \right]^2 k T_f \beta_T \quad (4-5)$$

where  $T$  is temperature,  $T_f$  is fictive temperature,  $\beta_T$  is isothermal compressibility,  $k$  is Boltzmann constant,  $\rho$  is density,  $\epsilon$  is dielectric constant, and

$$\rho \left( \frac{\partial \epsilon}{\partial \rho} \right)_T = \frac{(n^2 - 1)(n^2 + 2)}{3} \quad (4-6)$$

where  $n$  is the refractive index of the polymer system.

It is a simple model and holds for isotropic polymers. For the molecular anisotropy of a polymer, a correction factor must be applied to increase the value of the turbidity.

The correction factor is known to be the Cabannes factor and it is given by [4,17]:

$$C_u(90) = \frac{6 + 6\rho_u(90)}{6 - 7\rho_u(90)} \quad (4-7)$$

where  $\rho_u(90)$  is the ratio between the parallel and vertical component of the scattered light at the 90 degree angle when the incident light is unpolarized. For instance, the Cabannes factor is 2.7 for PS and 1.1 for PMMA [4,5].

With the values  $\beta_T = 2.55 \cdot 10^{-10}$  Pa<sup>-1</sup>,  $T_f = 90$  °C,  $\rho = 1.19$  g/cm<sup>3</sup> and  $n = 1.49$  the  $\tau$  at 650 nm is found to be about 9 dB/km for PMMA [17].

### 4.3 Extrinsic loss factor

It is caused chiefly by external contaminations in the fiber core and physical imperfections in the fiber.

#### 4.3.1 Absorption by contaminants

It has been well evidenced with glass optical fibers that the transition metal ions such as cobalt, iron, nickel and manganese incorporated during the manufacturing process, may cause a significant increase of the optical loss. Incorporation of such impurities may be unavoidable, and they induce light absorption caused by electronic transitions in the visible and near infrared region of the spectrum. Similar mechanisms or processes also can take place in POFs [5,7,37].

The presence of small impurities such as polymerization inhibitors, initiators, chain transfer agents, additives and polymerization byproducts are most likely be the organic contaminants in POFs can cause a significant increase of the attenuation either by light absorption or scattering [4,5,37].

Generally, polymers absorb a certain amount of water depending on their kind. The water absorption by POF core polymers can induce an increase in attenuation cause mainly by OH vibration absorption overtones and a minor scattering loss due to agglomeration of water molecules. According to Kaino [5, 47], the most influential OH absorption overtones are  $\nu_6^{\text{OH}}$ ,  $\nu_5^{\text{OH}} + \delta^{\text{OH}}$ ,  $\nu_5^{\text{OH}}$  and  $\nu_4^{\text{OH}} + \delta^{\text{OH}}$ , which appear in the visible wavelength region 520 nm, 562 nm, 614 nm and 674 nm respectively.  $\delta^{\text{OH}}$  is the OH bending vibration, and  $\nu_n^{\text{OH}}$  is the  $n^{\text{th}}$  OH stretching vibration. POFs made of PMMA and PS show a significant increase in the attenuation due to high water absorption as compared to POFs made of fluorinated and deuterated polymers. The impact of O–H and C–H vibrations absorption overtones to the total attenuation is comparable.

#### 4.3.2 Scattering due to physical imperfections

During the fiber drawing process many imperfections such as dusts, micro-voids, micro-cracks, core diameter fluctuation, orientation birefringence and core-cladding

boundary imperfections are accompanied in the fiber. These typical imperfections can increase the optical loss by light scattering, independent of wavelength.

Dusts, micro-voids and cracks can act as scattering centers and their physical size mainly decides the light scattering mechanism in the fiber. Mainly the environment of fiber production plant and fiber drawing temperature conditions introduce these defects [5,7,37].

Kaino et al. [5] have investigated the influences of core diameter fluctuations and found an increase of scattering intensity with increased core diameter fluctuations. The influence of such fluctuations may be very significant when it exceeds 10 %.

Polymers show a certain extent of molecular alignment or orientation. The extent of molecular orientation of an end polymer product is derived mainly by polymer processing techniques (e.g.: injection molding, blow molding, compression molding and extrusion.). It is also known that amorphous glassy polymers such as PMMA and PS can exhibit molecular orientation. Some studies have shown that orientation birefringence in glassy PMMA can cause of increased scattering intensity [4,46]. Dugas et al. [48,49] have found an increase of the optical loss due to structural inhomogenities in the PMMA core fiber caused by molecular orientation, which occurs as a result of fiber formation. Therefore, molecular orientation can be a serious issue for the fabrication of low loss POFs.

Core-cladding interface imperfections arise mainly owing to adhesion inferiority of the cladding [5,36,37]. It is known in optical fiber technology that one of the deciding factors of the light guiding efficiency of an optical fiber is the adhesion strength of the cladding [5,36,40]. Therefore, core-cladding imperfections can arise by materials of the cladding and fiber drawing process as well.

## **4.4 Reliability of POFs**

### **4.4.1 Environmental effects**

POFs and polymer based optical components are referred as technical products, and utilized for several optical applications under various environments. The environments can be mechanical, climatic, chemical, biological and radiometric. The

optical transmission performance is a key issue for assessing the consistency or reliability of POF systems for desired long-term applications. The environmental factors certainly affect the optical transmission performance as a result the lifetime of the POF system varies to a different extent. The optical transmission of a POF is determined mainly by its materials physical and chemical properties. Therefore, during the practical operation of POFs, environmental factors bring both physical and chemical changes of materials and hence the optical transmission stability fluctuates. Additionally, polymers themselves undergo aging, which result in a variation of physical and chemical properties. However, the optical transmission durability of a POF depends on other factors such as the nature, the extent, and the frequency of the imposed environmental stresses [3].

**Table 4-3:** *Classification of industrial environmental factors on POFs.*

<b>Nature of stress influence</b>			
<b>Mechanical</b>	<b>Climatical</b>	<b>Chemical and biological</b>	<b>Radiometric</b>
<ul style="list-style-type: none"> <li>▪ Static bend</li> <li>▪ Repeated bending</li> <li>▪ Flexing</li> <li>▪ Impact</li> <li>▪ Crush</li> <li>▪ Torsion</li> <li>▪ Vibration</li> <li>▪ Tensile force</li> </ul>	<ul style="list-style-type: none"> <li>▪ High humidity</li> <li>▪ Extreme temperature</li> <li>▪ Change in climatic conditions</li> <li>▪ Thawing</li> <li>▪ Freezing</li> </ul>	<ul style="list-style-type: none"> <li>▪ Lubricants</li> <li>▪ Fuels</li> <li>▪ Break fluid</li> <li>▪ Hydraulic oil</li> <li>▪ Acid and alkalies</li> <li>▪ Solvents</li> <li>▪ Oxygen</li> <li>▪ Ozone</li> <li>▪ Reactive gases</li> <li>▪ Micro organisms</li> </ul>	<ul style="list-style-type: none"> <li>▪ UV- rays</li> <li>▪ X-ray</li> <li>▪ High energetic radiations</li> </ul>
Also in various combinations			

#### 4.4.2 Industrial environmental stress factors of POFs

Industrial environmental factors of POFs can be different from those of the normal outdoor environment factors and therefore a proper classification is necessary. There are some studies conducted particularly to assess the POFs reliability under several industrial environmental stress factors [3,50]. According to those studies industrial environmental factors of POFs can be distinguished as shown in Table 4-3. These factors are the most probable stress factors, which directly influence the POFs durability during the cycle of industrial operations. It is very often that POFs might experience combination of different stress factors. As a result, its influences can be different from that of the case of single stress factor.

### 4.4.3 Climatic stability of POFs – State of the art

The industrial environmental factors are as discussed above (see Table 4-3) being the most probable factors but due to the increasing use of POFs in automotive field, much interest has been paid to climatic and mechanical reliability studies. Several research reports concerning POFs reliability can be found especially in Proceedings of the Polymer Optical Fibers International Conference have been conducted since 13 years.

There are only a few systematic investigations so far to understand the optical loss, in molecular level, caused by industrial environmental stress factors [5,42,47,51,52,53]. Kaino et al. [5,47] have extensively studied the influences of humidity in different POFs and found that water absorption leads to increase in optical loss due to light absorption by water. Takezewa et al. [42] have investigated the effects of high temperature (150 °C) exposure of crosslinked PMMA based POFs and found that oxidative degradation products of the core polymer cause an increase of the optical loss by light absorption. Schartel et al. [51,52] have studied the thermo-oxidative degradation behavior of PMMA based SI-POFs. They have found that the optical transmission stability of POFs is most likely be governed by the thermo-oxidative stability of the core.

Though the climatic reliability investigations made by Daum et al. [3 and related articles can be found in Proceedings of the POF conference] have come up with significant results in predicting the stability of POFs but unable to describe strong evidences for the instability caused by the climatic factors e.g.: temperature and humidity. However, they have proposed a model for the deterioration of the optical transmission under high temperature and humid conditions [3,54]. According to the model, the loss of optical transmission of SI POFs (cables) occurs in four steps: a definite loss of transmission within a short period (25 hours to 50 hours) after the exposure start, following a very slow deterioration of transmission, following a phase is characterized by rapid decline in the transmission and finally a uncommon but typical process of increase of the transmission to a higher level when the humidity is varied while the temperature is kept constant.

# 5 Thermal Oxidative Degradation of Polymers

## 5.1 Introduction - polymer degradation

The term *polymer degradation* [55] is used to denote changes in physical and chemical properties caused by chemical reactions involving the bond rupture (scission) of the backbone of macromolecules.

The basic reactions steps of polymer degradation are initiation, propagation and termination of radicals, which are the opposite processes of the polymerization of monomers. The chemical reactions that occur by degradation can be broadly divided into two mechanisms:

- Chain reactions.
- Non-chain (or single step) reactions.

Typically, chain reactions can lead to smaller fragments by the rupture of main chain bonds. Low molecular weight compounds evolved by the rupture of main chain and side chain bonds, elimination, crosslinking and cyclization reactions are commonly resulted from non-chain reactions.

## 5.2 Thermal oxidative degradation processes in polymers

It has been realized that highest temperatures to which a plastic material may be exposed outdoors ( $\approx 80\text{ }^{\circ}\text{C}$ ) do not supply sufficient thermal energy (290 kJ/mol to 375 kJ/mol) to cause the bond rupture of polymer chains [55,56]. Therefore in a polymer thermal degradation process, although temperature is important as rate controlling parameter, degradation by pure thermal energy is not a critical factor in climatic aging/exposure studies. Accordingly, in thermal aging or exposure tests, reactions of molecular oxygen have to be considered. Oxidation is an important phenomenon that takes place in the thermally induced polymer degradation process with the participation of oxygen. It is perhaps the fundamental cause for deterioration of most of the organic materials including polymers.

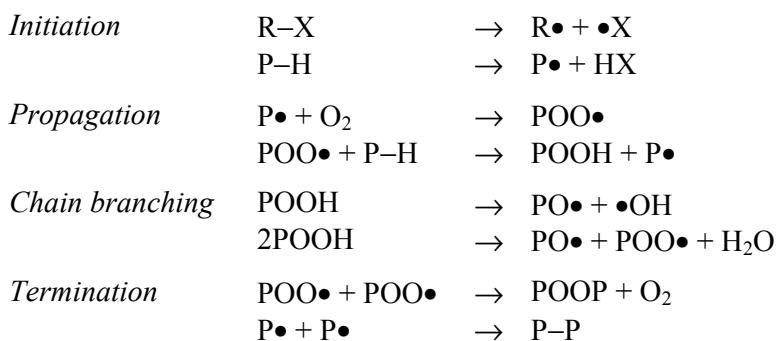
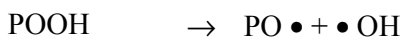


**Figure 5.1:** Schematic representation of the thermal oxidation process in linear polymers. R-X represents a low or high molecular weight species. P-H is the polymer.

Therefore, the role of oxygen is important in deterioration of plastic materials when exposed to atmospheric oxygen. The molecular reactions of oxygen in polymers are generally referred as *autooxidation* [55,56]. The radical chain reaction mechanism has commonly been observed in thermo-oxidative degradation of linear polymers. Molecules with carbonyl, hydroxyl and vinyl groups are known to form as a result of oxidative degradation. The basic oxidation reactions that involve in the thermal oxidative degradation process of linear polymers can be schematically represented as shown in Fig. 5.1 [57,58].

The formation of free radicals by bond cleavages induced by thermal energy is the primary process (initiation step) in both pure thermal and thermo-oxidative degradation processes. The secondary reactions of free radical and oxygen lead to the formation of hydroperoxides (POOH) (see also Chapter 6). The resultant hydroperoxides can have a role either as initiators of further reactions (propagation) or as intermediates (degradation products). The important role of hydroperoxides in thermal-oxidative degradation can be represented by the following two possible reactions:



The second reaction leads to the formation of true peroxides (as degradation products) but these are usually present in lesser concentration than POOH. Hydroperoxides are formed at many locations in the polymer chain, for instance, at sites where tertiary or secondary hydrogen is located. As a result varying degrees of stability exhibited by hydroperoxides. Therefore, the maximum concentration of hydroperoxides attainable in thermal oxidation will vary in different polymers as the steady state concentration often observed in photooxidation [55,56]. An elaborated discussion on hydroperoxides has been made in Chapter 6.

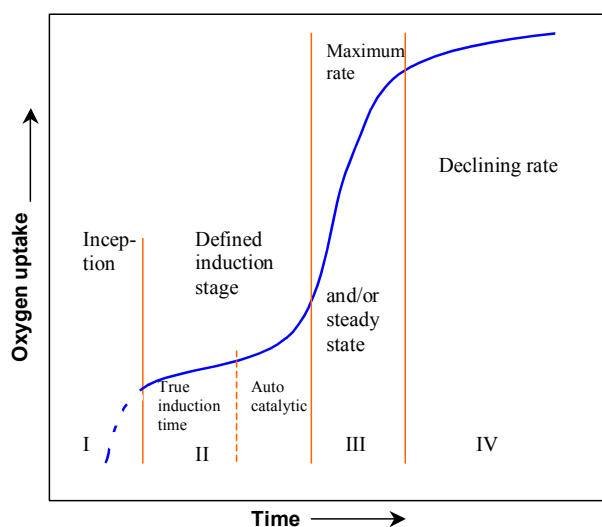


**Figure 5.2:** Schematic representation of the possible stages in the oxidative uptake history of polymer materials.

It is known that many polymer materials tend to deteriorate in stages during the thermal aging/exposure in the presence of atmospheric oxygen. The stages of deterioration can be related to the stages of oxygen uptake by polymer materials. Grassie and Feller [56] have discussed this subject in more detail. According to them the possible stages of oxidative history of a polymer sample can be schematically represented as shown in Fig. 5.2.

In the presence of weak bonds or links in the polymer chain the initiation of degradation (either pure thermal or oxidative) is more prone to occur than at the so-called stronger bonds (main chain and side chain bonds). The weak links or bonds are (e.g.:  $\pi$ -bonds and head to head linkages in the main chain) referred to molecular bonds of low dissociation energy [55,58].

### 5.2.1 Maximum rate of oxygen consumption or induction time

The *induction time* (also referred as *time to failure* of plastic materials) in oxidative deterioration that involves the formation of hydroperoxides may be precisely defined as the time of exposure before the maximum rate of oxygen consumption occurs under any given set of conditions [56]. The maximum rate of oxygen consumption can be generally related to the failure of the plastic material during the exposure tests. The induction time varies with the molecular nature and physical state of polymers substances. For instance, polyolefins and polyamides show a large variation in the induction time during their thermo-oxidative degradation [56].

### 5.2.2 Oxygen diffusion control in polymers

At room temperature, reactions of the polymer with oxygen are purely diffusion controlled and therefore the consumption of oxygen may be limited by the diffusion of oxygen into the interior of the polymer sample. The temperature controlled diffusion process in polymers can be expressed by the following Arrhenius type equation [29,59]:

$$D_c = D_0 \exp\left(\frac{-E_D}{RT}\right), \quad (5-1)$$

where  $D_0$  is independent pre-exponential,  $E_D$  is activation energy for diffusion,  $R$  is gas constant and  $T$  is absolute temperature. The  $E_D$  for rubbery materials is higher

than that for glassy materials. Therefore, the diffusion of oxygen is likely to be greater at higher temperatures usually employed in thermal degradation studies. The energy of activation for the diffusion is known to be lower (42 kJ/mol) than that of thermally induced chemical reactions (84 kJ/mol or higher). The sample thickness is also a limiting factor for the rate of reaction with oxygen relative to the rate of its diffusion to the reactive sites. However, the critical thickness will not remain same as thermal experiments are conducted at increasingly higher temperatures. Therefore, at higher temperatures the reaction rate may be independent of diffusion limitation differed by the thickness.

The diffusion of oxygen in a polymer substance of known thickness, under mild conditions, can be expressed by using the Fick's second law of diffusion according to the equation [56,59]:

$$\frac{\partial[O_2]}{\partial t} = D \frac{\partial^2[O_2]}{\partial x^2} = k[O_2] [R \bullet], \quad (5-2)$$

where  $t$  is time,  $x$  is depth and  $[\ ]$  represents the concentration.

Therefore, in a thermo-oxidative degradation process, the rate constant for the formation of peroxides depends on the concentration of oxygen in the polymer sample. Accordingly, the diffusion of oxygen directly relates the oxygen partial pressure in the sample.

### **5.3 The role of moisture in oxidative degradation of polymers**

Degradation of polymers usually is speeded up by the presence of moisture. Generally, there are four important effects related to water in climatic degradation of polymers [56].

- Chemical: hydrolysis of functional groups such as ester and amide.
- Physical: loss of the bond between the substrate and the polymer.
- Photochemical: generation of hydroxyl radicals or other chemical species.
- Physical/chemical: possible facilitation of ionization and the mobility of ionic entities.

Unfortunately, not much literature data are available regarding the particular role of water in thermal-oxidative degradation due to climatic exposure. Nevertheless, it is reported that water has a very little influence on free radical oxidation reactions that involve in thermo-oxidative and photooxidative degradation of polymers [56]. It is also reported that if the processes of thermal-oxidative deterioration depends on the concentration of water in the polymer (e.g.: yarns of Nylon and Kevlar), it is useful to consider the total rate of reaction meaning the combination of rate equations for thermo-oxidative and thermo-hydrolytic [56]. Startsev et al. [60] have stated that water can act as an activator for chemical reactions of deterioration and oxidation by an increase of the molecular motion of the polymer chain when exposed to the humid climate. Therefore, water could influence either directly or indirectly the degradation reactions of the polymers when exposed to humidity.

In thermal aging tests, the relationship of the rate of deterioration in relation to relative humidity (RH) is customarily considered. RH is the moisture content of air relative to the maximum possible content of water in air at a particular temperature and pressure. Therefore, the actual moisture content in a polymer substance is the controlling factor directly relates the partial pressure of water vapor in a given atmosphere. Because the moisture content is generally a result of an absorption process, in most polymers substances of known thickness, the commonly encountered deterioration response to relative humidity is an S-shaped curve [56]. The adsorption isotherm is the main reason for this kind behavior and it can be expressed by two well-known equations that are Freundlich and Langmuir's adsorption isotherm [59].

### 5.3.1 Dual mechanism of water transportation

Water transport in amorphous glassy polymers such as PMMA takes place with a dual mechanism. Part of water enters into the polymer network and causes the swelling of the polymer, and part of it accommodates into pre-existing micro voids (or defects). According to Turner [61], water uptake by the dual mechanism in PMMA may be expressed (at equilibrium) by the following equation:

$$w_D = f \cdot w, \quad (5-3)$$

where  $w_D$  indicates the weight percentage of water dissolved in the polymer and  $w$  is the total water percentage including the amount of water allocated into micro voids of

the polymer,  $f$  denotes the partitioning of water between two sorption modes and is a constant at a given temperature.

### 5.3.2 Reversible and irreversible physical influences of water

It is known that water acts as a polar plasticizer for several organic polymers [56,60]. The plasticization effect of water usually results in a reduction of the glass transition temperature ( $T_g$ ) (also a reduction of strength and elasticity modulus) and an increase of the thermal expansion co-efficient ( $\alpha_T$ ).

The reduction of  $T_g$  of polymers during the climatic aging in the presence of humidity, depends on the extent of water that is absorbed by the polymer and it may be expressed by the following equation [60,62]:

$$\frac{dT_g}{dw} = -k(T_g - T_{gm}), \quad (5-4)$$

with limiting conditions  $T_g = T_{g0}$  at  $w = 0$ ;  $T_g = T_{gm}$  and  $dT_g/dw = 0$  at  $w_m$ , where  $w_m$  is the maximum amount of absorbed water. At  $w > w_c$  (some critical concentration), the value of the exponent  $k$  indicator decreases.

The  $\alpha_T$  of polymers during the climatic aging in the presence of humidity, depends on the water concentration  $w$  according to the equation shown below [60,62]:

$$\alpha_T = \alpha_{T_0}(T)[1 + k(T)w] \quad (5-5)$$

where  $\alpha_{T_0}$  is the linear thermal expansion co-efficient,  $k(T)$  the co-efficient constant which depends upon the measuring temperature.

The above two equations follow the classical theories of free volume or lattice models and are true for a limited area of low concentrations of water.

The plasticizing effects of water in polymers during the climatic aging are completely reversible when the supramolecular structure of the polymer remains unchanged and chemical transformations are insignificant. This happens if the exposed polymer sample is not heated beyond  $T_g$  of disordered regions of the polymer because the molecular mobility of the segmental type is frozen at  $T < T_g$ . The plasticizing effects are completely irreversible when water interacts with the segmental mobility of polymer chains and this happens at  $T > T_g$ . This is often referred as *structural*

*relaxation* of polymers by water. The absorbed water acting as plasticizer, reduces  $T_g$  provides the segmental mobility and defreeze the physical process of structural relaxation.

### **5.3.3 Chemical interaction of water in polymers**

The transportation or absorption of water in polymer materials can lead to both physical and chemical changes through chemical reactions predominantly *hydrolysis* of the functional groups of the polymer [56]. The formation of *hydrogen bonds* between water molecules and polymer chains (functional groups) is the main result of chemical interaction of water with the polymer [63]. In some synthetic polymers such as poly(vinyl acetate) and in biopolymers complete hydrolysis can take place, however, several synthetic polymers undergo partial hydrolysis in the presence of water [30]. The partial hydrolysis may be referred as *hydration*. Nevertheless, the complete hydrolysis of the functional groups of a polymer is possible to take place under either acidic or basic medium condition in an exposure to water or humidity for longer period [56]. It is stated that during the acid hydrolysis some branching and crosslinking also take place and therefore the degradation reaction is quite indistinct [58]. Furthermore, the extent of the interaction of water with polymer chains on the other hand can lead to different states of the water content in the polymer.

## **6 Chemiluminescence Method of Investigation of Thermal Oxidative Stability/Degradation**

### **6.1 Chemiluminescence (CL) – General remarks**

If atoms or molecules are electronically excited by an external energy and emit this exciting energy, partly or totally, as radiation, this radiation is called *luminescence*. The time difference between excitation and emission is at least  $10^{-9}$  sec, but may reach up to  $10^5$  sec. The first case may be called as *fluorescence* and the latter as *phosphorescence* [64]

There are a lot of sources for the excitation, which are related to different luminescence technique such as thermo-, pyro-, photo-, radio-, electro-, tribo-, crysto-, bio- and chemi- luminescence. Eilhard Wiedemann [65] was the first to introduce the term *chemilunimescence* to describe light, generated by chemical reactions. More precisely, CL involves chemical reactions (often with oxygen), which produce atoms or molecules in electronically excited states in sufficient quantity. By relaxation to the ground state a broad spectrum of light is emitted, usually with wavelengths from 400 nm to 800 nm [65].

CL (also referred as oxyluminescence) takes its important place because of its inherent sensitivity and selectivity. It requires no separate external excitation source (in contrast to other techniques), only single light detector (e.g.: photomultiplier tube).

Many hundreds of inorganic and organic chemical reactions have been discovered which produce light. CL can occur in gases, in liquids, and at interfaces between solids and either gas or liquid phases. Lophine and luminol are the two organic chemiluminescent compounds most well studied. Oxidation of these compounds results in the light emission in the blue region of the spectrum [65].

CL of polymers is known from many years since the first effort made (in 1961) by Ashby, who observed the light emission from polypropylene on oxidation [66]. In the later years, Schard and Russell [67,68] studied the process further and found an inhibiting influence of antioxidants. With the introduction of low-noise photomultipliers an significant effort was made to understand the oxidative stability of various classes and types of polymers through the CL phenomenon, e.g.: polyolefins, which are the mostly studied class of polymers in terms of their oxidative stability because of their large use in outdoor.

## **6.2 Physical chemistry background**

### **6.2.1 Electronic excitation and bonding**

When a molecule absorbs a quantum of energy, the transition of electrons from the ground state to an excited state takes place. The result of the relaxation of excited state electrons to the ground state is the emission of photons via a radiative process. The photochemical processes can be generalized using the Jablonski diagram [59,64].

In CL the electronically excited state is generated by a chemical reaction initiated by a minimum amount of enthalpy. As a result the excited molecule, the product of the reaction, has a different atomic structure from the initial substrate. Though the Jablonski diagram [59,64] of simple luminescence is valid for CL, the energy pathway represented by the Franck-Condon principle may not apply since the electronically excited substrate is structurally different from the original substrate. A simplified energy pathway for CL can be represented as shown in Fig. 6.1 [65].

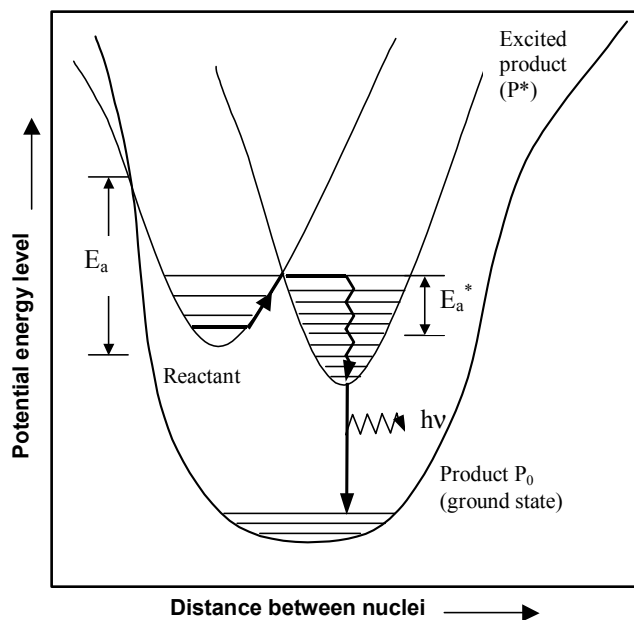
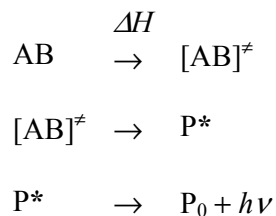


**Figure 6.1:** Energy pathway for chemiluminescence.

In a chemical reaction of reactant AB with sufficient enthalpy (thermal energy)  $\Delta H$  an activated complex  $[AB]^\ddagger$  (also called as primary excited state molecule) is formed. This intermediate state of high-energy transfers part of its energy to generate electronically excited state product  $P^*$ . The electronic excitation of a molecule results in electron transfer from a bonding orbital to an anti-bonding orbital. Such transitions effectively breaks the chemical bond between the two atoms and the result is structural rearrangement and instability of the molecule with different physicochemical properties from the ground state. When a minimum amount of enthalpy is supplied, the molecule dissociates into products. Therefore it involves both the chemistry of bond dissociation and physical processes of light emission by energy transfer to another species.

The relaxation of electronically excited state product ( $P^*$ ) to the ground state  $P_0$  is accompanied by the emission of a photon with energy  $h\nu$  resulting in CL at a wavelength  $\lambda = C/\nu$  ( $h$  is the Planck constant and  $C$  the velocity of light in vacuum).

The following scheme represents the entire reaction:



$\Delta H$  represents enthalpy of the reaction.

A chemiluminescent reaction has three essential features:

- A sufficient high level of energy must be generated by the reaction for the formation of an electronically excited state.
- There must be a pathway by which this energy can be supplied to form an electronically excited state.
- The excited state product must be capable of losing its energy as a photon by relaxation to the ground state.

### 6.2.2 Excitation by chemical reactions

Free energy ( $\Delta G$ ) of a chemical reaction is given by [59,64]:

$$\Delta G = \Delta H - T\Delta S \quad (6-1)$$

where  $T$  is temperature.

For the CL reactions the entropy change ( $\Delta S$ ) is very small, therefore  $\Delta H$  and  $\Delta G$  are very similar in magnitude.

A minimum energy has to be absorbed to initiate the chemical reaction, the activation energy ( $\Delta H_a$ ). With this activation energy and enthalpy of the reaction ( $\Delta H_R$ ), the energy available in a chemical reaction to produce a photon is given by:

$$\text{Energy available} = \Delta H_a - \Delta H_R \geq \Delta E^* \geq h\nu \quad (6-2)$$

where  $\Delta E^*$  is the energy required to generate an electronically excited product.

$\Delta E^*$  will be higher than the energy required to produce a photon since the energy will be lost during the complete process, however the required energy ( $\Delta E^*$ ) is  $\geq 290$  kJ/mol. The activation energy ( $\Delta H_a$ ) of a chemiluminescent reaction will not be too high if the reaction has to proceed to an observable rate. Normally,  $\Delta H_a$  required for

organic bimolecular and unimolecular oxidation reaction is  $\leq 150$  kJ/mol and  $\leq 100$  kJ/mol respectively. Therefore,  $\Delta H_R$  is the main contributor to the excitation energy in a chemiluminescent reaction.

The most common possible mechanisms with sufficient energy for generating an excited state product are:

- Electron transfer (e.g.:  $O + O + SO_2 \rightarrow O_2 + SO_2^* \rightarrow O_2 + SO_2 + h\nu$ ).
- Cleavage of linear or cyclic peroxides.

*Cleavage of linear or cyclic peroxides* is the most commonly observed reaction in organic CL reactions. The most common excited product in an organic CL reaction, where the oxidant is oxygen or its derivatives, is the carbonyl of a ketone.

### **6.2.3 Chemiluminescence and quantum yield**

The exact detailed reaction mechanism of chemiluminescence has not been identified, however some possible mechanisms that have been proposed so far are commonly accepted for the evidence of CL [65,69,70]. The proposed mechanisms (for liquid hydrocarbons) of the light emission are generally based on either a bimolecular termination of peroxy radicals or direct decomposition of hydroperoxides or metathesis reactions or molecular rearrangement, which are exoenergetic reactions in nature.

The Russell mechanism (Fig. 6.2) [69-73] is the most widely used mechanism for the description of CL in liquid phase oxidation of hydrocarbons but also discussed for organic polymers. In this mechanism, the light emission reaction is a bimolecular termination of alkyl (primary or secondary) peroxy radicals produced from the radical autooxidation mechanism. Recombination of two active peroxy radicals produces an excited carbonyl group directly through the cleavage of a six-membered ring as an intermediate. An alcohol and an oxygen molecule are resulted as termination byproducts. The formed excited carbonyl group stays directly in the triplet state, which upon relaxing to the singlet ground state results in the emission of photons.

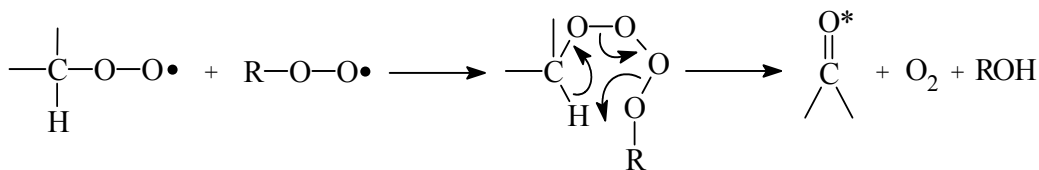


**Figure 6.2:** Schematic representation of the Russell mechanism.

The reaction (Fig. 6.2) discussed above stands for the emission of light from a single excited state molecule. When the overall quantum yield is independent of the conversion of such a system, the intensity of light  $I$  is proportional to the rate of termination reaction:  $I \sim K$ . Together with the CL quantum yield  $\phi_{CL}$ , and an instrumental constant  $G$ , the CL emission is given by [65,69-73,]:

$$I = G \cdot \phi_{CL} \cdot K \quad (6-3)$$

The  $\phi_{CL}$  is then defined as the ratio of the total number of photons emitted to the number of molecules reacting to produce those photons. The  $\phi_{CL}$  is made up of three components:

$$\phi_{CL} = \phi_{Che} \cdot \phi_{Exc} \cdot \phi_{Flu} \quad (6-4)$$

where  $\phi_{Che}$  fraction of molecules undergoing the necessary reaction,  $\phi_{Exc}$  fraction of molecules which react in the CL pathway to become electronically excited and  $\phi_{Flu}$  fluorescence quantum yield of an excited product. Therefore,  $\phi_{CL}$  is susceptible to modification of physical and chemical factors. The quantum yield is a material specific constant. As it may vary by several orders of magnitude and as it determines the CL emission as a factor, potentially different quantum yields have to be taken into account when comparing the CL result of different substances. Also, while normally assumed to be constant, the quantum yield may change in the course of a thermo-oxidative reaction being followed as CL. As it is very difficult to determine the quantum yield for a particular oxidation reaction, normally CL emissions are obtained as relative units rather than absolute ones.

The photo physical quantum yield decreases with increase of temperature, and the quenching of triplet state by molecular oxygen ( $^3\text{O}_2$ ) usually decreases the overall quantum yield of the CL emission to  $10^{-9}$ .

## **6.3 Evaluation of polymer oxidation processes**

Polymer long-term performance can imply many things, however one of the most important of those is the ability to resist the deteriorating effects of climatic exposures, to which oxidation is a prominent contributor. Basically, the oxidation process of polymers can be studied using the techniques such as differential scanning calorimetry (DSC) and infrared (IR), and also by analysis of reaction products. However, CL has attracted much attention because of its close association with oxidation and its extreme sensitivity, which permits the study of oxidative reactions at very early stages (much earlier than those at which IR and DSC become sufficiently effective) [65,69].

Ultraweak CL from oxidation of organic substances has been known for many years and the pioneering work of Ashby [66] and others [65-69], demonstrated CL from oxidation of a variety of polymers. These earlier studies have noticed the following:

- Significant light emission requires oxygen to be present, and the intensity is proportional to the partial pressure of oxygen in contact with the surface.
- The integrated emission intensity is proportional to the concentration of carbonyl groups produce in the oxidation process.
- Radical scavenging antioxidants decrease the intensity of light emission and introduce an induction time before a significant light emission is observed.
- Peroxide decomposing stabilizers also introduce an induction period in the CL curve.

### **6.3.1 Polymer oxidation scheme for chemiluminescence**

The oxidation scheme or model for organic polymers is based on the autooxidation mechanism as generally represented for oxidation of liquid hydrocarbons. The oxidation scheme for CL emission by polymers can be represented as shown in Fig. 6.3 [71-76].

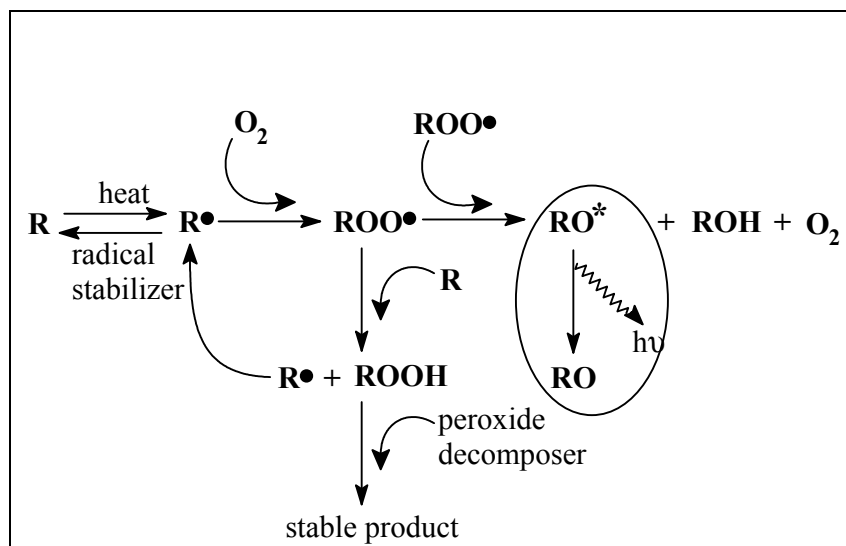
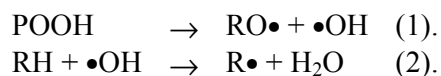


**Figure 6.3** Autooxidation scheme for chemiluminescence in organic polymers.

The *radical initiation* ( $R\bullet$ ) is a subject of many authors and several mechanisms have been discussed [55,58]. The formation of radicals by the cleavage of C–C or C–H bonds requires high thermal energy ( $> 800\text{ }^\circ\text{C}$ ). However, thermal initiation of radicals can occur via the cleavage of the weak bonds in the polymer chain. In contrast to this, the formation of radicals by the cleavage of peroxide and aliphatic azo bonds requires less dissociation energy of 130 kJ/mol to 170 kJ/mol, which is in the temperature range of  $70\text{ }^\circ\text{C}$  to  $150\text{ }^\circ\text{C}$ .

With peroxides (POOH) as initiators, the formation of radicals can be formulated as:



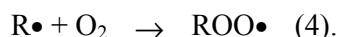
Radicals can be generated by the cleavage of the peroxide bond of hydroperoxide or another peroxide molecule. It is also possible that the direct reaction of the polymer with oxygen leads to the formation of radicals:



The above reaction requires a thermal energy of 120 kJ/mol to 190 kJ/mol. Since the required activation energy is of 170 kJ/mol to 230 kJ/mol, the above all reactions proceed slowly and selective in nature. The reactivity depends on the strength of the C–H bonding and it is in the order of tertiary  $>$  secondary  $>$  primary.

Radical scavengers (antioxidants) respond in an opposite way of the reactions (1), (2) and (3). They effect in a way that the reaction with free radicals forms stabilized radicals, which then suppress further propagation reactions.

The *chain propagation* starts with the addition of an oxygen molecule to the polymer radical, and forms an alkyl peroxy radical:

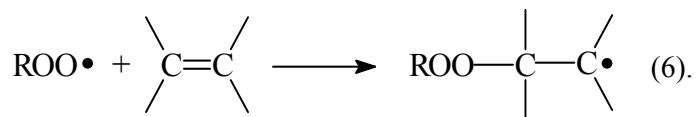


This reaction is faster and requires less activation energy, which is about 40 kJ/mol. The reactivity of oxygen mainly depends the structure of the polymer radical  $R\bullet$ .

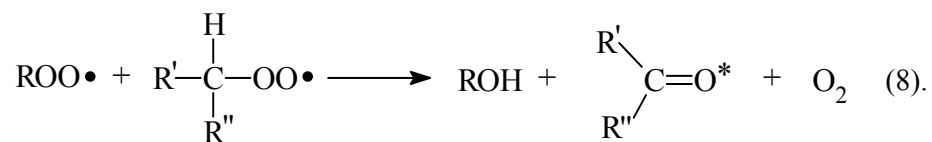
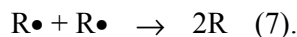
The second possible chain propagation step is the formation of hydroperoxide and polymer radical ( $R\bullet$ ) by the reaction of an alkyl peroxy radical with another polymer molecule. The generated new polymer radicals follow the reaction step (4) and therefore propagation is said to be autocatalytic in nature.



An alternative possible reaction for the formation of peroxy free radicals is the reaction of alkyl peroxy radicals with unsaturated C=C groups:



The *chain termination* occurs via radical recombination and disproportionation mechanisms. However, the radical recombination reactions have been found to occur effectively in polymers matrices at room temperature. The possible radical recombination reactions are as shown below:



From the above discussion the following generalized conclusions can be drawn:

- For CL the chain termination step is more important than the chain propagation step.
- A steady state prevails when the rate of radical chain growths initiated equals the rate of chain growths terminated.
- The formation of excited ketones in the termination step by peroxy radical recombination is proportional to the second power of the concentration of stationary peroxide  $ROO\bullet$ .

The CL intensity  $I$  relation is shown as (see Section 6.2.3):

$$I = G \cdot \phi_{CL} \cdot K .$$

In the stationary state condition (the rate of initiation equal to the rate of termination), the term  $K$  rate of reaction is then proportional to the concentration of peroxide. Thus  $K$  is given by:

$$K = \alpha [ROO\bullet]^2 . \quad (6-5)$$

Therefore in a chemiluminescent reaction a minimum of a pair of alkyl peroxy radical is necessary.

## **6.4 Types of measurements**

Two different types of CL experiments are generally performed [75] and they are:

- Stationary.
- Non-stationary.

In stationary experiments, the light emission by the sample is measured as a function of time of thermal oxidation. In non-stationary approach, the environment of the polymer is perturbed and change in the CL intensity is measured as material responds to the perturbation and then returns to the steady state. Both experiments differ significantly in the time required to complete the test. The former may require quite a long duration especially when applied to highly stabilized systems whereas the latter requires relatively short duration for both unstabilized and stabilized polymers.

Stationary experiments at temperatures approaching ambient involve measuring small changes in low intensities over a long period of time. For estimation of the oxidative stability of a polymer at nearly ambient conditions, the usual procedure is to measure the Arrhenius parameters at elevated temperatures and then extrapolate to room temperature on the assumption that there has been no change in the mechanism. But this route may not be precise because the stabilized polymers evidence to show change in the mechanism.

Increasing of free radicals in the polymer by perturbing the stationary state of oxidation is an alternative approach. This leads to an abrupt increase in the CL intensity followed by decay as the system returns to the steady state. This decay curve may be analyzed to supply the kinetic parameters for the oxidation reaction. This method has been widely used to determine the absolute value of termination rate constant and rate constant for radical scavenging by antioxidants in liquid hydrocarbons and solid polymers as well. UV-irradiation, gas switching (changing the gas atmosphere of the sample), temperature pulse and mechanical stress are the usual perturbation methods for solid polymers.

## 7 Experimental Details

### 7.1 Materials and sample preparation

#### 7.1.1 POFs and bulk material selection

For the present PhD work, commercially available data communication grade POFs made of poly(methyl methacrylate) (PMMA) were selected as a representative model as they are largely being used for various optical applications. The chemical structure and properties of PMMA are provided in Section 3.3.

In total, five POF samples were used. Two of them consisted core, cladding and jacket (referred as *POF cables*), and they were received from a customer of BAM for the basic research purpose. The other three samples consisted only core and cladding (referred as *bare POFs*) and were purchased from three different manufacturers. However, all the POF samples were step-index (SI) and multimode fibers with a typical diameter of about 1 mm (core and cladding). Specifications of POF samples are given in Table 7-1.

**Table 7-1:** Details of POFs (provided by the respective manufacturers/customers) and bulk PMMA used for the present investigation. “-” Indicates values were not provided by vendors.

No. <sup>1</sup>	Customer/ Manufactu rer	POF grade	Core material	Clad material <sup>2</sup>	Jacket material	Physical constants		
						Diameter [ $\mu\text{m}$ ]		Loss [dB/km] at 650nm
						Bare fiber	Core	
S1	Robert Bosch GmbH	PM4Y 1,0/2,2 OR	PMMA	Fluoro- polymer	Polyamide (PA12)	1000	-	180 - 220
S2	Robert Bosch GmbH	CXK- HT1001	PMMA	Fluoro- polymer	Polyethylene (PE)	1000	-	180 - 220
S3	Mitsubishi Rayon Co. Ltd.	Eska CK-40	PMMA	Fluoro- polymer	No jacket	1000	980	200
S4	Toray Industries Inc.	PGU-FB 1000	PMMA	Fluoro- polymer	No jacket	1000	-	150
S5	Asahi Chemicals	Luminous TB-1000	PMMA	Fluoro- polymer	No jacket	1000 $\pm$ 0.006	-	160
S6	Mitsubishi Rayon America Inc.	Acrypet V Color 001 (clear)	Bulk PMMA (granules) sample			Refractive index-1.49		

<sup>1</sup> These numbers are given temporarily to the corresponding samples for the convenience of naming. From this point onwards the corresponding components (either the bare POF or the core or the cladding) of POF samples and bulk PMMA name by these given numbers.

<sup>2</sup> In addition to these manufacturers data the experimental findings of claddings chemical compositions are provided in Section 8.1.3.

POF manufacturers/customers disclosed only few data (formulation and physical constants) of materials and this made the analysis of the unexposed and exposed samples somewhat difficult. Cladding materials of the POF samples were fluoropolymers, and jacket materials of two POF cable samples were PE and PA 12 (see Table 7-1). Despite the lack of data, the unexposed POF samples were characterized for the glass transition temperature ( $T_g$ ) and melting temperature ( $T_m$ ) and molecular weights using DSC and GPC, respectively (see Section 8.1.1 and

8.1.2). Claddings also were characterized for chemical compositions using FTIR (for details see Section 8.1.3).

Optical grade PMMA in the form of granules was used as a reference bulk material in a few cases. Some specifications are given in Table 7-1. The granule form is thought to be free of any kind of additives (e.g.: stabilizers and plasticizers), which are commonly incorporated into technical products to achieve a moderate performance.

### 7.1.2 POF sample preparation

During the POF sample preparation for optical measurements (online and spectral transmission, see Section 7.3.1 and 7.3.2) attention was paid to two main factors:

- Length of the fiber.
- Fiber end preparation.

*Length of the fiber* was optimized to about 10 m from the viewpoint of the fibers length-dependent mode mixing behavior, the length-dependent relative influence of fiber ends surfaces and applications (e.g.: automobile industry uses the fiber length in the order of about 10 m).

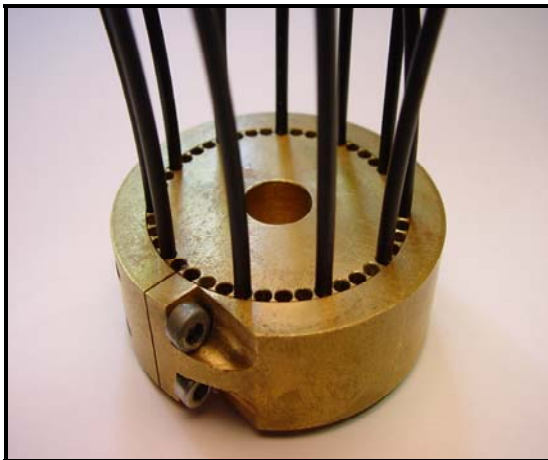


**Figure 7.1:** *Photograph of a prototype polishing tool.*

*Fiber end preparation* carried out by simple polishing using a self-built (BAM) metal tool, especially constructed for POFs. Fig. 7.1 shows a photograph of the polishing tool. The fibers were placed into individual grooves at the border of a cylinder in a way that their end-faces extend to a small but nearly equal length below the cylinder end-face. Then they were fixed by surrounding ring. By moving the tool with the fiber end-faces in a figure eight shape over grit abrasive papers end-faces were polished.

The polishing process started with a paper roughness of 40  $\mu\text{m}$  and went down to 0.3  $\mu\text{m}$  until the required surface smoothness of end-faces was obtained, inspected by using a simple microscope. An advantage of this tool is at a time as many as 10 to 15 (even more) fibers ends can be polished.

However, in a few cases a pair of specially adapted pliers (Rennsteig Werkzeuge GmbH, Germany) was used for fiber end cutting and end-face preparation.

The POF samples that were exposed and used for chemical investigations required no fiber end preparation and specific length. In the case of POF cables (both the exposed and unexposed), the jacket was first manually removed by using a wire-end stripper (Siemens) and then bare POF samples were utilized for chemical investigations.

## **7.2 Climatic exposures or aging**

### **7.2.1 Exposure conditions**

Out of the three most influential industrial environmental factors of POFs (see Section 4.4), climatic influences on both the optical transmission and the material stability were investigated. Table 7-2 provides details of climatic conditions that were applied to POFs for a longer period of time. Some of these climatic stress factors were applied for short period to investigate influences of individual climatic parameters on the optical transmission by varying one parameter and keeping other as constant. Table 7-3 displays details of the applied short-term climatic exposure conditions.

**Table 7-2:** Long-term climatic exposure conditions for POFs

No.	Temperature* [°C]	Relative humidity (RH) [%]	Exposure time [Hours]	Remarks
1	92 ± 1	95 ± 2	3300	For POF cables S1 and S2
2	92 ± 1	95 ± 2	> 1000	For bare POFs S3-S5
3	92 ± 1	50 ± 2	3380	For bare POFs S3-S5
4	50 ± 1	95 ± 2	1660	For bare POFs S3-S5
5	90 ± 1	<< 50	3290	For bare POFs S3-S5
6	100 ± 1	<< 50	4500	For bare POFs S3-S5
7	110 ± 1	<< 50	> 1000	For bare POFs S3-S5
8	120 ± 1	<< 50	> 1000	For bare POFs S3-S5

No. 1-4: Climatic parameters, temperature and humidity, applied in combination and these were intended and recorded values.

No. 5-8: Actually, temperature only was applied and measured but the humidity level was approximated (dry heat condition).

\* The uncertainty of the temperature refers to the place of the temperature sensor. This is valid for all temperatures given for climatic exposures.

**Table 7-3:** Scheme of short-term climatic exposures of POFs.

No.	Temperature	Relative humidity (RH)
1	Steady: (92 ± 1) °C	Cycle: 50 % / 48 h and < 10 % / 48 h, ... 80 % / 48 h and < 10 % / 48 h.
2	Cycle: (50 ± 1) °C / 48 h and 25 °C / 48 h, ... (90 ± 1) °C / 48 h and 25 °C / 48 h.	Steady: (95 ± 2) %
3	Steady: (25 ± 1) °C	Cycle: 50 % / 48 h and < 10 % / 48 h, ... 90 % / 48 h and < 10 % / 48 h.

## 7.2.2 Exposure tests

Using commercially available climatic chambers (VCS 4034-5/S and HC 4033, Vötsch Industrietechnik GmbH, Germany) and an oven (Heraeus Instruments GmbH, Germany) the long-term as well as short-term exposure tests (see Table 7-2, 7-3) were performed. Exposure tests to temperature in combination with humidity were carried out by using climatic chambers. Tests to temperature only were conducted by using both, the oven and climatic chamber.



**Figure 7.2:** *A photograph of an overview of the exposure test by using climatic chamber and multiplexer.*

In all the climatic exposure tests, about 10 m of each POF sample was placed inside the climatic chamber but for connecting it to the multiplexer, standing outside the chamber, the POF has to be prolonged by an additional length of about 3 m, which therefore was not exposed. So a total length of about 13 m was prepared instead 10 m as mentioned in the Section 7.1.2 and the optical measurements were performed for 13 m. An example for the exposure tests using climatic chamber and multiplexer is shown in Fig. 7.2.

For chemical investigations POF samples of known length (typically about 6 m length) and bulk PMMA samples were placed inside the chamber and exposed to known period.

All the POF samples were placed over ordinary glass plates inside the chamber because glass may avoid chemical changes (degradation processes) influence by metal (meshes) [77], which are commonly provided as sample holders in the chamber. The climatic chamber exposure tests were conducted in the ventilator generated air atmosphere. The oven exposure tests were conducted in an ambient atmosphere of circulating open air.

## 7.3 Optical transmission measurements

### 7.3.1 Measurements by using multiplexer

The optical transmission during the aging/exposure of POFs was measured using a self-constructed special device called as *multiplexer*. It recorded the transmission at three wavelengths regions, which were centered at 525 nm, 590 nm and 650 nm, which made it possible to measure the transmission every 5 minutes (e.g.: for three POF samples) during the exposure up to > 90 days. However, the transmission data presented in the following sections were obtained by averaging the data recorded as function of time at these three wavelengths. The multiplexer's detailed working principle can be found in [3,78].

The multiplexer mainly consists of three functional units:

- The light source unit: Three light emitting diodes (LED) were used as the light sources. Individual LED was launched into the individual POF by means of a controllable shutter and a coupler.
- The detector unit: A PIN photodiode followed by a low noise amplifier was employed as a detector. Both the detector and the light source units were set on an adjustable platform of the positioning system.
- The positioning system: POF ends were inserted into the multiplexer via a fixed special receptacle, uniformly spaced on a single plane. Switching between POFs to be tested was executed by the linear positioning system using a stepping motor.

First, the optical transmission of POF samples was measured before the aging/exposure started. This initial transmission value was considered as 100 %. Then the subsequent transmission values were recorded during the exposure and related to the initial value 100 %. Therefore, the outcomes of measurements were relative transmission values.

However, these transmission values (%) can be converted to attenuation ( $\alpha$ ) values in dB/km using the equation 2-7. For calculations of  $\alpha$ ,  $P_0$  is not absolutely 100 % because there will be always a small loss of the transmission at the fiber ends faces due to a small air gap between the POF connectors (this loss also is referred as Fresnel

reflection loss) [11]. Therefore  $P_0$  for PMMA based POFs is calculated to be about 92 %. The calculated  $\alpha$  values for the POF length 13 m are presented in Table 7-4.

**Table 7-4:** Attenuation values for the corresponding relative transmission values.

Relative transmission [%]	Attenuation [dB/km]
90	9
80	48
70	93
60	145
50	206
40	280
30	376
20	512
10	743
0.1	2282

### 7.3.2 Measurements by using miniature spectrometer

If it was sufficient to measure the optical transmission/loss of POF samples before and after the exposure a self-built *miniature spectrometer* was used.

The spectrometer consists of two main parts:

- The light source: Halogen lamp HL-2000 (TOP sensor systems, Sentronic GmbH, Germany).
- The detector: Charge-coupled device (CCD) S2000 (Sentronic GmbH, Germany) scanning the visible spectral range from 380 nm to 800 nm with the resolution 5 nm.

## 7.4 POF cladding extraction

As the bare POF is made of two optically clear components, the core and the cladding, much interest was paid to study these components separately. Material details of the studied POF samples can be found in Section 7.1. Since most of the fluoropolymers show insolubility in common organic solvents, the cladding extraction was achieved by dissolving only the core i.e. PMMA, which has a number of solvents. Chloroform (trichloromethane) was used as a solvent for the PMMA core and non-solvent for the cladding (fluoropolymer). The treatment of bare POF samples (excluding the sample

S5 because its core and cladding both were dissolved in the same solvent) with this solvent was found as a best way of the separation of the cladding from the core.

First, bare POF samples were cut into small pieces of about 3 cm to 4 cm and soaked in chloroform for more than 12 hours for complete dissolution of the core. In the case of POF cable samples, the jacket was first removed (using a wire-stripper) and then bare POF pieces were soaked-in. Then the non-dissolved cladding samples were taken out from the solution of the core and washed them for about 3 to 4 times using the same solvent in a separate glass container. Then samples were pressed smoothly between soft papers to remove a large volume of the solvent. Finally, the remaining solvent was removed by drying at below 55 °C in a vacuum oven. The cladding samples obtained in this way appeared like hollow cylinders.

A few experiments were conducted for only the fiber core. To achieve the separation of the core fiber from the cladding 1,4-dioxane (diethylene dioxide) solvent was used, which dissolves the core but swells the cladding. The core fiber was separated by the following simple way: bare POF samples were cut into small pieces and immersed in dioxane for 7 to 10 minutes. Then, samples were taken out from the dioxane container and immediately removed the cladding just by stripping using hands with the soft paper. It is attributed that during the immersion solvent penetrates the interface of core and cladding and swells up the cladding, it allows easy stripping of the cladding, remaining the core in the fiber form. Finally, core fiber samples were dried (at about 60 °C) in a vacuum oven to remove the solvent on the surface.

## 7.5 Chemiluminescence experiments

It is seen in Section 6.3 that the CL intensity can be expressed in the form:

$$I = G \cdot \phi_{CL} \cdot K,$$

where  $K$  = rate of the luminescent reaction,  $G$  (takes a value between 0 and 1) = a constant that incorporates all factors influencing the detection efficiency for photons being emitted and quantum efficiency  $\phi_{CL}$  (takes a value between 0 and 1) = the product of a fraction of potentially luminescent reactions which produce the excited states and a fraction of such states emit light. Therefore, variation in  $I$  can be due to changes in  $G$ ,  $\phi_{CL}$  or  $K$ . In practice,  $G$  can be calculated for any instrument.

Determination of  $\phi_{CL}$  is very difficult, however typical values in the range  $10^{-3}$  to  $10^{-10}$  are known to be exhibited by organic compounds and solid polymers [74,79,80]. Yet, it is still possible to detect the weak emission of light through sensitive detection by single photon counting ( $G \approx 1$ ) and the fact that photon flux increases linearly with a number of reactive species.

CL curves of the investigated samples were recorded with the help of an own built (BAM) set-up, Fig. 7.3 shows a flowchart of the experimental set-up used in the present CL experiments.

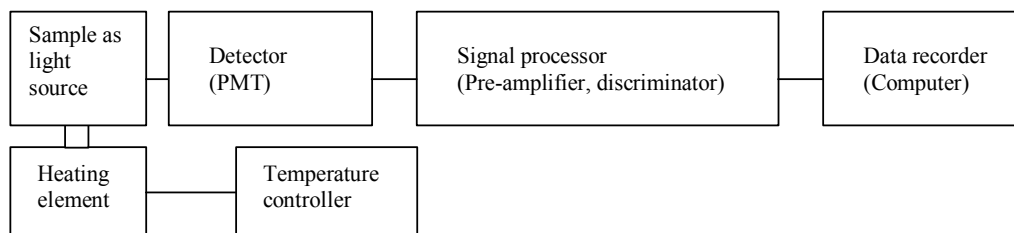


**Figure 7.3:** *Flowchart of the CL set-up.*

### 7.5.1 Instrumentation

The basic instrumentation consists of a heating arrangement for the sample in a light-tight chamber, a photomultiplier tube (PMT) to sense the CL emission, an amplifier to measure the PMT output current and a chart recorder to record the current as a function of temperature or time.

An own built (BAM) sample chamber [79] was used for sample heating, done by electrically, controlled by using a Lake Shore 340 (Westerville OH, USA) temperature controller. This chamber consists of a gas inlet and outlet, space in its middle for placing the sample and a quartz window on its top connecting to the PMT. Fig. 7.4 shows a photograph of different parts constructed in the sample chamber that used for the present CL set-up.

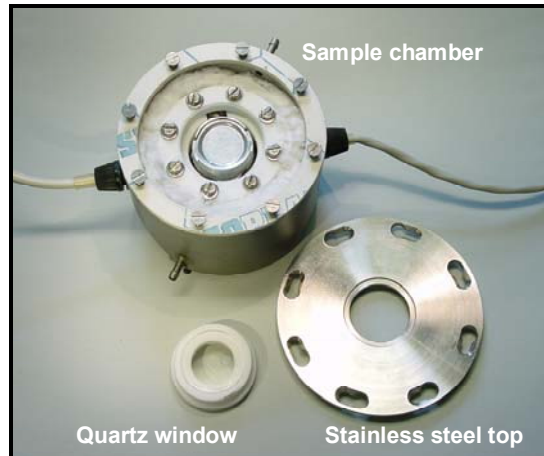


**Figure 7.4:** *A photograph of an overview of the own built sample chamber.*

The chamber was constructed in two parts, an outer and inner part. The outer part (see Fig. 7.4) was made of stainless steel, airtight and had a gas inlet and outlet. The gas from the inlet is fed through the space between this and an inner part and was filled with steel wool to preheat the inflowing gas. A thermally insulated (from the outer part) inner ceramic layer (see Fig. 7.4) was constructed inside the outer part but connected to it via the gas inlet. Within the inner part, first a pile of resistors to heat and then a PT 100 resistor to measure the temperature were installed. A removable sample holder aluminum pan of 25 mm in diameter was placed on top of the PT 100 resistor. The temperature processing was done by means of a temperature controller and read out from there by a computer. The inner ceramic part consists of a screw type cover on its top, which was also made of ceramic. However, the center of this cover was made open but covered with a quartz window containing a small hole at the center to allow the gas flow outwards. The outer chamber was covered using a detachable stainless steel plate (which also covers the inner part since its height is constructed shorter than that of the outer part) and it contains another quartz window without a hole in its center. During the measurements, the sampling chamber was connected to the housing of a side-on low noise cooled PMT (Hamamatsu R1527P) via outer chamber cover.

All materials used for the chamber construction were inspected (especially those in view of the photomultiplier) before to be as low emissive as possible in terms of photons released at an applied temperature range.

The output of the PMT was processed by a Perkin Elmer/EG&G/ORTEC (Oak Ridge, TN, USA) single photon counting device in which a pre-amplifier VT120C, discriminator 935 and counter 994 were in-built.

The photon counter and temperature controller were connected via an IEEE bus to a computer recorded the signal and controlled the temperature using an own-programmed Turbo Pascal software.

### 7.5.2 Sampling

In all the CL experiments, samples in their original form were used because the sample preparation from one form to another (e.g.: powder and solution casting) may affect their CL behavior significantly [80]. However bare POF, core and cladding samples were first cut into 2 mm to 3 mm pieces in length and then horizontally placed in the aluminum pan sample holder, which was mounted on a resistor in the sample chamber (see Section 7.5.1). Prior to the use of new aluminum pan in each sampling, it was washed by acetone and dried by heating in an oven to remove the presence of contaminants like grease and oil etc. that could affect the CL emission from the sample.



**Figure 7.5:** *An example for the sampling in CL experiments.*

Since it has been demonstrated that PMMA based POFs exhibit comparatively weak CL emission at temperatures below (PMMA)  $T_g$  [51,52], as much sample as possible was placed in the sample holder. Almost the same weight (or surface to volume ratio) was maintained in all the CL measurements. Fig. 7.5 shows an example for the sampling (in particular bare POF samples) used in CL experiments.

### 7.5.3 Measurements

Temperature ramp measurements were carried out for all the investigated samples. However, temperature was held stationary with the accuracy  $\pm 0.1$  K for about 60 minutes at each desired value in the range from 37 °C (310 K) to 177 °C (450 K). The

heat-up rate was 5 K min<sup>-1</sup>. The applied temperature program was as shown along with the corresponding CL curves presented in the subsequent sections. The CL emission (counts per second, cps) was recorded as a function of time and temperature under a constant flow rate of pure oxygen.

One of the reasons to choose this type of measurements may be that it is useful to determine differences in the oxidation state of samples of comparable shape and degradation history.

The registration of photons was done as integral emission without spectral resolution. The spectral characteristics exclusively are determined by the PMT (within the UV/VIS range of concern to the present work). The two quartz windows in the light path only show a negligible influence on the spectral transmission behavior. A postulated emission of singlet oxygen in the near infrared (NIR) region in the course of oxidation would already be beyond the spectral sensitivity of the PMT used here.

Before recording spectra of the samples, blank measurements (without the sample but with the aluminum pan sample holder) were carried out to ensure the CL emission from the aluminum pan was too less to be accounted. Also, to confirm negligible emission from the experimental set-up, measurements without the sample and the holder were performed.

## **7.6 FTIR measurements**

FTIR spectra of bare POF, core and cladding samples were separately recorded using a commercially available FTIR instrument NEXUS 670 (Nicolet Instruments Corp. USA). The number of scans performed for each sample was 256 and the recorded wavenumber range was 4000 cm<sup>-1</sup> to 600 cm<sup>-1</sup> with a resolution of 4 cm<sup>-1</sup>.

For recording spectra of POF core samples, first core polymer solutions of known concentration were prepared as described in Section 7.4. Then capillary films were formed on sodium chloride IR transparent discs. Finally, the film samples were vacuum dried (at below 55 °C) for an over night in an oven to remove the contents of solvent in the samples.

## 7.6.1 Attenuated total reflection (ATR) - FTIR

ATR is a constructive and widely applicable technique for obtaining FTIR spectra of samples such as rubbers, fibers, food materials, cured resins, liquid samples and powders without any sample preparation [81].

### 7.6.1.1 Practical aspects

Basically, this method uses the principle of the Snell's law of refraction (see Section 2.1). The application of ATR in spectroscopy is based on the fact that although complete internal reflection occurs at the interface, radiation does in fact penetrate a short distance into the rarer medium. This penetrating radiation is called as the *evanescent wave*. It can be partially absorbed by placing a sample in optical contact with a dense medium (so called the internal reflection element, IRE, usually either a prism or multireflection element) at which reflection occurs (see Fig. 7.6). To increase the sensitivity a number of subsequent reflections can be used, the higher the angle of incidence and thinner or longer the multireflection element the larger is the number of reflections.

The reflected radiation can result in absorption spectrum that closely resembles the transmission spectrum of a sample. However, the actual pattern depends on several parameters; including refractive indices of the prism (or multireflection element) and the sample, the angle of incidence of the radiation, penetration depth, the number of reflections and the wavelength of radiation.

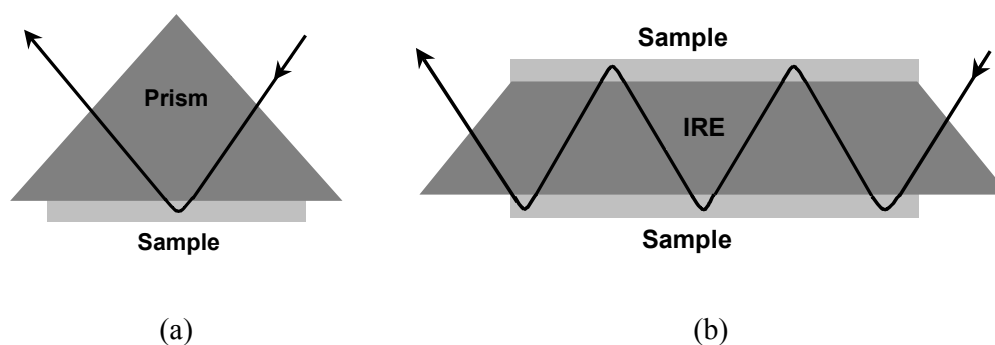


**Figure 7.6:** Schematic representation of attenuated total reflectance in: (a) single reflection prism; (b) multireflection element.

*Refractive indices* of the prism and the sample are among the most important affecting factors. The refractive index difference between these two ultimately results in penetration depth of the evanescent wave. The larger the difference the shorter is the penetration depth and the lower is the spectral contrast. However, when the refractive index of the sample close to the same of the prism, the deeper is the penetration and the higher is the spectral contrast. Germanium (Ge), zinc-selenide (ZnSe) and silicon (Si) are the mostly used as prism materials having refractive indices  $> 2.2$ ,  $2.41$  and  $2.2$  to  $2.41$  respectively.

ATR prisms can be constructed with different incidence angles ( $45^\circ$  and  $60^\circ$  are common). However, the *angle of incidence* ( $\theta_i$ ) must be greater than the critical angle ( $\theta_c$ ) for the total internal reflection to occur (see Section 2.1). Since  $\theta_c$  varies across an absorption band,  $\theta_i$  should be considerably greater than  $\theta_c$ . The penetration depth decreases with increasing  $\theta_i$ , therefore, choosing a very large  $\theta_i$  for general use is not recommended.

The *penetration depth* is normally a fraction of a wavelength and determined by the refractive index difference between the sample and prism,  $\theta_i$ , the wavelength and the pressure used to hold the sample (solid hard samples only) against the prism. The effect on the spectrum is that bands at longer wavelengths are more intense than those at shorter wavelengths, relative to the transmission spectrum of the same material.

### 7.6.1.2 Measurements

ATR-FTIR spectra of bare POF and cladding samples were registered using a commercially available *smart golden gate–single reflection–diamond–ATR unit* (L.O.T.-Oriol GmbH, Germany). It had an IRE (prism) made out of Type-IIa-Diamond with the incident angle  $45^\circ$ . The refractive index and the penetration depth of the IRE were  $2.4 \mu\text{m}$  and  $4.4 \mu\text{m}$ , respectively. Using this ATR unit the spectral range registered was  $4000 \text{ cm}^{-1}$  to  $650 \text{ cm}^{-1}$ . The number of scans and the resolution were same as measured in transmission FTIR (see Section 7.6).

It was found that the ATR-FTIR spectrum of the bare POF (core and cladding) was equivalent to the spectrum of its cladding when measured them separately.

## 7.7 Supplementary measurements

**Differential scanning calorimetric (DSC)** measurements were carried out to determine  $T_g$  and  $T_m$  of POF samples employing a Seiko DSC 220C instrument. Alumina pan served as the reference and the heating/cooling rate was  $10 \text{ K min}^{-1}$ .

**Gel permeation chromatography (GPC)** method was used to characterize the molecular weights of POF core samples by a Polymer Lab GPC 210 instrument. Tetrahydrofuran (THF) was employed as an eluent with a flow rate of  $1 \text{ ml min}^{-1}$ . A refractive index detector analyzed the elutants. GPC columns were calibrated with a PMMA standard. POF samples ( $1 \text{ mg ml}^{-1}$ ) were first dissolved in THF and then the solutions were filtered to remove the non-dissolved cladding prior to the injection.

**UV/visible** transmittance measurements were performed utilizing a commercially available Varian Cary 300 Scan spectrophotometer. To record spectra (in a range of 180 nm to 850 nm) of core samples, solutions were prepared using spectrograde dichloromethane solvent. Cladding samples obtained by the procedure as described in Section 7.4 were directly taken for registering spectra. However, a special slit (a width of less than the diameter of the bare POF or cladding) was self-built since the diameter of cladding samples was 1 mm, which was too small to measure using the provided one for normal film samples.

**Thermogravimetry (TG)** method was applied to analyze the thermal stability of POF samples by using a TGA/SDTA 851 (Mettler Toledo GmbH, Germany) instrument. The heating rate was  $10 \text{ K min}^{-1}$  under both air and nitrogen atmosphere.

**Scanning electron microscope (SEM)** pictures were taken from a Philips SEM 515 (pw6703) apparatus to analyze morphological changes of POF samples.

## 8 Results and Discussion

### 8.1 Characterization of the unexposed POFs

#### 8.1.1 Glass transition ( $T_g$ ) and melting temperature ( $T_m$ ) by DSC

DSC is a technique in which the difference in heat flow between the sample and a reference is monitored as a function of temperature and time, while the sample is subjected to a controlled temperature program. With this technique, characteristic temperatures (glass transition, melting, and crystallization temperature), melting and crystallization behavior, specific heat capacity, heat of reaction, reaction kinetics, oxidative stability and thermal stability can be studied. The glass transition ( $T_g$ ) and melting temperature ( $T_m$ ) are the characteristics of amorphous and crystalline materials, respectively.

The DSC determined  $T_g$  and  $T_m$  of POF and PMMA samples are provided in Table 8-1. DSC experimental curves shown in Fig. 8.1 can serve as a model for the bare POF, cladding and core, which are compared with the reference bulk PMMA sample.

**Table 8-1:** Experimentally determined values of  $T_g$  and  $T_m$ , and molecular weight characteristics (weight  $M_w$ , number  $M_n$  average molecular weights and polydispersity PD) of POF and PMMA samples. On-set and off-set describe the starting and ending temperatures of the transition, respectively. “-” Indicates no value could be found by the methods followed in the present investigation.

Samples	Glass transition ( $T_g$ ) and melting temperature ( $T_m$ ) / [°C] ( $\pm 1$ %)				Molecular weight [g/mol] ( $\pm 1 \cdot 10^2$ )		
	On-set	Off-set	$T_g$	$T_m$	$M_w$	$M_n$	PD = $M_w/M_n$
S1 Bare POF	113.9	124.4	119.6	-	-	-	-
	132.4	145.1	-	137.4	-	-	-
	114.4	123.6	118.6	-	$1.07 \cdot 10^5$	$5.65 \cdot 10^4$	1.89
Cladding	63.7	153.8	-	124.4, 137.5	-	-	-
S2 Bare POF	115.0	124.8	119.8	-	-	-	-
	-	-	-	-	$1.10 \cdot 10^5$	$5.95 \cdot 10^4$	1.85
	105.0	120.9	112.7	-	-	-	-
S3 Bare POF	116.5	126.2	121.0	-	-	-	-
	133.1	145.1	-	137.4	-	-	-
	112.9	123.4	118.1	-	$1.11 \cdot 10^5$	$6.15 \cdot 10^4$	1.77
Cladding	69.6	154.1	-	125.1, 139.5	-	-	-
S4 Bare POF	113.6	124.6	119.2	-	-	-	-
	133.9	147.5	-	139.9	-	-	-
	112.9	123.0	117.9	-	$1.00 \cdot 10^5$	$5.65 \cdot 10^4$	1.78
Cladding	65.3	155.0	-	126.7, 141.0	-	-	-
S5 Bare POF	113.6	123.5	118.0	-	-	-	-
	-	-	-	-	$1.12 \cdot 10^5$	$6.15 \cdot 10^4$	1.82
	-	-	-	-	-	-	-
S6 Bulk-PMMA	103.9	111.4	107.6	-	$1.36 \cdot 10^5$	$7.08 \cdot 10^4$	1.92

Three bare POF samples (S1, S3 and S4; all Type 1) exhibited two distinct transition temperatures  $T_g$  and  $T_m$ . While the other two (S2 and S5; all Type 2) exhibited only  $T_g$ . The bulk PMMA sample (S6) exhibited typical  $T_g$  as the normal PMMA does (see Table 8-1 and Fig. 8.1).

The bare POF is a physical blend of core and cladding polymers. If these are of different kinds, DSC could result in two distinct transition temperatures. Hence,  $T_g$  and  $T_m$  demonstrated by Type 1 samples can be attributed one of that to the core and

other to the cladding. Furthermore,  $T_g$  is believed to be of the core because it is PMMA, which is well known to exhibit the same. Additionally, DSC measurements to the core and cladding samples resulted in the same temperature region of  $T_g$  and  $T_m$  as displayed by bare POF samples. Therefore, this result confirms that between these two transitions,  $T_g$  should be of the core and obviously the other transition  $T_m$  should be of the cladding. It reveals that the cladding is probably of crystalline in material nature. Moreover, chemical compositions analysis by FTIR shows (see Section 8.1.3) claddings of Type 1 probably be either a fluorinated polyolefin or a copolymer of olefins and fluoroolefins, which is known for the crystalline material nature and exhibits  $T_m$ .

Type 2 samples exhibited only  $T_g$  as a consequence of might be similar kinds of polymers of the core and cladding, having the transition in the same temperature region. This result indicates that Type 2 claddings are most likely of amorphous in material nature. Additionally, the FTIR analysis reveals (see Section 8.1.3) that Type 2 claddings resemble PMMA and therefore single  $T_g$  can be expected from them.

Nevertheless, all bare POF samples displayed  $T_g$  of about 119 °C and  $T_m$  of three of them was of about 137 °C (Table 8-1).

Samples of only the core displayed single transition temperature i.e.  $T_g$  and it was found to be of about 118 °C, which is almost the same as obtained for bare POF samples. This result verifies the fact that the obtained  $T_g$  of bare POFs samples should be  $T_g$  of the core. However, for both the samples it was found higher compared to the literature value (about 105 °C for atactic PMMA) and the experimentally found value (Table 8-1) for the bulk PMMA sample S6. It indicates that PMMA of the core in the POF could be having either a different structural configuration (syndio- or iso- tactic) or molecularly orientated.

In the case of POFs, the structural configuration may not be the major source influencing the optical properties. The higher the amorphous nature of the polymer (the core) the lower is the optical loss (scattering loss) [3,4,15,25,36,37]. Syndio- and iso- tactic natures of the polymer are known to exhibit higher degrees of crystallinity, which can result in more optical loss due to scattering. Therefore polymers with these configurations are less preferred. But the other fact, the molecular orientation, which

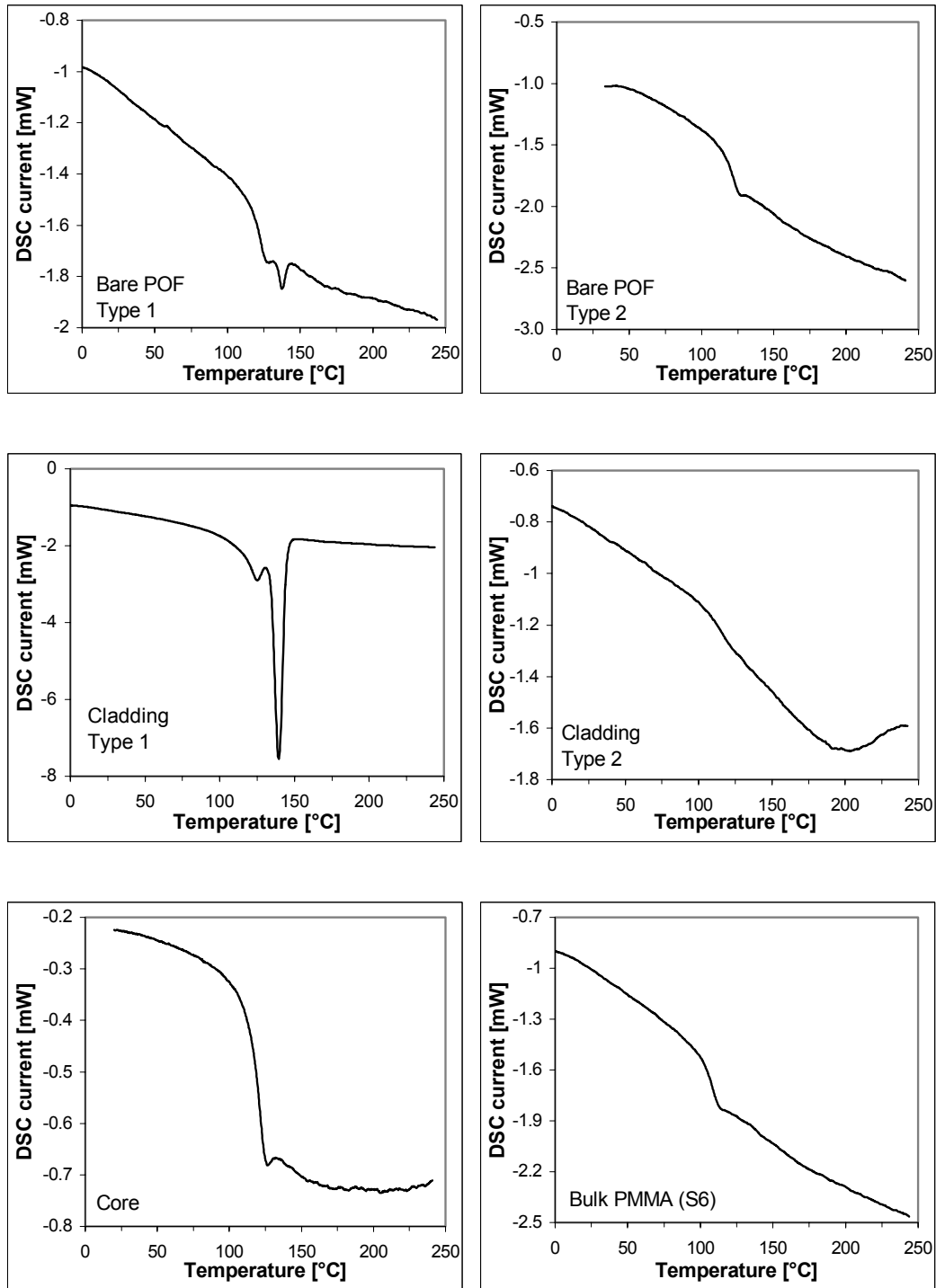


**Figure 8.1:** DSC second heating curves for bare POFs, claddings, core and bulk PMMA (S6).

is reported to occur in the core during the fiber drawing process, could result in an increase of  $T_g$  of the polymer and also the scattering loss due to the orientation birefringence [48,49]. Additionally, heating/cooling conditions that employ during the fiber drawing process can result in the formation of different crystallite structures, which have influences on  $T_g$  of the polymer [82]. Therefore, the molecular orientation seemed to be the main cause for the obtained large  $T_g$  of POF and core samples.

Two melting temperatures ( $T_m$ ) in the range from 124 °C to 137 °C were found for three cladding samples (S1, S3 and S4; Type 1) (see Fig. 8.1). This could be a result of either different crystallites (e.g.: different size) present in the polymer or a (block) copolymer nature or a blend of two kinds of polymer of the cladding material. The other cladding samples (S2 and S5; Type 2) exhibited only  $T_g$  and it was of about 112 °C. It is little lower than the value obtained for core (only) samples may be an indication of the similar material nature of the cladding and the core (PMMA). The FTIR results reveal a molecular similarity of these claddings with PMMA and it is discussed in more detail in the later section.

From the DSC findings the followings can be claimed:

- $T_g$  of different POF samples was measured and compared with individual counter parts (the core and cladding) and their typical DSC curves are shown in Fig. 8.1.
- $T_g$  of all bare POF and core samples lies in the same region and it was higher than that of the bulk PMMA sample.
- Regardless of claddings materials all bare POF samples showed almost similar  $T_g$ , which indicates less influence of the cladding.
- Either different crystallites or two different kinds of polymers should be responsible for the obtained two melting temperatures of cladding samples.

### 8.1.2 Molecular weights by GPC

Experimentally found values of the molecular weights and polydispersity (PD) are tabulated in Table 8-1. These values are corresponding to the core of POF samples except the sample S5 because its cladding and core were both dissolved in the solvent (THF) used for the experiments. The core of POFs possessed the molecular weight ( $M_w$ ) in the range from  $1.07 \cdot 10^5$  to  $1.12 \cdot 10^5$  g mol<sup>-1</sup>.

A comparison of the molecular weights of different cores (PMMA) of POFs may infer that PMMA as a POF core should possess  $M_w$  in the order of  $10^5 \text{ g mol}^{-1}$  and PD of about 1.8.

### 8.1.3 Chemical compositions analysis by FTIR

FTIR transmission spectra of the core of S1, S2, S3, S4 and S5 samples displayed almost the same characteristic bands of PMMA, an additional evidence for the PMMA core.

In contrast to the similar PMMA core, POF samples differed by cladding materials as evidenced by ATR-FTIR. The cladding material of samples S1, S3, and S4 was found to be similar in their chemical structure and their spectra are as shown in Fig. 8.2. However, these claddings differed from the cladding material of the sample S2, its spectrum is as displayed in Fig. 8.3. The cladding material of the sample S5 varied from the other cladding materials, its spectrum is as shown in Fig. 8.4. For the comparison, the bulk PMMA sample (S6) transmission spectrum is provided in Fig. 8.5. The absorption bands of this PMMA were found almost in the same wavenumber regions as established IR data of PMMA in the literature [83].

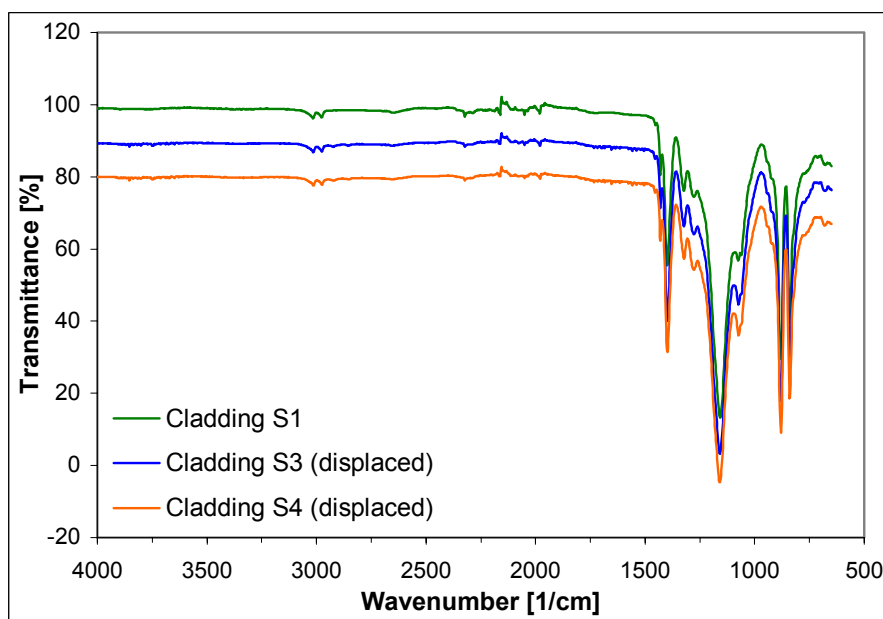


**Figure 8.2:** ATR-FTIR spectra of claddings S1, S3 and S4.

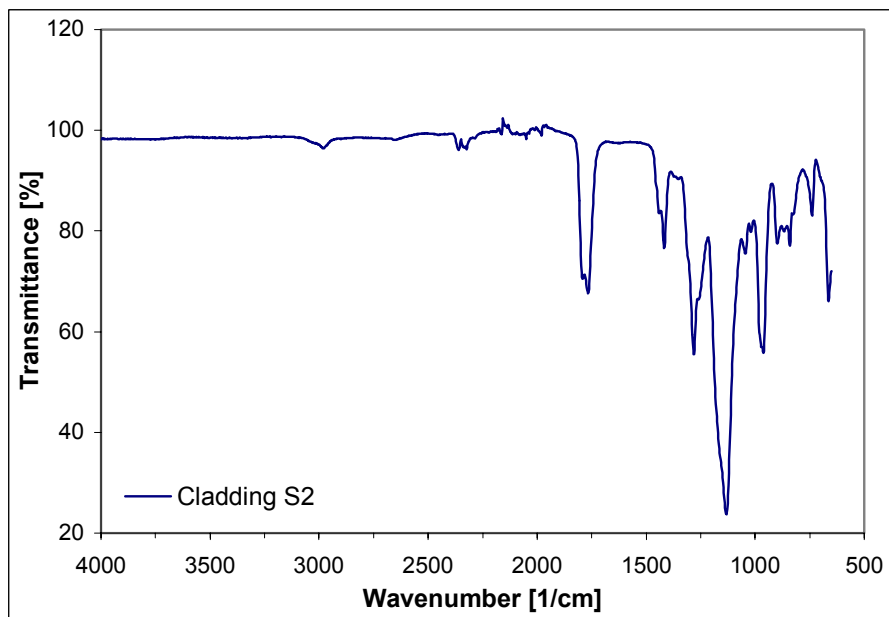


**Figure 8.3:** ATR-FTIR spectrum of the cladding S2.

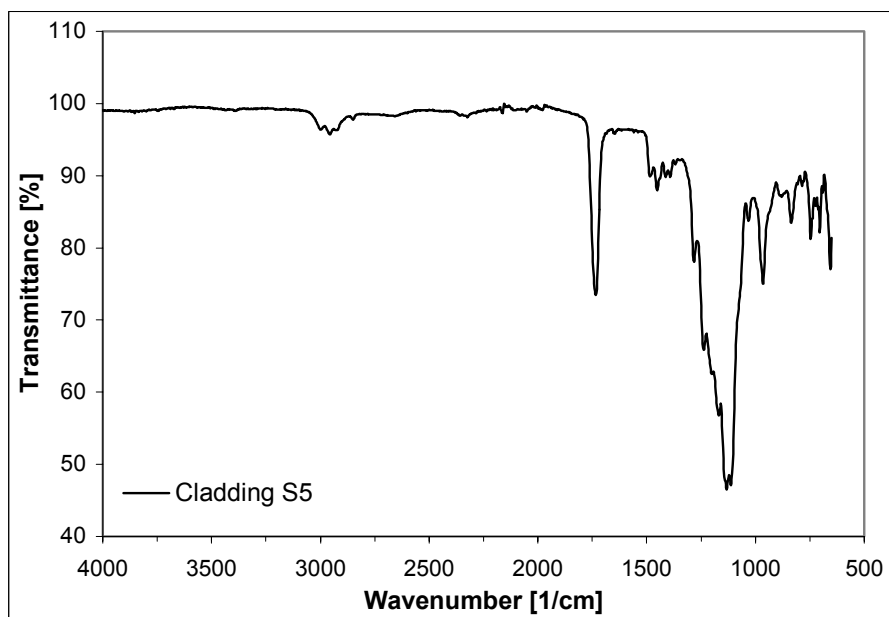


**Figure 8.4:** ATR-FTIR spectrum of the cladding S5.

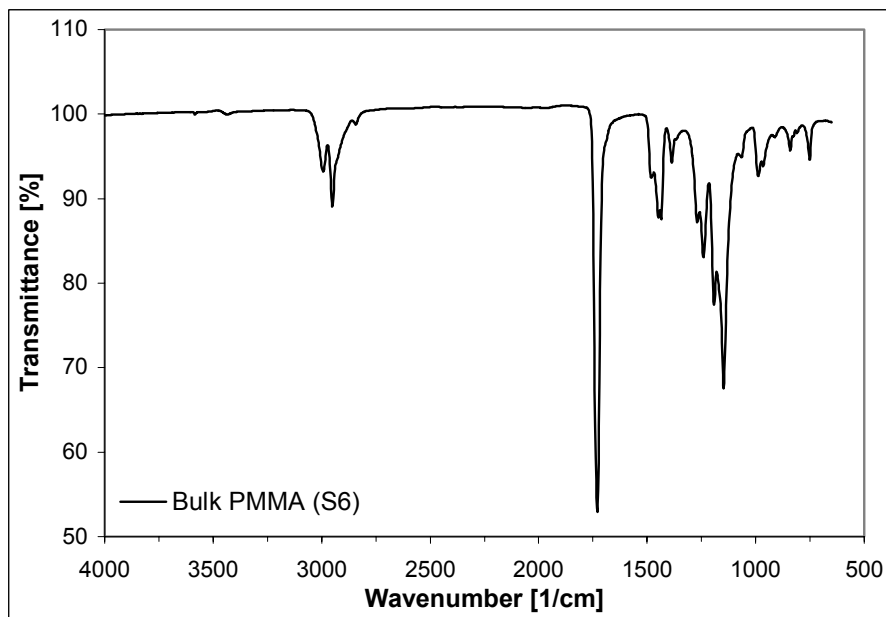


**Figure 8.5:** FTIR spectrum of the bulk PMMA (S6).

Spectra of claddings S1, S3 and S4 show strong absorption bands in the region between  $1100\text{ cm}^{-1}$  and  $1400\text{ cm}^{-1}$ , which strongly evidence vibrations absorption of C–F bonds in the polymer chain. This direct interpretation is made with the information that claddings are fluoropolymers as disclosed by suppliers. Very small absorption bands in the region between  $2970\text{ cm}^{-1}$  and  $3015\text{ cm}^{-1}$  reveal the presence of a few C–H groups. Two strong absorption bands in the lower wavenumber area between  $835\text{ cm}^{-1}$  and  $880\text{ cm}^{-1}$  indicate could be the deformation vibrations absorption of C–H (Fig. 8.2).

From these results it can be claimed that the cladding material of samples S1, S3 and S4 might be either a fluorinated polyolefin (polyfluoroolefin) or a copolymer of olefins and fluorinated olefins or could be a blend of polyolefins and fluorinated polyolefins. However, the most probable composition is a copolymer of fluoroolefins since some reports have disclosed the possible applications of this type as claddings of POFs (see Section 3.3.2). Between S1, S3 and S4 claddings there can be differences in chemical compositions, which could not be detected with FTIR.

**Table 8-2:** Comparison of vibrations absorption bands (the units are in  $\text{cm}^{-1}$ ) of S2 and S5 with PMMA [83].  $\nu$  and  $\delta$  represents the stretching and bending vibrations, respectively. Subscripts 's' and 'a' represents the symmetric and asymmetric vibrations, respectively.

Vibration	PMMA [83]	Cladding S2 ( $\pm 1 \text{ cm}^{-1}$ )	Cladding S5 ( $\pm 1 \text{ cm}^{-1}$ )
$\nu(\text{C}=\text{O})$	1734	1789, 1766	1734
$\delta(\text{CH}_2)$	1485	1443	1485
$\delta_a(\text{CH})$ of $\alpha\text{-CH}_3$	1448	Not compared	1450
$\delta_s(\text{CH})$ of $\text{OCH}_3$	1436	1418	1431 (shoulder)
$\delta_s(\text{CH})$ of $\alpha\text{-CH}_3$	1387	Not compared	1415, 1392
$\nu_s(\text{C}-\text{C}-\text{O})$	1273, 1242	1281, 1260 (shoulder)	1279, 1237
$\nu_a(\text{C}-\text{O}-\text{C})$	1193, 1147	1131 (broad)	1164, doublet 1131 and 1019
$\nu(\text{C}-\text{C})$	1063	1044	1030
$\text{OCH}_3$ rock	989	Overlapped at 963 (broad)	965
$\alpha\text{-CH}_3$ rock	966	Not compared	May be overlapped at 965
$\text{CH}_2$ rock	843	842	834
$\nu_a(\text{C}-\text{C})$	754	740	747

The spectrum of the sample S2 resembles that of PMMA however a shift in the position of main absorption bands was observed and compared with the available IR data of PMMA (see Table 8-2). As it can be noticed from Fig. 8.3 and Table 8-2 the sample S2 showed a significant shift in the position of the  $-\text{C}=\text{O}$  absorption band to higher wavenumbers (doublet;  $1789 \text{ cm}^{-1}$  and  $1766 \text{ cm}^{-1}$ ) and  $-\text{CH}_2$ ,  $-\text{OCH}_3$  and  $-\text{C}-\text{O}-\text{C}-$  (broad) absorption bands to lower wavenumbers ( $1443 \text{ cm}^{-1}$ ,  $1415 \text{ cm}^{-1}$  and  $1131 \text{ cm}^{-1}$  respectively) in comparison to the same of PMMA (see Table 8-2). These results strongly suggest effects of the fluorination environment in the polymer chain. Similar effects can also be seen with other bands, but it was difficult to assign these to an exact nature of the molecular groups since the extent and the site of fluorination were not known. However, some reports have disclosed various fluorinated acrylate polymers for the use in as cladding materials of POFs but no FTIR spectral characterization can be found (see Section 3.3.2).

Nevertheless, the appearance of the  $-\text{C}=\text{O}$  band at the higher region ( $1789 \text{ cm}^{-1}$  and  $1766 \text{ cm}^{-1}$ ) strongly implies that fluorination is most probably at the  $-\text{OCH}_3$  group of

the polymer [84]. The broad and doublet of the  $\text{-C=O}$  band may also indicate could be a copolymer of fluoroacrylate and non-fluoroacrylate monomer. The absorption band of  $\alpha\text{-R}$  ( $\text{CH}_3$ ) was not compared due to lack of spectral information however it is possible that  $\text{-R}$  can be either  $\text{CH}_3$  or H or F [34]. The broad absorption band of  $\text{-C-O-C-}$  in the lower region  $1131\text{ cm}^{-1}$  reveals a overlap of C-F vibrations. The fluorination at  $\text{-OCH}_3$  is most probably the substitution of hydrogen by fluorine atoms but also could be the substitution by a linear fluorinated alkyl chain.

With these findings it can be claimed that the cladding of S2 should be an poly(fluoroalkyl acrylate) (PFA).

The spectrum of S5 cladding shows more similarity in contrast to that of S2 with the spectrum of PMMA (see Fig.8.4 and 8.5, and Table 8-2). However, a shift in the position of absorption bands due to fluorination was observed. The main absorption bands were compared and presented in Table 8-2. The broad and small absorption bands in the region between  $1060\text{ cm}^{-1}$  and  $1300\text{ cm}^{-1}$  show a big influence of C-F groups. The comparison of absorption bands with that of PMMA evidences the fluorination is most likely be at the  $\text{-OCH}_3$  group of PMMA (see Table 8-2). Because no shift in the position of the  $\text{-C=O}$  band compared to that of PMMA was observed, the fluorination might be the substitution of hydrogen atoms by a linear fluorinated alkyl chain [85].

The results support that the cladding S5 should be a poly(fluoroalkyl methacrylate) (PFMA) but the extent of fluorination was found difficult to assign. It is also possible that a copolymer or a blend of non-fluoroacrylate and fluoroacrylate polymers could be the material of the cladding.

Although these findings give an overview of most likely chemical compositions of claddings, the exact composition elucidation is very complicated since each manufacturer/researcher use their own formulation to achieve better optical properties (see Section 3.3.2 for details of cladding materials).

## 8.2 Climatic exposure of POF cables

The optical transmission stability of two POF cables S1 and S2, which are exposed to a climate of 92 °C / 95 % relative humidity (RH), is investigated. The possible causes for the loss of optical transmission due to climatic exposure are researched by several means.

The chemiluminescence (CL) technique is applied to investigate the thermo-oxidative degradation/stability of the unexposed and exposed samples. FTIR, TG, GPC and UV/visible transmittance measurements are carried out to investigate climatic exposure effects on POFs.

### 8.2.1 Online optical transmission measurements

The results of multiplexer measured optical transmission data of POF cables (S1 and S2) are presented in Fig. 8.6. It is the average value of the three wavelengths (see Section 7.3.1) transmission data, which were acquired as a function of time during the exposure to the climate 92 °C / 95 %RH.

The transmission values (%) also can be expressed in dB/km, which is presented in Table 7-4 and it can serve as a reference table.

The results clearly evidence a difference in the optical transmission stability between the two POFs although they possessed the same core material PMMA. The sample S2 exhibited higher optical stability than that of the sample S1. Moreover, the transmission loss behavior displayed by these samples was dissimilar from each other as can be perceived from Fig. 8.6.

Within about 50 hours of the exposure, the optical transmission of both the POFs decreased by a certain extent (about 6 %) and during this reduction they exhibited similar behavior. These observations are similar to the findings by Daum et al., who have investigated the reliability of different PMMA based POFs [3,54]. They have proposed the initial reduction of the transmission to initial fluctuation of humidity in the POF. Schartel et al. have proposed it to chemical changes mainly by oxidation of low molecular weight species in the fiber core [51,52]. However, the initial reduction of the transmission observed in the present case is attributed mainly to physical changes (like softening of the polymer by mainly water molecules, for details of such

processes see Section 8.3.1) and minor to chemical changes. A similar exposure experiment (92 °C / 95 %RH) to bare POF samples (S3, S4 and S5) resulted in a large initial reduction of the transmission (see Section 8.3.1), which shows large physical influences of both temperature and humidity on the optical transmission stability of POFs. Furthermore, CL experiments to bare POF samples (bare POF samples from POF cables, and bare POF samples of S3, S4 and S5) indicate the presence of either low molecular weight species or may be chemisorbed water, which cause chemical changes by oxidation (see Section 6.3.1). Therefore, the observed reduction of the transmission can be due to overlap of physical and chemical changes of POFs.

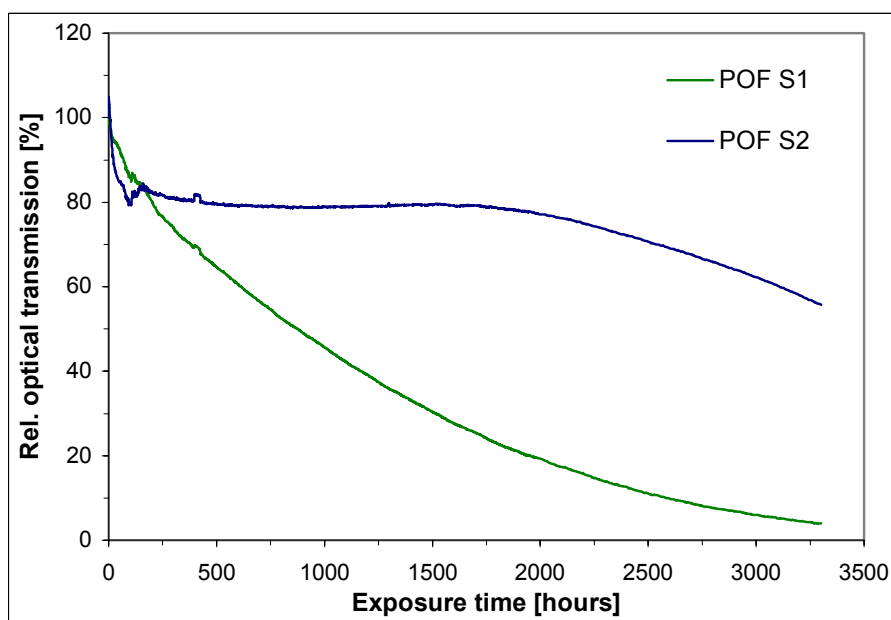


**Figure 8.6:** *Optical transmission (averaged over three wavelengths) through POF cables S1 and S2, measured as a function of time during the exposure to the climate 92 °C / 95 %RH.*

After the small transmission reduction at the start of the exposure, the behavior of transmission loss exhibited by both POFs was different as can be seen in Fig. 8.6. Both exhibited a continuous decrease of the transmission but the sample S1 showed higher time dependency than sample S2. At some point of initial stages, the sample S2 displayed a reversible increase and decrease of the transmission to a certain extent and then a very slow decrease. While the sample S1 demonstrated a continuous fast decrease with the exposure time. The variation in the transmission of the sample S2 is

assigned to mainly additional physical changes, as chemical reactions alone would show a monotonic decrease of the transmission. Physical changes are most likely due to the presence of humidity, and the extent of reversible transmission change could depend on the materials properties of core, cladding and jacket. However, from the position of the slow decrease of the transmission registered by the sample S2 and the continuous decrease by the sample S1, the changes are attributed mainly to the oxidative degradation of the polymer brought by the thermal energy. The results of CL, FTIR, TG, UV/visible transmittance and GPC experiments demonstrate the occurrence of degradation in the exposed samples, which might be the major cause for the observed transmission loss of POFs.

### **8.2.2 Investigation of thermo-oxidative stability/degradation using CL**

Exposures/aging of polymers results in changes of both chemical and physical properties through undesired irreversible aging processes, which are related to oxidation (see Chapter 5). The aging or exposure of polymers in presence of climatic parameters (e.g.: temperature, and temperature and humidity), without UV exposure, is thermo-oxidative in nature, which also is the case for CL and hence its results can be directly used to assess their stability.

The utility of conventional methods such as FTIR coupled with TG, and DSC is limited by their lacking sensitivity to monitor the thermo-oxidative degradation of polymers. In contrary, the CL technique has been known for many years for monitoring the thermal oxidation in many organic compounds and organic polymers [65-76]. The basic auto-oxidation scheme for polymers is discussed in more detail in Chapter 5 and 6. The CL emission in first approximation is proportional to the oxidation reaction rate, higher emission meaning lower thermo-oxidative stability of the sample under investigation and vice-versa. Therefore, it gives more straightforward evaluation of the residual stabilization of the polymer than the other techniques. Since the development of single photon counting technique, CL has been demonstrated to be a powerful tool to investigate the thermo-oxidative stability of many commodity and engineering polymeric materials, especially polyolefins [66-76] and polyamides [69,75,86]. Recently, it has been successfully extended to study the thermo-oxidative degradation behavior of optical polymers such as PMMA (POFs)

[51,52] and conjugated polymers [87]. These investigations have centered on modeling of the oxidation behavior at a specified temperature range.

Bare POF and cladding samples (S1 and S2) both were investigated for their thermo-oxidative stability using CL in the temperature range 107 °C (380 K) to 177 °C (450 K). The applied temperature program was as presented along with CL curves shown in subsequent paragraphs. Both the samples exhibited CL with no induction period (see Section 5.2.1) in the selected temperature range. Because the investigated samples maintained the same form and a constant initial weight, the results are comparable and reliable. With bare POF samples (S3 and S4) it is modeled that the total CL emission of the bare POF (core and cladding) is the contribution from both the core and cladding (see Section 8.3.2).

#### **8.2.2.1 Initial peak and plateau behavior**

Both the unexposed bare POF and cladding samples exhibited an initial peak and subsequent plateau CL emission behavior, which is shown in Fig. 8.7 for the bare POF S1 and S2.

The observed peak and plateau CL emission behavior are similar to the findings of previous studies (but the sampling technique is different from the present case), showing the consistency of the CL method [51,52,87]. The initial peak behavior observed in both the samples can be proposed to an extent of the consumption of low molecular weight species such as monomer could present in the polymer matrix reacting with oxygen and/or to the reaction of a fraction of the polymer accessible in excess with already available or trapped oxygen in the polymer matrix. Therefore, the reaction may be independent of diffusion of surrounding oxygen. Some previous studies on CL of the cellulose polymer have reported such an initial peak, which is mainly due to the chemisorbed water in the polymer [88]. If the second interpretation is adopted the observed initial peak would represent an amount of the absorbed humidity in the present samples (bare POF and cladding).

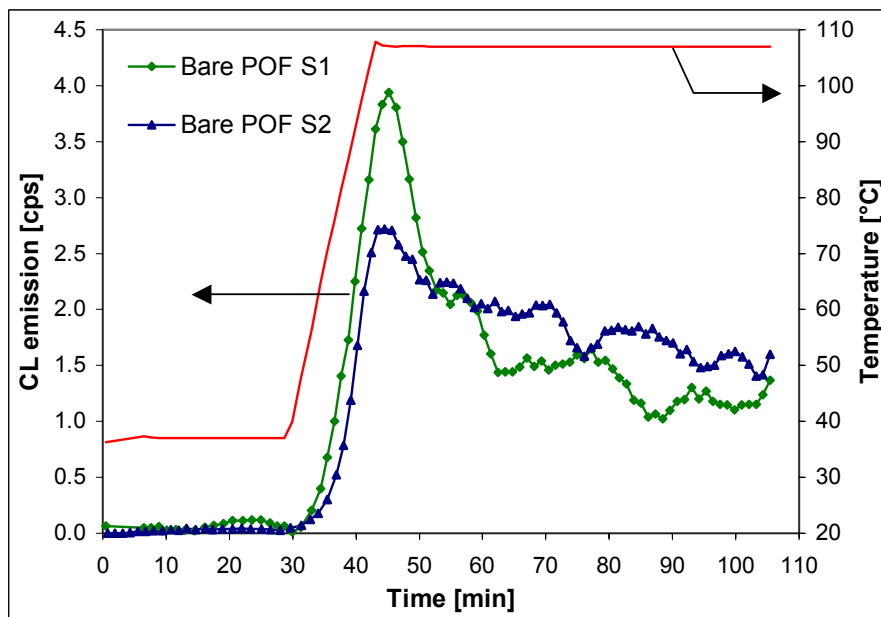


**Figure 8.7:** *CL emission curves (peak and plateau behavior) (at 107 °C) of the unexposed bare POF samples S1 and S2.*

Out of the pathways of both the interpretations (monomer or chemisorbed water) it can be concluded that a small difference in the CL emission between the samples would be due to their processing and conditioning histories. Furthermore, either of monomer or chemisorbed water presence in the polymer, the CL peak emission could be connected with the observed initial reduction of the transmission. However, the extent of which may not be precise to relate to the height of the peak, as the relation does not hold (almost a constant reduction of the transmission was observed in both the POFs but they displayed a difference in their CL peak height). Of course, CL measurements and exposure conditions were different. Nevertheless, this fact was verified with S3, S4 and S5 bare POF samples, where the extent of initial transmission loss and the peak height did not relate each other (see Section 8.3.2). Nonetheless, the initial CL peak was, indeed an clear indication of chemical changes by oxidation, but the resultant loss of transmission might be overlapped with the transmission loss caused by physical changes, which are the main sources imposed by climatic parameters.

The CL plateau emission behavior (see Fig. 8.8, for instance) can be regarded as the availability of polymer molecules to the thermally activated oxidation given by a

constant rate of the diffusion of oxygen taking place in the sample. The plateau CL emission can be proposed to be a constant loss of the transmission induced by purely oxidative degradation with an additional transmission loss due to physical changes in the POF.

As stated earlier both the samples, bare POF and cladding (unexposed), exhibited the peak and plateau behavior. Therefore, it was not clear whether the observed initial loss of transmission was due to chemical changes (oxidative degradation) in the cladding or core. Nevertheless, CL and other experiments to the exposed samples show higher degradation of the cladding than of the core (see subsequent Sections), indicating the transmission loss of POFs arising mainly due to changes in the claddings properties.

#### 8.2.2.2 CL of the unexposed bare POFs

CL curves for the unexposed bare POF sample S1 and S2 are shown in Fig. 8.8. Although both the samples consisted the PMMA core, their thermo-oxidative stability was not the same. Both exhibited similar CL characteristics with respect to the initial peak and plateau emission behavior. At the initial temperature step (107 °C), the CL peak emission from the sample S2 was more or less equal to that of the sample S1.

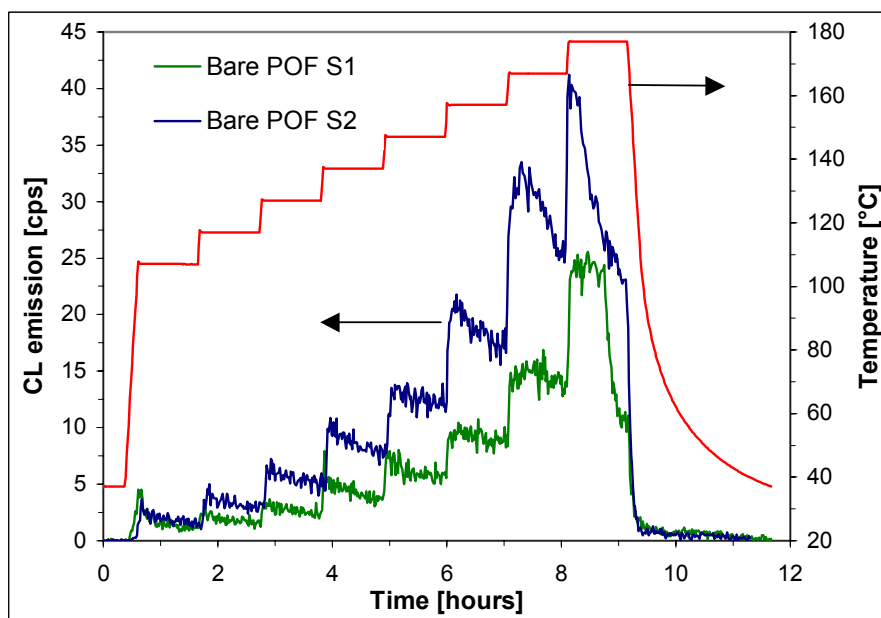


**Figure 8.8:** CL curves for the unexposed bare POFs S1 and S2.

However, in the subsequent temperature steps, the CL emission from the sample S2 was greater than that of the sample S1 but both showed an increasing trend. Possible explanations are an increase of the mobility of polymer chains that are spatially separated and an increase of the diffusion or dissolution of oxygen in the polymer matrix. The polymer chain mobility could be additionally increased by the plasticization of degradation products. At higher temperatures (167 °C and 177 °C), the plateau behavior of the sample S2 marked to vanish but attained a broad maximum and then decreased. This may not be surprising because higher temperatures could result in the accumulation of reaction products that can quench the excited state carbonyls, as a result a fast decay of the CL emission may be expected [89]. The decay rate of CL could be enhanced by the mobility of both excited state molecules and oxidation products due to melting of the polymer. The influence of temperature on the decay rate can be seen in Fig. 8.8 in the fact that the CL emission shows a less pronounced declining slope at 167 °C than at 177 °C. However, detail investigations may be necessary to confirm these characteristics and will be done in a future research.

The CL emission from the sample S2 was higher and appeared to be less thermo-oxidative stable as compared to the sample S1. The difference in the CL emission between the two samples is attributed predominantly due to a difference in the chemical compositions of claddings because the core of both was PMMA. Additional influencing factors could be polymer formulation, manufacturing and fiber drawing conditions. But these differences are believed to be less significant because POFs producers can use a similar formulation and drawing conditions in order to achieve the transparency as high as possible. Therefore, the claddings should be responsible for the observed differences in CL of bare POF samples. So it is believed that the CL behavior of the bare POF is almost a model of cladding CL, except for lower emission from the former mainly owing to the sample physical structure. CL of the claddings is discussed in the subsequent section. It is known that the core (950  $\mu\text{m}$  to 980  $\mu\text{m}$  in diameter) is a major part of the bare POF. But oxidation (using new oxygen from the surrounding) of the bare POF sample starts first at the cladding and then spread to the core because the cladding (50  $\mu\text{m}$  to 20  $\mu\text{m}$  in thickness) acts like a protective layer. Therefore, it is possible to assume that the thermo-oxidative degradation of the core should mainly depend on the diffusion constant of the cladding polymer. The

subsequent experimental results indeed provide the importance of the cladding in thermo-oxidative degradation of POFs.

### 8.2.2.3 CL of the unexposed claddings

CL of the unexposed claddings (sample S1 and S2) is presented in Fig. 8.9. For both samples similar CL characteristics (initial peak and plateau behavior) were observed as in the bare POFs CL. The CL emission from the cladding sample S2 was higher showing lower thermo-oxidative stability compared to the cladding sample S1. These results are consistent with CL of bare POF samples. Hence, it can be a qualitative but clear indication that the CL emission from the bare POF results mainly from the cladding. This finding is in good agreement with the results obtained for samples S3 and S4 discussed in Section 8.3.2.

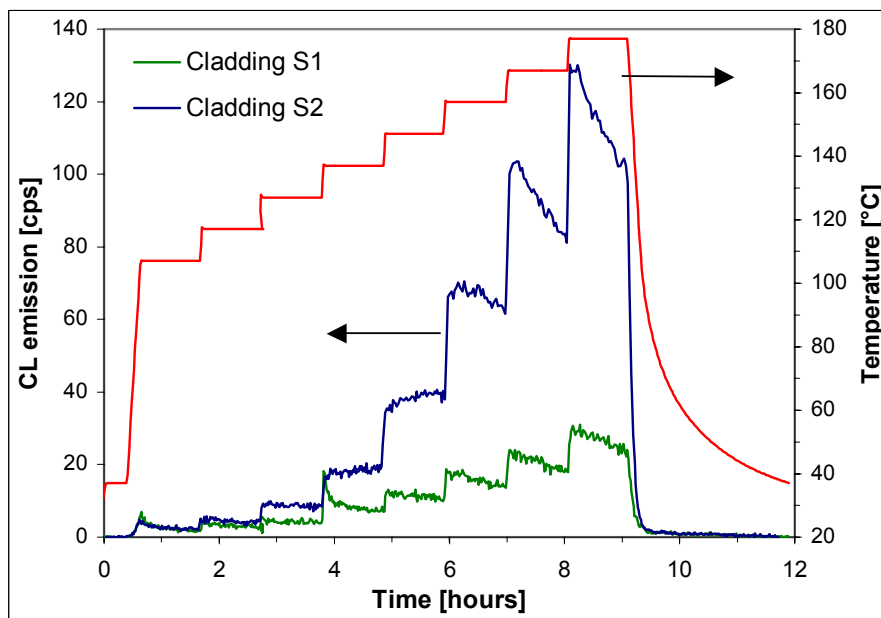


**Figure 8.9:** CL curves for the unexposed claddings S1 and S2.

By comparing the CL emission from the corresponding unexposed bare POF and cladding samples, it is seen that the total CL emission from the cladding was all the time higher than that of the bare POF. A few factors are involved regardless of chemical structural differences between the core and cladding. Physical factors that strongly appear could be the hollow cylindrical structure (see Section 7.4) and the sample thickness. Due to the hollow structure, the diffusion of oxygen through a

nearly doubled surface appears to be more efficient to the sample. Owing to a smaller thickness of the cladding compared to the core, the dissolution of oxygen in the sample can be promoted by the efficient diffusion. Therefore, these effects could largely influence the degradation rate of the cladding. The influences seem to be more effective at higher temperatures (see Fig. 8.9), imply an increase in the diffusion rate and polymer chain mobility.

While the physical structural factors are believed to be the major cause for the higher CL emission from the cladding than that of the bare POF, the difference in the claddings CL emission can mainly be arisen from chemical structural differences. Using Fourier transform infrared (FTIR) spectroscopy both the unexposed claddings were characterized (see Section 8.1.3). It was found that probably the cladding S1 be either a highly fluorinated polyolefin or a copolymer of fluoroolefins, and the cladding S2 be a poly(fluoroalkyl acrylate) (PFA). The CL results reveal that PFA polymer is more prone to the oxidative degradation than that of a highly fluorinated polyolefin or a copolymer of fluoroolefins. A primary reason can be the availability of C–H groups (numbers or -I inductive effect, groups in  $\alpha$ -position) for the subsequent oxidation process. Additionally, other factors such as chain branching and functional groups could influence the CL emission and its behavior as well [66-69,75,86]. Therefore, different claddings materials oxidize to a different level as a consequence uneven stability of POFs in spite of identical core material. Accordingly, the extent of oxidative degradation of the core mainly depends on the material type as well as thickness of the cladding, which is the starting component in the oxidative degradation of the bare POF.

#### **8.2.2.4 CL of the exposed bare POFs and claddings**

The exposed bare POFs as well as claddings S1 and S2 exhibited some changes due to climatic exposure, Fig. 8.10 and 8.11 show their CL curves. The fact that the CL emission was much higher for the exposed samples than for the unexposed samples clearly indicates the thermo-oxidative degradation occurrence as a result of climatic exposure.

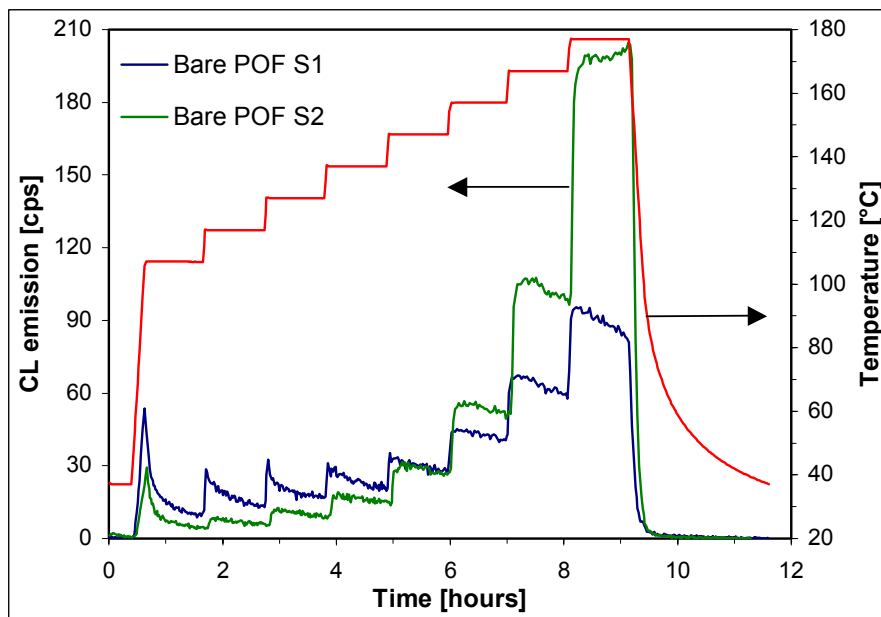


**Figure 8.10:** *CL curves for the exposed bare POFs S1 and S2.*

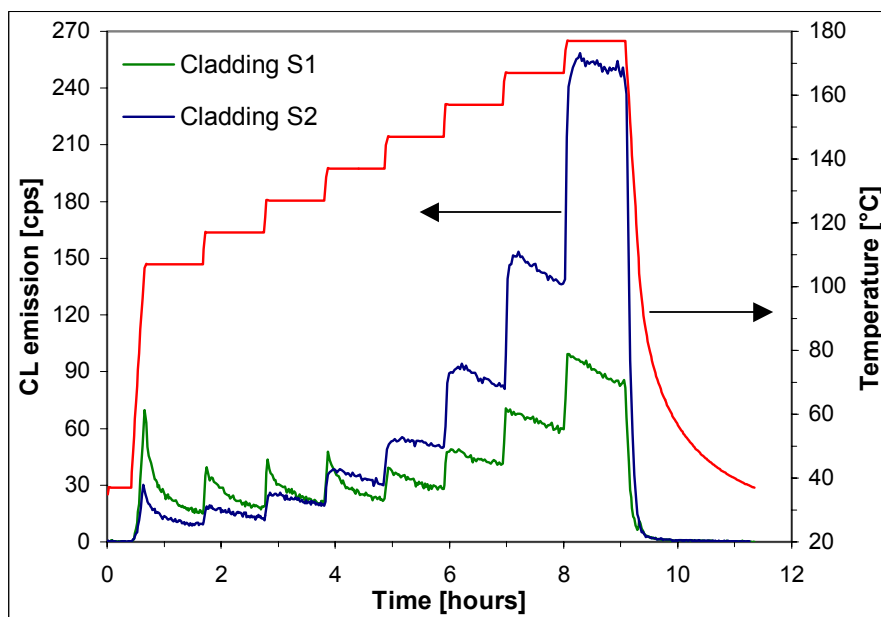


**Figure 8.11:** *CL curves for the exposed claddings S1 and S2.*

CL of the exposed bare POF as well as cladding samples S1 and S2 show an intense sharp peak at 107 °C (Peak 1). However, CL of the same of the sample S1 demonstrates continuous peaks (Peak 2, 3 and 4; at 117 °C, 127 °C, and 137 °C) in

contrast to plateaus of the sample S2 for the subsequent temperature levels. The CL peak behavior clearly implies the consumption of one of the reacting components of the oxidation process. This could well be one or more of the involved low molecular weight degradation products formed as a result of thermo-oxidative degradation by climatic exposure. The peaks (Peak 1, 2, 3 and 4) could be interpreted as being due to differences in oxidizing ability of various degradation products. The CL emission of Peak 1 may be independent of the diffusion of external oxygen because in the polymer matrix the use-up of dissolved oxygen itself may still be adequate to generate peroxy radicals. To study the potential influence of external oxygen, CL of the exposed bare POF samples under nitrogen atmosphere instead of oxygen was investigated. The re-occurrence of Peak 1 was found though with lower emission and with much lower emission of all the subsequent peaks and plateaus. It shows a requirement of enough oxygen, which is necessary to oxidize the reactants completely. Yet, the exposed samples peak behavior can be a direct indication of readily oxidizable degradation products and therefore the peak intensity can be a measure of an extent of the consumption of these products, at a particular temperature.

A comparison of the CL emission from the exposed sample S1 and S2 indicates lower emission exhibited by the sample S2 at the initial four temperature steps (see Fig. 8.10 and 8.11). However, in the subsequent temperature steps, sample S2 exhibited much higher CL emission than sample S1. This suggests that CL of the exposed sample S2 might involve one or more degradation mechanisms. Thermal aging of polymers may lead to both degradation and crosslinking of polymer molecules [55,58]. In view of this fact, the intensity of Peak 1 of the sample S2 could be related to the decomposition of degradation products that are accumulated only at the surface of the sample. Consequently, the first three plateaus (see Fig. 8.10 and 8.11) can be proposed mainly to thermally activated oxidation of the available part of the crosslinked polymer and their emission rate is controlled by the diffusion rate of oxygen. Since crosslinking reduces the diffusion rate, the emission for the first three plateaus was lower compared to that of sample S1. However, it was still higher than that of the corresponding unexposed samples, which is probably due to the decomposition of the remaining surface accumulated degradation products having uneven thermo-oxidative stability. For the subsequent temperature levels (from 147 °C to 177 °C), the CL emission from the sample S2 started increasing and was

much higher than that of the sample S1. It can be due to the decomposition of dissolved degradation products in the polymer matrix and an increase rate of oxygen diffusion. Owing to high temperature the polymer can melt. As a result the plasticization can positively influence the diffusion rate. Therefore, oxygen diffuses efficiently into the polymer matrix and is utilized in the decomposition of dissolved degradation products and an available part of the polymer as well.

From the above discussion of the results, the interpretation of the CL data so far can be summarized as follows:

Up to the temperature level of 140 °C, the sample S1 exhibited four consecutive peaks with higher emission and the following plateaus with lower emission as compared to that of the sample S2. The fact that the CL emission from the exposed samples is higher than for the corresponding unexposed samples clearly indicates the thermo-oxidative degradation as a result of climatic exposure. The CL peaks imply mainly the consumption of available readily oxidizable active species that newly become available upon first reaching a new, higher temperature level. The following plateaus emission derived mainly from oxidation of an available part of the polymer under stationary conditions and governed by the individual diffusion rate of (new) oxygen into the material. As compared to a variation (first decrease and then increase) of the CL emission from the exposed sample S2, sample S1 displayed no such significant variation. Therefore, it suggests that thermo-oxidative degradation could be the main result of climatic exposure of the sample S1 in contrast to both thermo-oxidative degradation and crosslinking of the sample S2.

A comparison of the total CL emission (integration of CL over time) shows a higher value for the sample S2 than for the sample S1. It clearly evidences higher thermo-oxidative degradation of the sample S2 as compared to the sample S1, as a result of climatic exposure. This outcome is congruent to CL of the corresponding unexposed samples that sample S2 exhibited lower thermo-oxidative stability than the sample S1.

Of course, other factors such as humidity and POF jacket were not taken into account in the present CL experiments to the unexposed samples, although the actual climatic exposure test was conducted in the presence of them. These factors could influence CL of the bare POF and cladding as well. Not much data are available in regard to influences of these factors. However, a previous investigation has found a decrease of

the CL emission as a result of water saturation in POFs [52]. But it was not observed in the present CL experiments. Nevertheless, it is known that water absorption in polymers such as acrylate polymers can lead to both physical and chemical changes (see Section 5.3). Polymer swelling can be a physical change for instance. No considerable swelling was observed in both the POF samples. Water can be chemically interacted via hydrogen bonding and can very slowly hydrolyze the functional groups such as esters. These changes can be expected in the present samples more particularly in the cladding type of the sample S2 (PFA) and in the PMMA core and only to a much lower extent in the cladding type of sample S1 (an highly fluorinated polyolefin or a copolymer of fluoroolefins). Such chemical changes could lead to a complex thermo-oxidative degradation resulting in formation of complex products as a result of climatic exposure. Accordingly, an exact qualitative explanation for CL of the exposed samples may be very complicated. Nonetheless, CL experiments show that absorption of water in POFs could result in an increase rate of the thermo-oxidative degradation.

Another factor, the jacket of POF samples, could influence the rate of thermal oxidation by controlling the rate of diffusion of oxygen and water vapor as well during the exposure. Therefore, a variation of materials of the jacket could alter the diffusion rate. Polyamide 12 (PA 12) and polyethylene (PE) were the jacket materials of the POF sample S1 and S2 respectively (see Section 7.1.1). It is known that oxygen diffusion coefficient of PE is higher than that of PA12 whereas the water absorption by PA 12 is higher compared to PE [90]. Though, this information gives a broad idea about a potential influence of the jacket but real effects of these factors on degradation of the bare POF might be complicated. This, for the present case, could be explained by two ways. First of all, the jacket itself might experience thermo-oxidative degradation due to exposure as a result its original diffusion properties will be varied to some extent. Secondly, effects of the jacket were difficult to assign due to different materials of the cladding although with the identical core. Nevertheless, investigation of real causes of individual factors humidity and jacket remains as a challenging work in a future research.

As it is investigated in the CL analysis of the unexposed samples that CL of the bare POF (see Fig. 8.8) was almost a replica of CL of the cladding (see Fig. 8.9).

Extremely consistent qualitative results were obtained with CL of the exposed samples (see Fig. 8.10 and 8.11). Therefore, the CL results strongly support the conclusion that climatic exposure of POF cables leads to thermo-oxidative degradation of the cladding predominantly and only to a minor degree the core. FTIR, TG, DSC and UV/visible transmittance measurements sustain the above made conclusion.

### 8.2.3 Investigation of climatic exposure influences using FTIR

FTIR is one of the known methods to analyze molecular changes in polymers exposed to various physical and chemical parameters, an example for studying degradation of PMMA can be found in [91]. Combining attenuation total reflection (ATR) technique with FTIR allows studying the surface of polymer films and fibers etc. [83].

The exposed and unexposed core and cladding samples were analyzed by FTIR method for molecular changes due to climatic exposure. Spectra of the corresponding samples are displayed below.

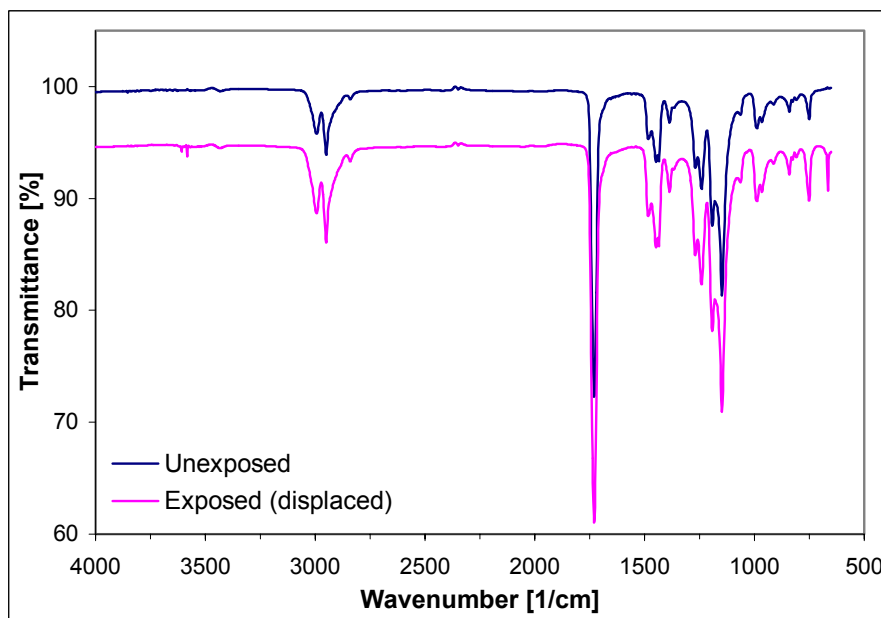


**Figure 8.12:** FTIR spectra of the unexposed and exposed core S2.

Almost no qualitative spectral changes were found with the exposed core polymer spectra (Fig. 8.12) of both S1 and S2 compared to the unexposed one's (see example for the sample S2 in Fig. 8.12) which shows that of no significant degradation of the

core as a result of climatic exposure could be detected by FTIR. One possible reason may be too small detection efficiency of this method. Consequently, small chemical changes occur in the core particularly at its surface cannot be recognized.

In contrast to the not existing spectral changes of the core, the exposed cladding samples displayed some significant changes, especially the cladding sample S2. The spectrum of the exposed cladding S1 shows only a few little changes that are small absorption bands in the region between  $1660\text{ cm}^{-1}$  and  $1630\text{ cm}^{-1}$  and a small band at around  $3355\text{ cm}^{-1}$  (see Fig. 8.13). These bands can be clearly visible in the difference IR transmittance spectrum (exposed minus unexposed) shown in Fig. 8.15. The former can be assigned to stretching vibrations of C=C bonds and the later to stretching vibrations absorption of peroxide OH groups. These results may indicate that formation of double bonds by elimination of hydrogen atoms and the oxidative degradation could be the major processes as a result of climatic exposure. Additionally, it is known that irradiation of fluoropolymers (e.g.: polyvinylidene fluoride, PVDF) leads to both elimination and oxidative degradation [92]. Nasef et al. have verified these types of results by using FTIR method [93]. Nevertheless, since the observed changes detected by FTIR were very small, it is risky to make a conclusion for the occurrence of degradation as well as for a degradation mechanism. However, CL, TG and UV/visible transmittance measurements indeed prove the occurrence of degradation and therefore it can be stated that climatic exposure resulted in degradation of the cladding S1.

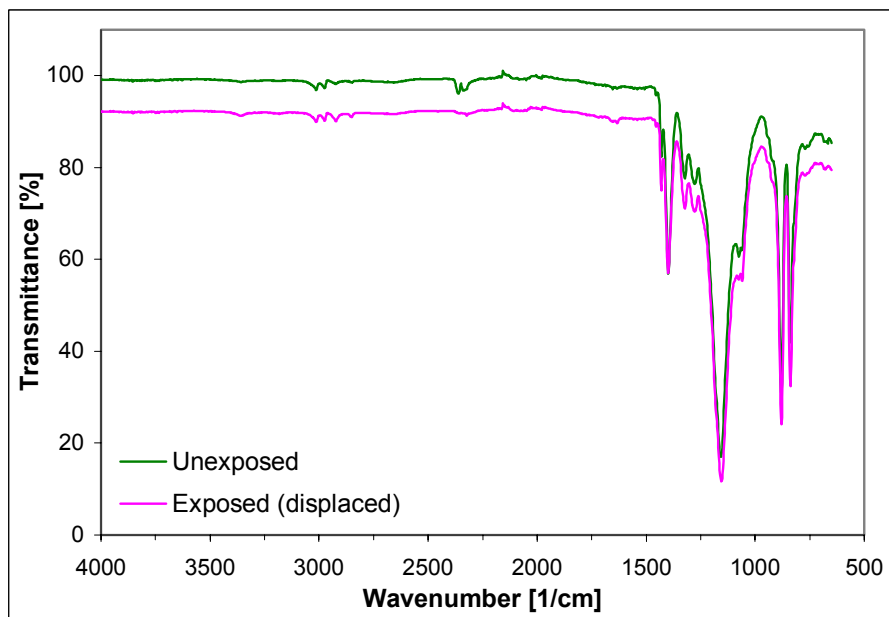


**Figure 8.13:** ATR-FTIR spectra of the unexposed and exposed cladding S1.

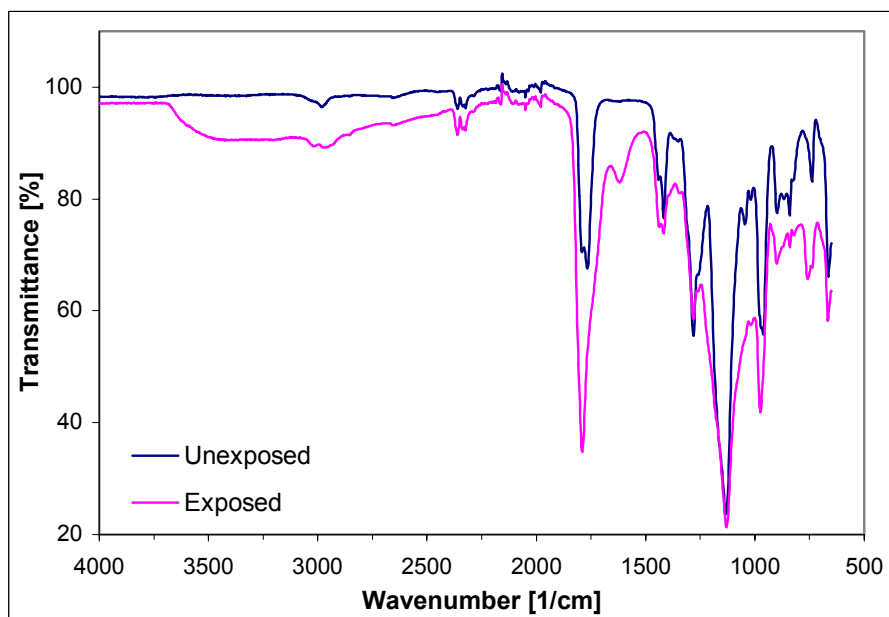


**Figure 8.14:** ATR-FTIR spectra of the unexposed and exposed cladding S2.

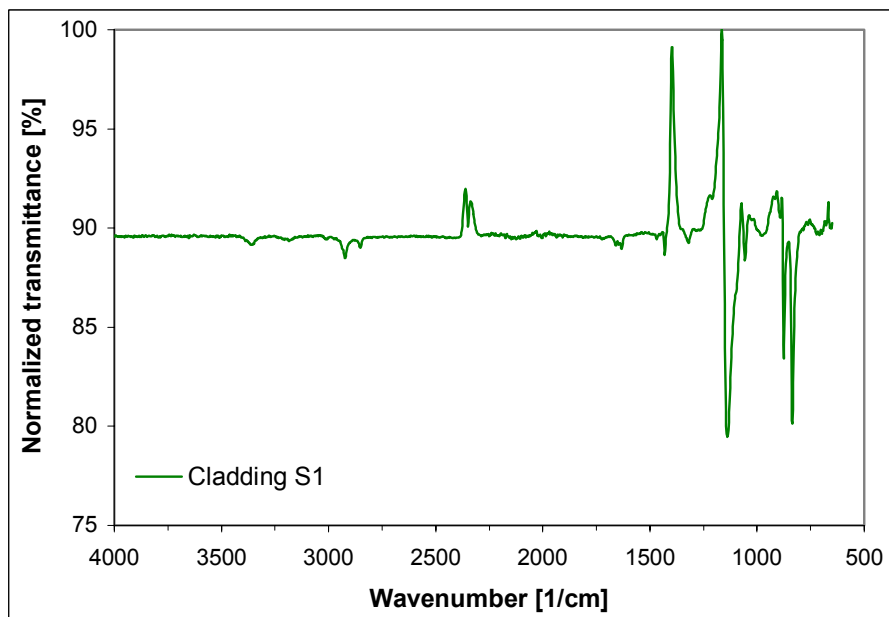


**Figure 8.15:** *Difference IR spectrum (ATR-FTIR spectrum of the exposed minus unexposed cladding S1).*

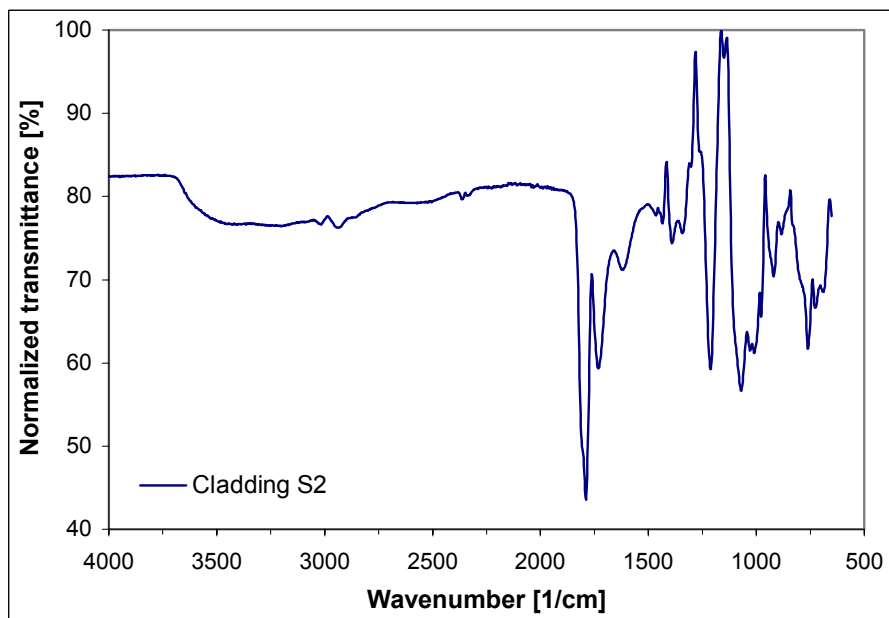


**Figure 8.16:** *Difference IR spectrum (ATR-FTIR spectrum of the exposed minus unexposed cladding S2).*

The following are the observed changes in the spectrum of the exposed cladding S2 compared to the unexposed one (see Fig. 8.14):

- A decrease of the transmittance or an increase of the absorbance. This result clearly evidences degradation of polymer molecules as a result of exposure.
- The formation of new absorption bands between  $3680\text{ cm}^{-1}$  to  $2500\text{ cm}^{-1}$  (very broad) and  $1620\text{ cm}^{-1}$  (broad). These consequences reflect the effects of water absorption and oxidative degradation of the polymer. The first absorption band can be assigned to O–H stretching vibration absorption and the second to the deformation vibration absorption. The absorption bands between  $3680\text{ cm}^{-1}$  and  $2500\text{ cm}^{-1}$  show a large variety of O–H groups, which might have been formed in the cladding S2. Bulk water has polymeric hydrogen bonds, which shows a broad absorption band in the region between  $3700\text{ cm}^{-1}$  and  $3000\text{ cm}^{-1}$  and this water is referred as clustered water [63,84]. Therefore, in the present exposed cladding sample, presence of clustered water can be expected as a result of exposure to high humid condition. This type of water is physically absorbed without molecular bonding to polymer molecules. The presence of the functional groups such as ester in polymers can react with water molecules, and the resultant products (e.g.: carboxylic acids) have characteristic O–H absorption bands in the region generally between  $3560\text{ cm}^{-1}$  and  $3500\text{ cm}^{-1}$  [84]. Consequently, a partial hydrolysis of the polymer of the cladding S2 can be expected since it includes saponifiable ester groups. Hence, the reaction products can have an absorption in the region of carboxylic acids. In general, intra and inter hydrogen bondings of water molecules to polymer chains determine the position of the O–H absorption band [84] and therefore a variety molecular bonding of water to polymer chains appeared to form in the cladding polymer. Additionally, the thermo-oxidative degradation is known to form peroxides which have the absorption in the region between  $3400\text{ cm}^{-1}$  and  $3500\text{ cm}^{-1}$  and therefore it can be expected in the exposed cladding. The products of thermal-oxidation of PMMA are reported to be conjugated molecules [42,52,55,77,94], which normally have characteristic absorption at about  $1600\text{ cm}^{-1}$  belonging to vibrational absorption of double bonds. Since the present cladding polymer was characterized to be a PFA (see Section 8.1.3), such products may be expected here, too. Therefore the observed broad absorption band near  $1620\text{ cm}^{-1}$  can be expected due to vibrations of double bonds but might be overlapped with O–H band.

- Shift in the position of absorption bands. Broadening and transforming from doublet to singlet at  $1790\text{ cm}^{-1}$  and broadening and a slight shift at  $1130\text{ cm}^{-1}$ , reflects the effects of degradation of the polymer. The cladding S2 was characterized to be a PFA (see Section 8.1.3) but its composition could be also a copolymer of different fluoroalkyl acrylates or fluoroalkyl acrylate and methyl methacrylate [36-39]. Therefore, for the later composition degradation seems to result in formation of two separate ester groups one with fluorine atoms and another without. This result can be clearly seen with the difference IR spectrum (Fig 8.16) as it shows two absorption bands at  $1789\text{ cm}^{-1}$  and  $1732\text{ cm}^{-1}$ , which can be assigned to fluorinated C=O and to the normal ester C=O vibrations, respectively. Furthermore, the broad absorption band at  $1130\text{ cm}^{-1}$  becomes doublet ( $1163\text{ cm}^{-1}$  and  $1135\text{ cm}^{-1}$ ), as it can be clearly seen with the difference spectrum, may support the presence of two types of C–O–C groups may correspond to fluorine and no fluorine substituted acrylate groups. However, elucidation of a degradation mechanism is very complicated because climatic exposure was conducted in the presence of both humidity and temperature, which can have combination effects on POFs. Nevertheless, climatic exposure results in formation of variety of degradation products having different structures as evidenced by FTIR.
- A few changes in the region between  $900\text{ cm}^{-1}$  and  $660\text{ cm}^{-1}$ . These changes are most likely being due to the formation of new molecules (of types stated above) with different structures having characteristics deformation vibrations.

## 8.2.4 Investigation of climatic exposure effects using supplementary methods

### 8.2.4.1 Thermal stability analysis by thermogravimetry (TG)

Thermogravimetry is a technique in which the mass loss of a polymer sample is monitored as a function of temperature and time, during the exposure to a controlled temperature program under a defined atmosphere like  $\text{N}_2$  or He or  $\text{O}_2$ . The rate of mass change can determine the decomposition rate, and characteristic decomposition temperatures can be identified. Additionally, it is useful to monitor the thermal stability, composition (e.g.: moisture, solvent, additives and fillers), dehydration,

decarboxylation, oxidation or decomposition. This permits investigating possible material changes due to external influences like climatic exposures.

Numerous research reports on thermal degradation or stability of polymers analyzed by TG method can be found in the literature [94,95]. Kashiwagi et al. [94] and Manning et al [95] have extensively studied the thermal degradation mechanism of PMMA using TG method.

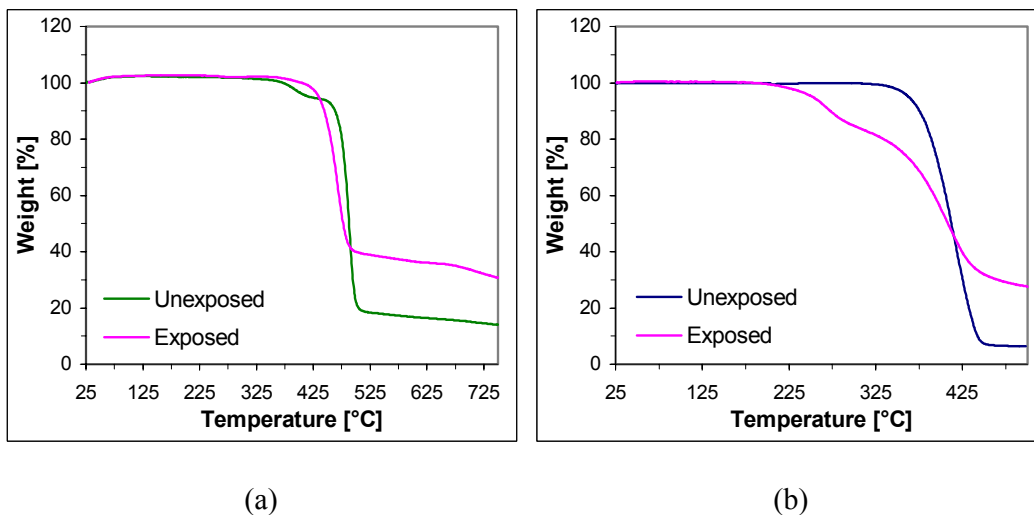


**Figure 8.17:** Thermograms recorded under nitrogen atmosphere at a heating rate of  $10 \text{ K min}^{-1}$  for: (a) cladding S1 and (b) cladding S2.

The thermal stability of the unexposed and exposed cladding samples was analyzed by TG method. Thermograms were recorded of the form weight loss as function temperature and time under nitrogen and air atmosphere. TG curves of both cladding samples are provided in Fig. 8.17. Both the exposed cladding samples S1 and S2 exhibited differences in their thermal stability compared to corresponding unexposed one's.

The unexposed cladding S1 exhibited two-step degradation behavior. The first small degradation step was at around  $395 \text{ }^\circ\text{C}$  and the second and main degradation step at around  $488 \text{ }^\circ\text{C}$ . The first step could be cost by any kind of impurities (e.g.: additives), and the following step may correspond to the main chain scission degradation of the polymer [94]. The corresponding exposed cladding sample displayed a single step degradation behavior and the main decomposition was at about  $470 \text{ }^\circ\text{C}$  (see Fig. 8.17a). These results show the lower stability of the exposed sample probably induced

by degradation products and their decomposition was followed by the main chain scission of the polymer. Furthermore, the residue of both the samples was compared and found that the exposed sample exhibited a higher residue (about 30 %) compared to the unexposed sample (about 14 %). From the experience, the residue contains carbon black and inorganic fillers. The higher the carbon black the more unsaturated is the organic polymer. This outcome strongly indicates the presence of unsaturated and/or crosslinked products of the polymer formed as a result of climatic exposure. However, it was verified by measurements under air and the result is the residue of the exposed sample was found about 4 % and that of the unexposed sample was about 9 % implying the decomposition of both unsaturated and crosslinked products in the presence of oxygen produces volatiles. Therefore, it can be said that climatic exposure leads to the formation of more unsaturated and/or crosslinked products owing to degradation.

The unexposed cladding S2 exhibited single-step degradation behavior and the main degradation step was at about 418 °C, which is the main chain scission of the polymer. The corresponding exposed sample marked two-step degradation behavior and main degradation steps were at about 270 °C and 410 °C respectively (see Fig. 8.17b). These results evidence lower stability of the exposed samples due to climatic exposure. The first step clearly evidences volatilization of low molecular weight species formed as degradation products. The second decomposition step follows the first step by main chain scission. Additionally, the residue of the exposed cladding sample was found to be higher (about 28 %) than that of the unexposed sample (about 6 %). The difference in the residue of the samples, here too, strongly implies that unsaturated and/or crosslinked products were formed in the exposed cladding owing to degradation as a result of climatic exposure. It was supported by the results of measurements conducted under air, where the residue of both the exposed and unexposed samples was found to be nearly 0 %. These outcomes may suggest the same conclusion as drawn to the sample S1.

It can be compared from Fig. 8.17a and 8.17b that both the exposed cladding samples S1 and S2 exhibit lower thermal stability compared to the unexposed one's. Nevertheless, sample S2 appeared to be more affected by the climatic exposure as it shows two clear degradation steps compared to a single degradation step by the

cladding S1. This result is in accordance with the lower stability of the cladding S2 compared to S1, resulting from CL measurements. One of the main reasons could be a different chemical nature of polymers that S2 cladding was characterized to be a fluorinated acrylate polymer and S1 to be a polyfluoroolefin (see Section 8.1.3). It also could be one of the main reasons for the less thermal stability of the unexposed cladding S2 compared to S1.

#### **8.2.4.2 UV/visible transmittance**

As can be seen by bare eyes, the exposed samples, especially the sample S2, appeared yellowish in color in contrast to the colorless unexposed bare POF samples. It is thought to be mainly a change in the color of the core but separation of the cladding from the core using solution method (see Section 5.4) revealed a yellowish color of cladding samples. However, the UV/visible transmittance experiments clearly evidence more changes in the cladding as compared to the core (see Fig. 8.18 and 8.19). The exposed core samples exhibited only a minor change in the transmittance as a result of the climatic exposure (see Fig. 8.18a and 8.18b). Whereas the exposed cladding samples, particularly the sample S2, showed a big change in the transmittance (see Fig. 8.19a and 8.19b). This result directly supports higher degradation of the cladding than of the core as a result. Both cladding samples showed more changes in the region of UV and near visible. The cladding S2 showed a big drop in the transmittance in the region between 220 nm and 500 nm strongly suggesting this new absorption of light should be due to a variety of chromophores formed as a result of thermo-oxidative degradation. Overall, the UV/visible transmittance experiments data are strongly in accordance with the CL, FTIR and TG experimental results that climatic exposure of POF cables leads to more degradation of the cladding than the core.

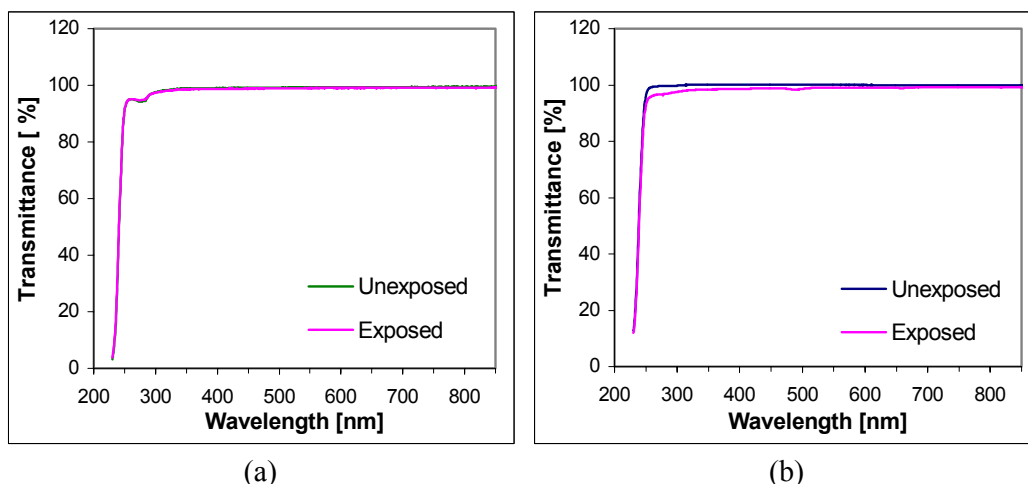


**Figure 8.18:** UV/visible transmittance spectra of the core: (a) sample S1 and (b) sample S2.

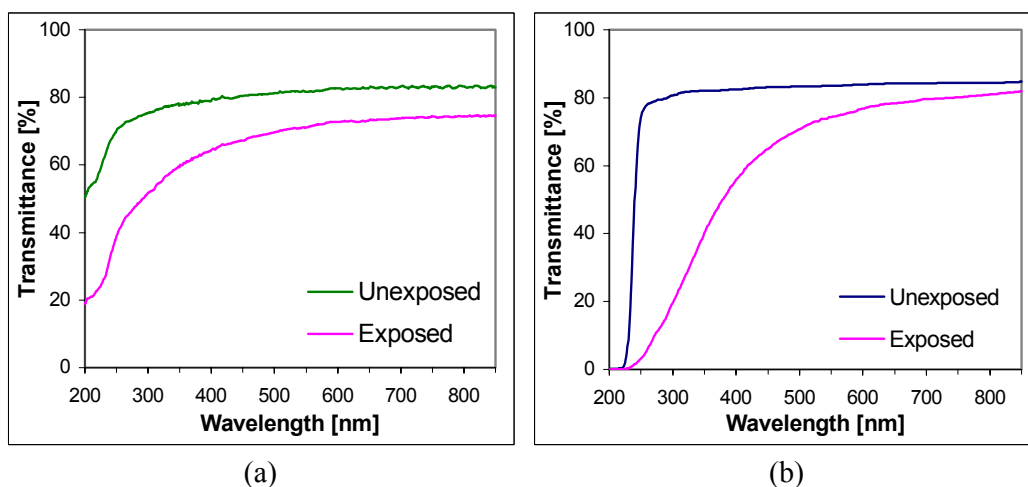


**Figure 8.19:** UV/visible transmittance spectra of the cladding: (a) sample S1 and (b) sample S2.

### 8.2.4.3 Molecular weight analysis

The occurrence of degradation in the polymer leads to changes in molecular weight distribution, which can be monitored using GPC technique. In this technique, the polymer solution is injected into the gel-phase column and different sizes of molecules are eluted as a function of time at constant temperature. It is one of the known techniques to monitor degradation by analyzing changes in molecular weights [55,58].

The exposed samples of the core were analyzed for the occurrence of degradation due to climatic exposure and the results were compared with the unexposed samples. It

was found that no considerable changes in the molecular weight distribution could be detected with GPC. This result additionally supports that the core of POF was less affected by climatic exposure.

### 8.2.5 Spectral transmission measurements

The optical transmission of the unexposed and exposed POF cables S1 and S2 was recorded in the wavelength range from 400 nm to 800 nm, using miniature spectrometer. Spectra are displayed in Fig. 8.20. The same of the exposed samples S1 and S2 was compared and spectra are provided in Fig. 8.20c.

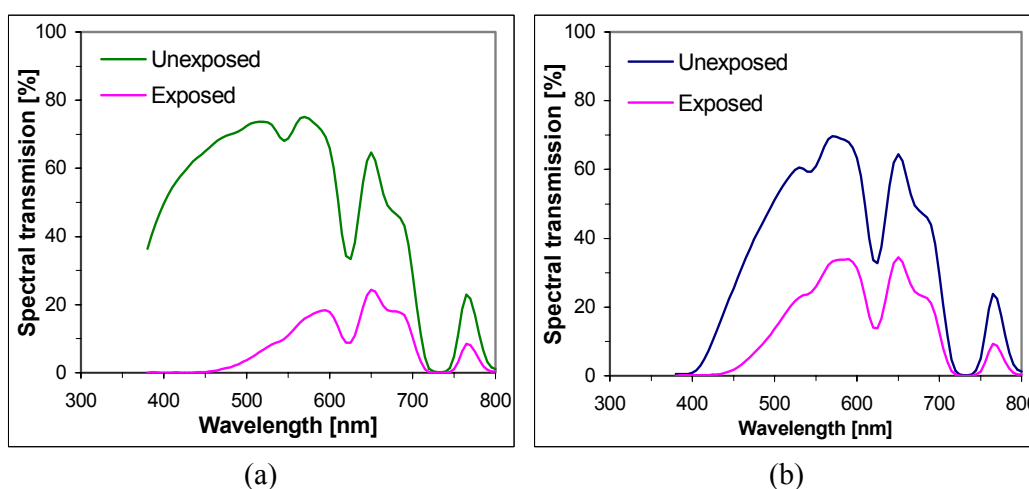


**Figure 8.20:** Spectral transmission of the unexposed and exposed POFs: (a) POF S1 and (b) POF S2.

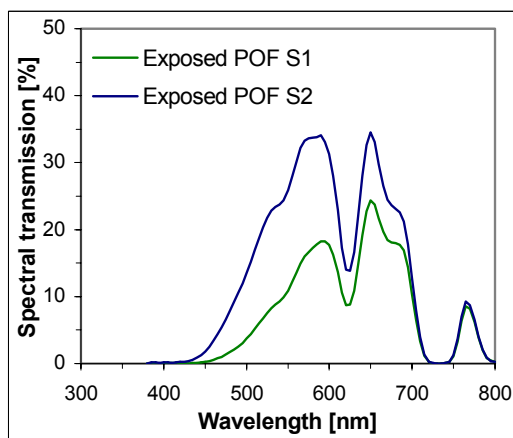


**Figure 8.20c:** Spectral transmission of the exposed POFs S1 and S2.

As it can be noticed from the transmission spectra (Fig. 8.20a and 8.20b) of both the unexposed samples that though both the samples consisted the same material PMMA, their spectral transmission is different in the wavelength range 400 nm to 600 nm. The

transmission of the POF S1 was found to be higher than that of the POF S2. These results suggest that could be different claddings of these POF samples are responsible for the observed difference in the transmission. In fact UV/visible transmittance measurements to the unexposed claddings samples (see Section 8.2.4.2) show a difference in transmittance characteristics as similar to the findings here. Therefore, different claddings could be one reason for the observed difference in the transmission characteristics of POFs S1 and S2. However, other factors such as formulation of polymers could lead to differences in the transmission characteristics of POFs.

A significant decrease in the transmission was found in both the exposed POF samples indicating climatic exposure effects. However, both showed a large decrease at the lower wavelength region, which could be an indication of a large absorption of light by chromophores that could form due to degradation as a result of climatic exposure. This large absorption could induce the absorption loss at higher wavelength regions according to Urbach's rule (see Section 4.2.2). A comparison of the transmission of the exposed POF samples (see Fig. 8.20c) shows more transmission loss in POF S1 than in POF S2 as found in the online transmission measurements.

Both the POFs displayed a transmission loss probably due to absorption of light could be in both the core and cladding. However, the chemical investigations strongly reveal that the cladding of POFs was affected more than the core by climatic exposure. Therefore, it is possible that the observed transmission loss in both the POFs could be due to more absorption of light in the cladding and less in the core. Nevertheless, the transmission loss can arise from different mechanisms owing to physical and chemical changes of both the core and cladding.

### **8.2.6 Optical transmission loss - possible explanation**

CL, FTIR, TG, UV/visible transmittance and GPC investigations show degradation mainly of the cladding and minor of the core as a result of climatic exposure. In view of the investigated results, it is proposed that the observed loss of optical transmission in POFs could be derived mainly from an increase in light absorption by degradation products of both the cladding and core and scattering of light owing to core-cladding boundary imperfections.

Takezewa et al. [42] have reported that aging of (crosslinked) PMMA based POFs at 150 °C results in thermo-oxidative degradation of the core and due to which a significant loss of transmission is observed. They have proposed that the loss of transmission in POFs is mainly due to an increase in light absorption by conjugated carbonyl compounds formed as degradation products.

It strongly agrees with our hypothesis that the loss of transmission most probably due to increase in light absorption by the core and cladding as well. However, according to the chemical analysis result, the core is less degraded than the cladding and therefore higher light absorption losses by the cladding are possible.

When light is guided through the fiber by total internal reflection at the border between the core and cladding a fraction of light goes into the cladding (so called the evanescent light, see Section 7.6.1), is transported a small distance (in the order of some wavelength units) in the cladding parallel to the fiber axis, and then goes into the core. If the border is disturbed, e.g.: by degradation, not only the evanescent light reaches the cladding but refracted light, too. So both can be absorbed in the cladding. As a result, the basic fiber optic phenomenon, the total internal reflection within the fiber, might be substantially reduced, causing a significant optical loss.

It is also possible that a large degradation of the cladding due to climatic exposure could lead a change of the refractive index ( $n$ ), which result in a variation of NA of the fiber (see also Section 8.3.1.1). This change of NA relates the optical transmission property of the POF. Therefore, it is likely that a loss of transmission could arise also from a variation of  $n$ .

Further on, degradation of the cladding also could lead to change in its adhesion strength, the extent of which may depend on its material. It is known in the POF technology that one of the main requirements for the cladding is good adhesion, as this significantly determines the functional property of the POF [5,36-40]. Therefore, an improper adhesion can lead to core-cladding boundary imperfections, too, causing scattering of light and resulting in an increase of the optical transmission loss. Accordingly, climatic exposure could be assumed to decrease the adhesion strength of the cladding of both the POF samples. Although the cladding sample S2 found to be more degraded than the cladding sample S1, their corresponding POFs exhibited contrary in optical transmission loss (POF S1 exhibited more transmission loss than

the POF S2, see Fig. 8.6). Therefore, it could be assumed that the adhesion strength of the cladding of sample S1 should be decreased to a larger extent than that of sample S2 because the core material of both was PMMA. It becomes obvious that mainly the material chemical nature determines the adhesion property of the cladding. However, the respective quantitative contributions of each source to the total transmission loss remain to be studied in a future research.

### **8.3 Climatic exposures of bare POFs**

The optical transmission stability of three bare POF (core with clad only) samples S3, S4 and S5 is investigated. They are exposed to the climates 92 °C / 95 %RH, 92 °C / 50 %RH, 50 °C / 95 %RH, 120 °C / low humidity, 110 °C / low humidity, 100 °C / low humidity and 90 °C / low humidity. Here the “low humidity” should be understood as a value of  $\ll 50$  %RH (dry heat condition). The possible causes for the loss of optical transmission due to climatic exposures are discussed.

The chemiluminescence (CL) technique is mainly applied to investigate the thermo-oxidative degradation/stability of the unexposed and exposed samples.

#### **8.3.1 Online optical transmission measurements**

##### **8.3.1.1 Exposure to temperature-humid climates**

The optical transmission loss behavior of bare POF samples S3, S4 and S5 exposed to the climates 92 °C / 95 %RH, 92 °C / 50 %RH and 50 °C / 95 %RH, was monitored by the multiplexer as a function of exposure time. The results presented in Fig. 8.21, 8.23 and 8.24, respectively, are the average values obtained at three wavelengths (550 nm, 590 nm and 650 nm).

The experiments clearly evidence a difference in the optical transmission stability between the three POFs although they consisted the same core material PMMA. The results also evidence strong influences of imposed humidity on the transmission stability of POFs.

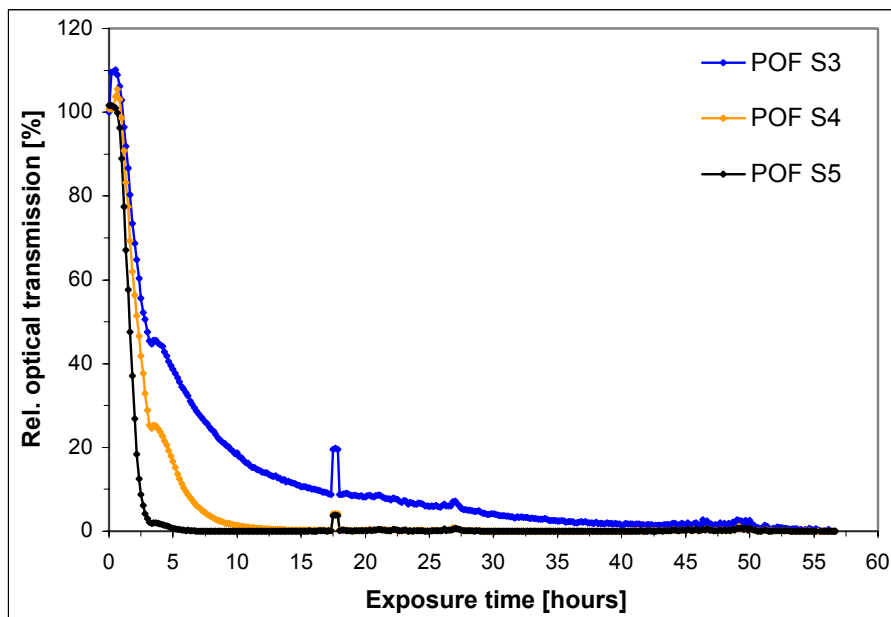


**Figure 8.21:** *Optical transmission (averaged over three wavelengths) through bare POF S3, S4 and S5, measured as a function of time during the exposure to the climate 92 °C / 95 %RH.*

All the three bare POFs exposed to the climate 92 °C / 95 %RH exhibited poor transmission stability in view of their long-term reliability as they reached < 1 % transmission within an exposure time of about 50 hours (see Fig. 8.21). The transmission peaks at the very start of the exposure may be related to structural relaxation of the polymer may improve the adhesion between the core and cladding [54] and the ones at about 17 hours to a malfunction of the measuring system. However, between the three POFs there is a marked difference in their transmission stability as each POF sample took its own duration in reaching 50 % and < 1 % transmission. The optical performance of the three POFs appeared to be similar up to 50 %, and it may be called as linear behavior. While the dissimilar optical performance in reaching < 1 % from the point of 50 % may be called as non-linear behavior. The exposure times for reaching 50 % transmission were 96 minutes, 127 minutes and 168 minutes, for reaching < 1 % transmission 5 hours, 12 hours and 60 hours in sample S5, S4 and S3 respectively. A similar separation in linear and non-linear transmission loss can also be observed from the results of the exposure of the same POFs to the climate 92 °C / 50 %RH (see Fig. 8.23). All these results indicate

that both imposed temperature-humid condition and POF material properties could influence the transmission stability of POFs.

In both the cases, the linear behavior and non-linear behavior, it seems that mainly the absorption of water (humidity) by POFs plays an important role in causing the transmission loss. As mentioned above the transmission of POFs reached nearly  $< 1\%$  in about 50 hours. But the same POFs exposed to  $100\text{ }^{\circ}\text{C}$  / low humidity and  $90\text{ }^{\circ}\text{C}$  / low humidity for more than 3000 hours exhibited a transmission loss of about  $65\%$  and  $20\%$ , respectively (see Fig. 8.26 and 8.27). Moreover, the exposure of POFs to  $92\text{ }^{\circ}\text{C}$  /  $50\%$ RH led to a transmission loss of about  $50\%$  at the end of about 3000 hours (see Fig. 8.23). These results could be the strong evidence for large influences of high humidity and nearly total transmission loss at  $92\text{ }^{\circ}\text{C}$  /  $95\%$ RH should be due to mainly the water absorption by POFs. It appears to be very much influenced by the imposed high temperature because the same POFs exposed to the climate  $50\text{ }^{\circ}\text{C}$  /  $95\%$ RH displayed a transmission loss of  $< 10\%$  at the end of 1500 hours (see Fig. 8.24).

Fig. 8.21 shows that an increase of water absorption in POFs decreases the optical transmission down to  $< 1\%$ . It can be thought that the core of POFs is mainly responsible for water absorption because it is thicker ( $\sim 980\text{ }\mu\text{m}$  in diameter) than the cladding ( $\sim 20\text{ }\mu\text{m}$  in thickness). The core material of the three POFs was the same i.e. PMMA, and water absorption or transportation in it occurs in a dual behavior as already discussed [61] (see Section 5.3.1). The presence of impurities such as micro voids and cracks in the core fiber depends on the fiber drawing history of POFs. To reduce the optical loss, POF producers may use precise drawing methods and drawing parameters to avoid the incorporation of impurities that could cause a large loss by scattering. Therefore, in general, the presence of impurities such as micro voids, cracks and dusts in the fiber will be neglectable small in number or even absent at the state of the delivery, which was confirmed for the present POFs S3, S4 and S5 (the length of tested fibers was about 13 m) by back scattering measurements with an optical time domain reflectometer (OTDR) [3]. It can be concluded that the water transportation into micro voids should be insignificant to induce the transmission to  $< 1\%$  in few hours at  $92\text{ }^{\circ}\text{C}$  /  $95\%$ RH.

Nevertheless, water transportation into the polymer matrix inducing the swelling of the polymer has a significant effect on the transmission stability of POFs. The swelling causes volume expansion of the polymer material, for instance, which may be reversible in nature and is related to phenomena of wetting (sorption) and drying (desorption). In the present case, too, a process of swelling in the sense that a systematic increase of the diameter was observed (at the stages of 50 % and nearly 100 % loss of transmission) in all the three POF samples. Table 8-3 provides the measured diameter of the POF samples. Yet, it appears to be irreversible because almost no decrease in the diameter was found after heating the samples under a dry condition and moreover they became brittle after bringing down to the room temperature-humid condition. Additionally, the increase in the diameter resulted in a significant contraction of the length of fibers. In view of this fact, the phenomenon of swelling may not be suitable to explain the observed irreversible increase of the diameter of POFs.

**Table 8-3:** Diameter of the unexposed and exposed (92 °C / 95 %RH) POF samples, measured by using a simple electronic screw gauge (Mitutoya).

Bare POF	Diameter [ $\mu\text{m}$ ] ( $\pm 5$ )		
	Before the exposure	At 50 % loss of transmission	At nearly 100 % loss of transmission
S3	1000	1030	1110
S4	1000	1041	1145
S5	1000	1090	1200

Nevertheless, it could be explained on the basis of water in polymers acting as a plasticizer accompanied by an increase in the thermal-coefficient of expansion and a reduction of the glass transition temperature ( $T_g$ ) [60,62]. Amorphous polymers including PMMA exhibit a known order of anisotropic thermal expansion. The anisotropic nature of expansion mainly depends on the polymer processing history (e.g.: extrusion, injection molding, compression and blow molding). In other words, polymers exhibit the anisotropic expansion when the orientation of polymer chains takes place [82]. Furthermore, the expansion co-efficient is believed to be lower in the direction of the orientation than in the direction perpendicular. These effects are related to the free volume theories of glassy polymers [60,62]. Such anisotropic behavior of polymers can also be expected in the fiber core material PMMA of the

present investigated POFs because the core of them exhibited a  $T_g$  of about 118 °C, which suggests the occurrence of the orientation of polymer chains. In the case of isotropic behavior a  $T_g$  of about 105 °C would be expected. Dugas et al. have studied the structural anomalies in PMMA core fibers and found an anisotropic nature of the core due to the orientation of polymer chains [48,49]. Therefore, in the present POF samples more expansion in the transversal direction than in the longitudinal direction can be predicted. The anisotropic behavior of expansion of polymers can be well seen when they are heated to their  $T_g$  and then cooled down. In the contemporary case of climatic exposure, the set temperature was only 92 °C, which is far below the observed  $T_g$  (of both core and POF samples). To cause the expansion in the duration of 50 hours (at which all POFs had lost nearly all the transmission) is far earlier than predicted by Dugas et al. [48,49]. Therefore the observed significant increase of the diameter and a contraction of the length of fiber samples should be due to plasticizing effects of water in the core of POFs. That means water in POFs reduced their  $T_g$  by increasing the chain mobility. As a result the expansion occurred in a faster rate than it would take when exposing to only 92 °C. Furthermore, the plasticizer effect seemed to be irreversible because the observed expansion (diameter and contraction of length) and brittle nature of the cooled samples is an indication of the occurrence of molecular disorder. The irreversible plasticizing effect of water in polymers may be referred as structural relaxation.

As already discussed, the poor stability of the three POFs is different for all of them. The sample S5 had reached < 1 % transmission much earlier (5 hours) than the other ones (12 and 60 hours). A possible explanation could be a difference in the cladding material. As found by FTIR, the cladding of sample S5 has to be a poly(fluoroalkyl methacrylate) (PFMA) and that of S3 and S4 be a polyfluoroolefin or a copolymer of olefin and fluoroolefin (see Section 8.1.3). It is well known that acrylate polymers are hydrophilic and fluoroolefin polymers are hydrophobic in nature. Therefore, it appears that the acrylate cladding of the sample S5 supported the process of water absorption by the core. Whereas the polyfluoroolefin type cladding of S3 and S4 acted as a barrier. Consequently a difference in the rate of water absorption and thereby a difference in the transmission loss rate between POFs can be expected. Therefore, it can be stated that the more polar is the cladding, the faster is the migration of water into the core. However, the observed difference in the transmission stability between

S3 and S4 may be due to a small difference either in chemical compositions of claddings or physical structural anomalies in the core.

In general, significances of water absorption or water transportation in polymers are changes in their both physical and chemical properties [60,62] (see Section 5.3). Therefore, causes for an early drop off of the transmission in POFs could be changes in both their physical and chemical properties. Most probable physical changes, for instance, that could occur in POFs are volume expansion and refractive index change. They induce inhomogeneities and/or imperfections, which are strongly responsible for the optical loss by any type of scattering in POFs. Chemical changes, for instance, that could occur in POFs are interaction of water with the functional groups and molecular degradation. They are most probably responsible for the loss due to absorption of light (see Chapter 4).

In the present exposure case, physical changes appeared to be the main sources for the total loss of transmission of POFs because chemical changes that could be detected by using chemiluminescence (CL), FTIR and GPC were insignificant to cause to the total loss of transmission in a duration of < 50 hours. It is most likely that physical changes are the main sources, e.g.: the observed increase in the diameter and contraction of the fiber length resulting in total in a volume expansion. A change of the fiber diameter, mainly related to change in the core diameter, is one of the important parameters that influence the optical transmission [3,5,]. Therefore, the observed increase of the diameter may be of one the main sources for the total loss of transmission in POFs. The volume expansion (see above) of oriented glassy polymers generally means a return of the molecular disorder from the ordered structure. Certainly such process can be expected in the core fiber of the present samples, too, which induces structural anomalies or inhomogeneities within the core fiber resulting in a decrease of the transmission due to scattering of light.

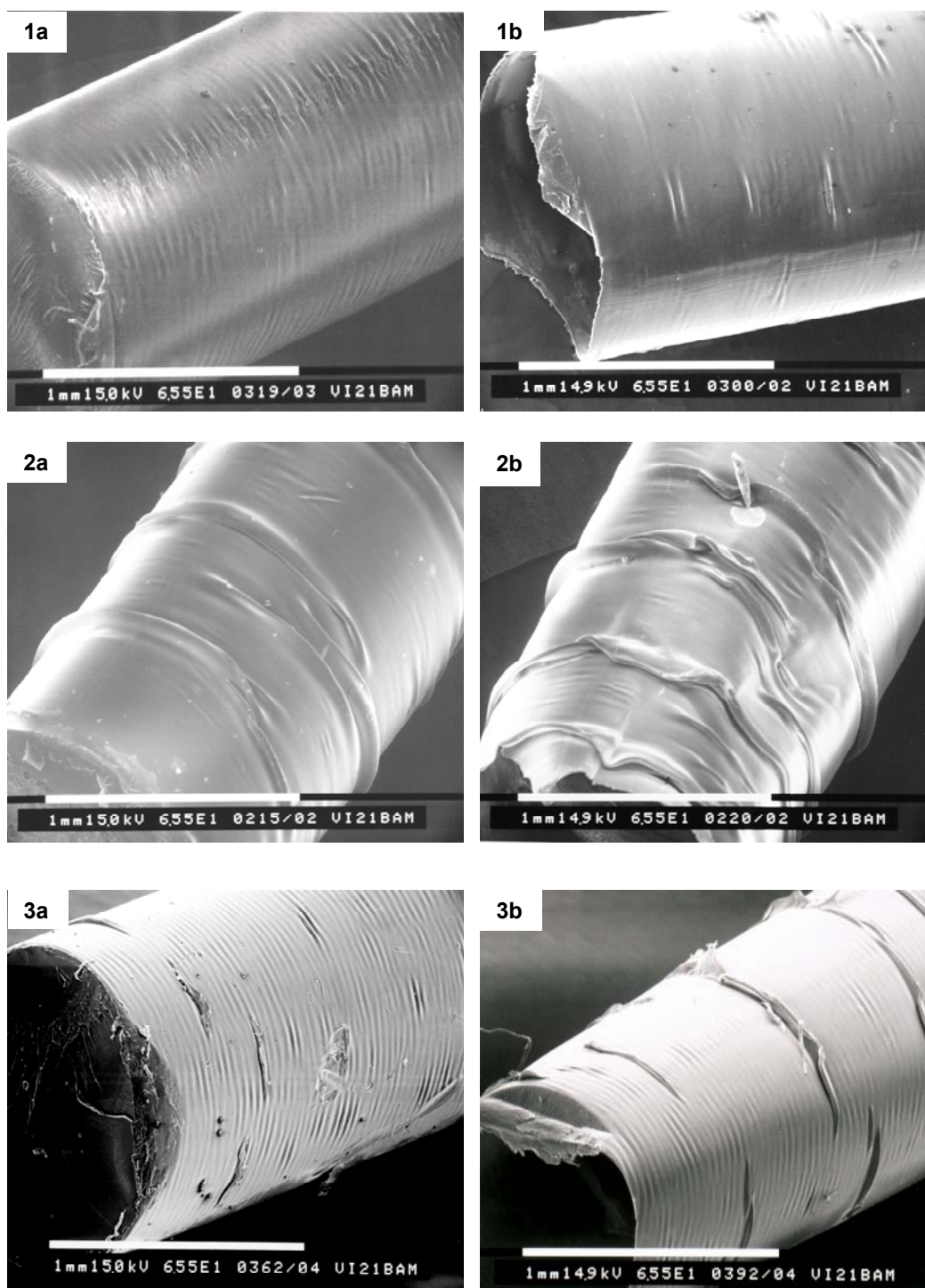


**Figure 8.22:** SEM photographs of the exposed POF (a) and cladding (b) of the sample S4: 1a & 1b. Exposed to 92 °C / 95 %RH; 2a & 2b. Exposed to 120 °C / low humidity and 3a & 3b. Exposed to 110 °C / low humidity.

Moreover, the expansion of POFs' diameter could develop imperfections in the core and at the core-cladding interface. Some microscope pictures by means of scanning

electron microscope (SEM) were taken to observe the surface morphology of the post-exposed samples. Fig. 8.22 shows SEM photographs of both the POF and cladding of the sample S4 as an example. A kind of shrinkage/folding on the surface of POF samples (except in the sample S5) was found (see Fig. 8.22, 1a). An identical shrinkage/folding was found in claddings, too (see Fig. 8.22, 1b). Therefore, it can be realized that shrinkage/folding is related to the cladding not the core. A cause for the shrinkage/folding could be the applied high temperature-humid condition (92 °C / 95 %RH) creating a state, which is near to the melting temperature of claddings. This seems to be possible because for the same POF samples exposed to 120 °C and 110 °C with very low humid condition, the SEM shows a more pronounced shrinkage/folding than for the samples exposed to 92 °C / 95 %RH (see Fig. 8.22). Consequently, such shrinkage/folding structures could create structural imperfections mainly at the core-cladding interface during the early stages of the exposure. As a result a large increase of the optical loss due to scattering can be expected. Therefore, the formation shrinkage/folding structures should be one of the main causes, too, for the total loss of transmission in POFs.

Previous investigations have showed that PMMA and some fluoropolymers exhibit a negative thermo optic coefficient (TOC) [96], which describes a change of the refractive index  $n$  with temperature  $T$ . Prod'homme derived an equation that relates  $dn/dT$  to volume expansion (or density) and electronic polarisability of the materials, as shown in equation (8-1) [97],

$$\frac{dn}{dT} = f(n)(\varphi - \beta) \quad (8-1)$$

where  $\beta$  is the volume expansion co-efficient,  $f(n)$ , is defined as

$$f(n) = \frac{(n^2 - 1)(n^2 + 2)}{6n}, \quad (8-2)$$

and  $\varphi$  is the temperature co-efficient of electronic polarisability  $P$ , defined as

$$\varphi = \frac{1}{P} \frac{dP}{dT}. \quad (8-3)$$

According to this theory, TOC depends on the terms  $\varphi$  and  $\beta$ . Most of the optical polymers exhibit negative TOC (e.g.: PMMA shows a negative TOC in the order of

$10^{-4}$ ), which suggests that the term  $\beta$  dominates over the term  $\varphi$ , because  $f(n)$  is always positive. In view of the Prode'homme theory it can be assumed that POFs exhibit a negative change in the refractive index. At the exposure condition 92 °C / 95 %RH, the temperature itself could influence the volume expansion, which will be well enhanced by the water absorption process. Therefore a considerable change in the refractive index can be expected to take place in POFs. Consequently the variation in  $n$  within the fiber generating inhomogenities mainly in the core cause more microscopic scattering loss (e.g.: Rayleigh scattering), as it is known. Additionally, a change of  $n$  results in a variation of NA, which governs the transmission property of POFs. Therefore, a significant contribution to the total optical loss from refractive index changes is possible.

Additionally, it is observed that all the three POF samples exhibited very similar transmission losses at all the three wavelengths, which suggests that scattering happened at inhomogenities, with extensions much larger (geometrical optics) or much smaller (Rayleigh scattering) than the wavelength. In the first case it could be a supplementary evidence for the transmission loss mainly due to physical changes in POFs. Therefore, physical changes appear to play an important role to cause the total loss of transmission in POFs when exposed to the climate 92 °C / 95 %RH. Finally, under this exposure climate, the optical transmission stability of the three POFs can be characterized in the following order: POF S3 > POF S4 > POF S5.

As can be noticed from the optical measurements at the climatic exposure 92 °C / 50 %RH all the three POFs exhibited quite a good optical stability compared to that of the same exposed to 92 °C / 95 %RH (see Fig. 8.21 and 8.23). The peaks on the curves in Fig. 8.23 are the noise probably creating by a small variation in humidity of the system. The results of this exposure can be a clear indication of the large effect of high humidity on the optical stability of POFs. However, the optical performance exhibited by each of them was different as can be seen from the experimental data shown in Fig. 8.23. The POF sample S5 exhibited higher performance compared to S3 and S4. The sample S5 displayed only about 25 % loss (75 % transmission) whereas the sample S3 and S4 displayed about 60 % loss (40 % transmission) and 52 % loss (48 % transmission), respectively, at the end of about 3380 hours. However all the

three samples showed the linear and non-linear loss behavior as observed in the case of 92 °C / 95 %RH (Fig. 8.21).

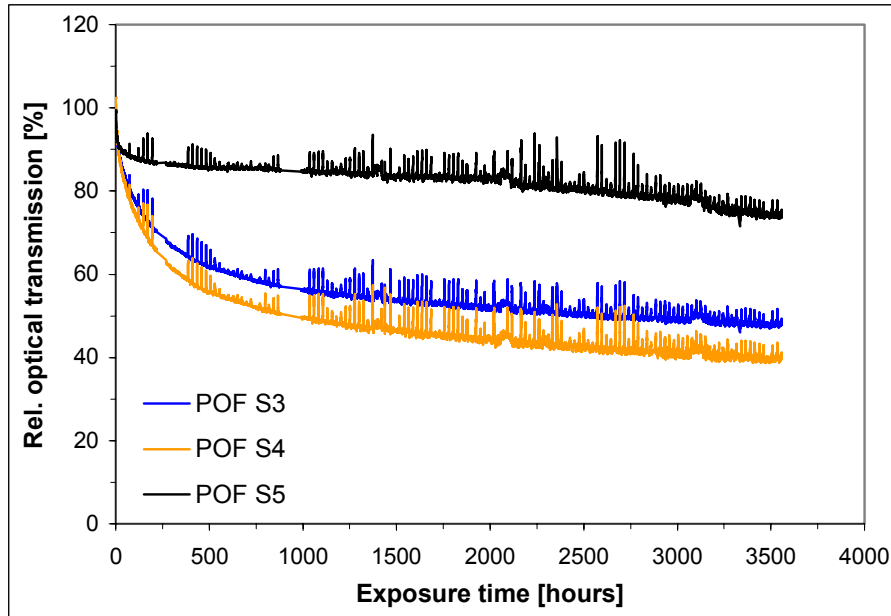


**Figure 8.23:** *Optical transmission (averaged over three wavelengths) through the bare POFs S3, S4 and S5, measured as function of time during the exposure to the climate 92 °C / 50 %RH.*

The initial transmission loss (linear behavior) was less than 5 % and it can be ascribed to physical changes mainly due to imposed humidity as chemical changes by oxidative degradation of the polymer are less likely to cause as discussed before (see earlier paragraphs). After the initial reduction, the transmission performance (non-linear behavior) exhibited by POFs may be explained by their thermo-oxidative stability. The thermo-oxidative stability investigation of these unexposed POFs by means of CL technique reveals that thermo-oxidative stability of the POF sample S5 should be higher than that the other two samples S3 and S4 (see Section 8.3.2.2). This result seems to be in good agreement with the obtained optical results that POF sample S5 exhibited higher optical stability than that of S3 and S4. Therefore, it is possible that changes due to thermal oxidation of the polymer mainly drive the optical stability of POFs. However, the imposed humidity also could influence the transmission loss in addition to the loss mainly due to chemical changes. Influences of humidity can be both physical and chemical as discussed before. However, such

processes are very slow to occur because the imposed humidity of 50 % RH is quite low as compared 95 %RH. On other hand, it has been reported that water has a very little effect on free radical oxidation reactions that involve in thermal- and photo-oxidation processes [56]. Nevertheless, a major influence of water in polymers on chemical reactions of deterioration and oxidation processes could be as an activator [56,60,62]. It may increase the chain mobility, which then could increase the rate of reaction. Therefore, water can influence both directly and indirectly on the optical stability of POFs.

Furthermore, CL measurements to the exposed POF samples indicate the occurrence of degradation (see Section 8.3.2), which suggests that the observed loss occurs mainly due to absorption of light. However only small changes in CL curves were found, the extent of degradation was difficult to assign for each POF sample. As it is investigated the CL emission from the POF sample is the combined emission from the cladding and core (see Section 8.3.2.1). But the cladding emission was found to be higher than that of the core, which suggests the cladding is more prone to degradation than the core. Therefore, it could be possible that occurrence of degradation reactions in the cladding lead to cause of a transmission loss mainly by absorption of light and by other mechanisms as discussed earlier (see Section 8.2.6). The optical stability of the three POF samples under the climate 92 °C / 50 %RH can be characterized in the following order: POF S5 > POF S4 > POF S3.

The results of optical performance of POFs S3, S4 and S5 exposed to 50 °C / 95 %RH (see Fig. 8.24) show that the optical performance is quite different from that of the exposure 92 °C / 50 %RH. But, it appears that humidity seems to have similar effects (water transportation into the core) as observed from the experimental results of the exposure 92 °C / 95 %RH (see Fig. 8.21).

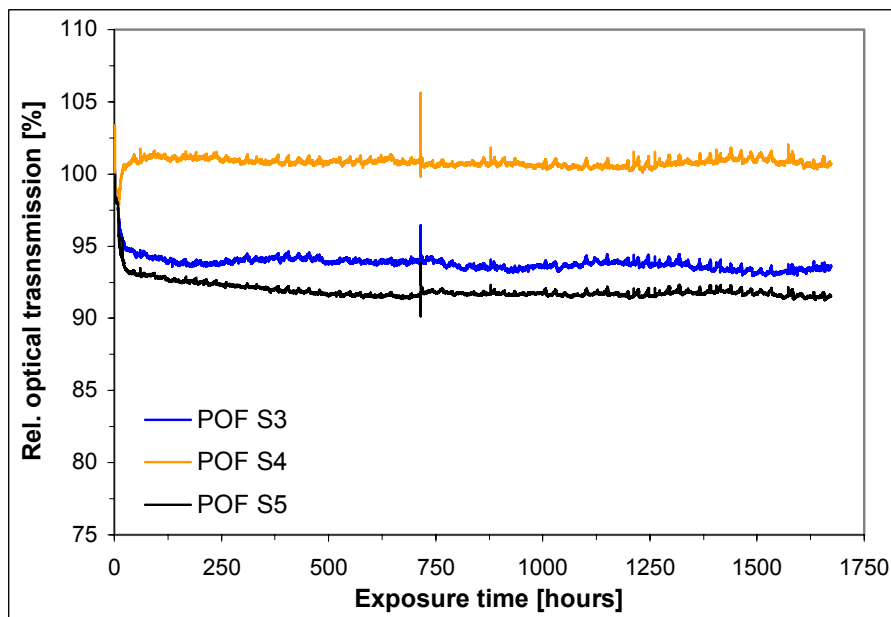


**Figure 8.24:** *Optical transmission (averaged over three wavelengths) through the bare POFs S3, S4 and S5, measured as a function of time during the exposure to the climate 50 °C / 95 %RH.*

However, the POF sample S4 in Fig. 7.24 behaved differently than the other two samples. It exhibited initial increase in contrast to the reduction of the transmission as observed in the other two samples S4 and S5 and usually observed in all the previous exposure test results. A reason for an increase of the transmission could be the occurrence of some processes like recover of core-cladding boundary imperfections. Therefore, the climate 50 °C / 92 %RH appears to have a positive influence on the transmission stability of the sample S4. However, for samples S3 and S5 it seems to have a negative effect that they displayed the loss of about 7 % (93 % transmission) and 12 % (88 % transmission) respectively. Since the applied temperature was too far from  $T_g$  of the core, the imposed high humidity was of 95 %RH, should be the main parameter that influencing the transmission performance by generating physical imperfections in POFs. Nevertheless, chemical reactions like deterioration and oxidation are possible to occur at temperature 50 °C but at a very slow rate and they, too, could be influenced by humidity as discussed earlier. Physical imperfections (e.g.: fluctuations in fiber core diameter) that are generated by humidity should be responsible for a loss of transmission by any kind of scattering of light in POFs. The

optical stability of the three POF samples under the climate 50 °C / 92 %RH can be distinguished in the following order: POF S4 > POF S3 > POF S5.

Short-term exposure experiments to these POFs more clearly reveal effects of individual climatic parameter on the optical stability, which will be discussed in the later section.

### 8.3.1.2 Exposure to temperature with very low humid climates

The experimental results of the optical performance of POFs S3, S4 and S5 exposed to 110 °C / low humidity, 100 °C / low humidity and 90 °C / low humidity are shown in Fig. 8.25, 8.26 and 8.28, respectively. The presented data are again the average value of the data for three wavelengths and recorded as a function exposure time.

The results clearly evidence the importance of temperature that alone would be sufficient to tear down the transmission of POFs to a different extent.

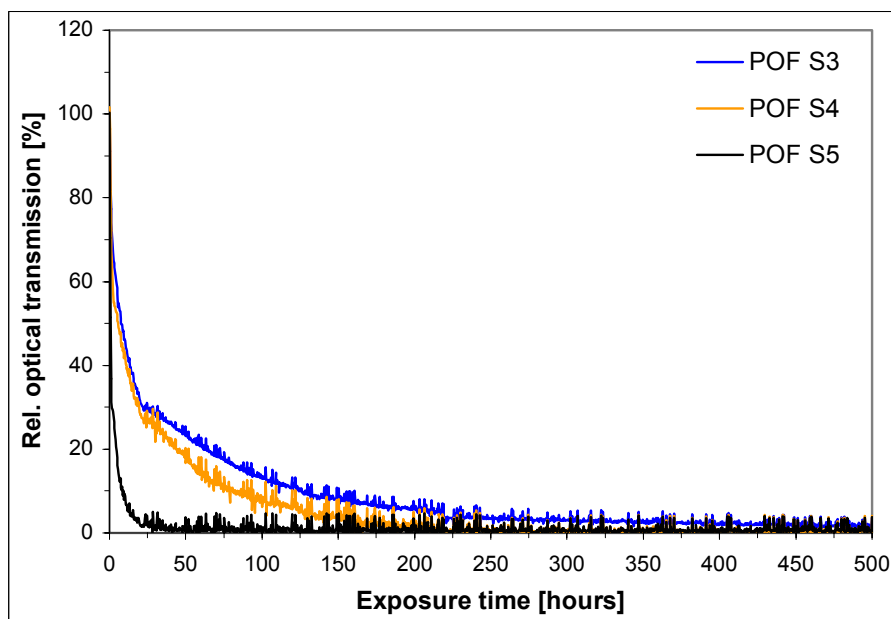


**Figure 8.25:** *Optical transmission (averaged over three wavelengths) through bare POFs S3, S4 and S5, measured as function of time during the exposure to the climate 110 °C / low humidity.*

At a first step, POF samples S3, S4 and S5 were exposed to 120 °C / low humidity. They exhibited the total loss of transmission as soon as the temperature had reached the set point; therefore no figures for the optical transmission are presented.

Obviously, the reason is a mechanical softening and subsequent loss in optical properties at high temperature, which was above the observed  $T_g$  (of about 118 °C) of the core and near to the observed melting point (of about 127 °C) of claddings. A significant increase in diameter, brittleness, and shrinkage/folding of the cladding were observed, which is similar to the results obtained from the exposure test at 92 °C / 95 %RH. However the changes were more pronounced under the exposure 120 °C / low humidity (see Fig. 8.22).

The exposure of POFs S3, S4 and S5 to the climate 110 °C / low humidity resulted in similar consequences as observed in the exposure of 92 °C / 95 %RH and 120 °C / low humidity. The optical transmission performance of these POF samples is represented in Fig. 8.25. The transmission curves are very similar to the ones observed by the exposure to the climatic 92 °C / 95 %RH (see Fig. 8.21). The outcomes of both the exposures were compared and indicate similar changes to cause total loss of transmission in both the cases. However, the influencing parameter in the former case is temperature and in the later case is humidity. Yet, the rate of transmission loss exhibited by POFs under the climate 110 °C / low humidity was low compared to that of under 92 °C / 95 %RH. The loss of nearly all transmission occurred in the duration of about 28 hours, 210 hours and 590 hours in S5, S4 and S3 respectively. It may suggest that the combination of high temperature and humid climate generate a condition, which is stronger than the condition 110 °C / low humidity. As a result, a faster rate of the transmission loss was observed in the former case. Nevertheless, here too, main sources for the transmission loss are expected to be physical changes of POFs, because well-pronounced changes like increase in diameter, brittleness and shrinkage/folding were found. For example, the shrinkage/folding observed through SEM is shown in Fig. 8.22. Therefore, the observed loss of transmission can be ascribed mainly to scattering. However, chemical reactions could also take place to some extent and they are known to cause the loss by light absorption.

The optical measurements consequences of the exposure to 100 °C / low humidity are presented in Fig. 8.26. They show a strong initial drop-off of the optical transmission

as soon as temperature had reached 100 °C (linear behavior). The transmission of POFs turned stable after a drop-off when the set temperature became stable (non-linear behavior). The linear behavior of the transmission loss in the three POFs was quite different that sample S5 exhibited more loss (transmission about 35 %) than that of the other two samples S3 and S4 (transmission about 72 %). The linear loss behavior is attributed mainly to physical changes. Since the exposure temperature was near to  $T_g$  of the core, molecules can set-in motion, which influences the polymer physical structure significantly. Molecular motions of polymer chains perhaps cause softening and volume change, which result in imperfections in the core as well as at the core-cladding interface, as discussed earlier (see Section 8.3.1.1).

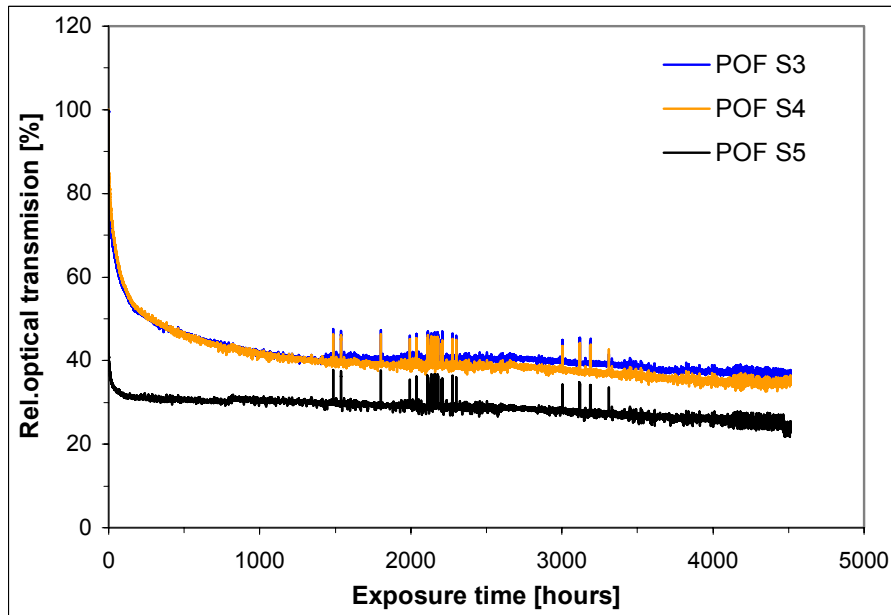


**Figure 8.26:** *Optical transmission (averaged over three wavelengths) through bare POFs S3, S4 and S5, measured as function of time during the exposure to the climate 100 °C / low humidity.*

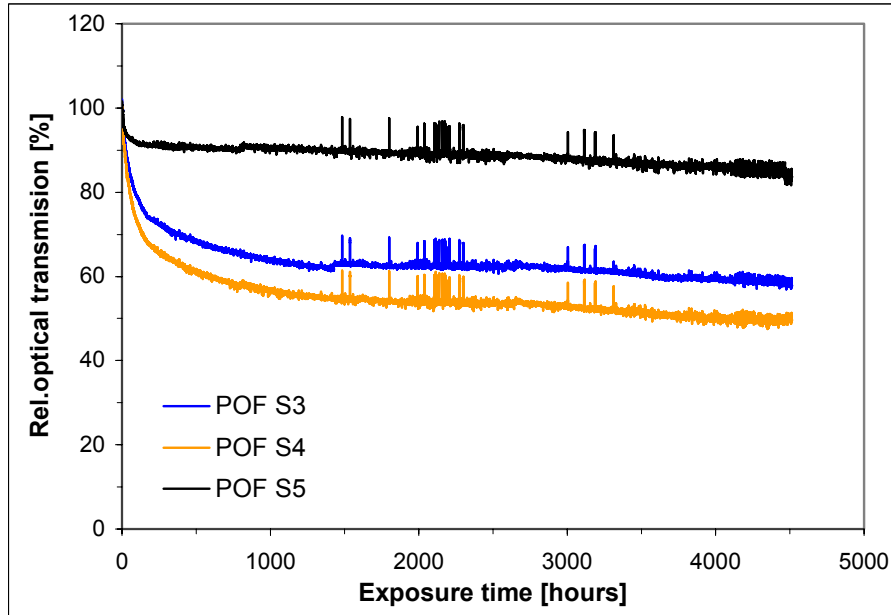


**Figure 8.27:** Assumed optical transmission function of time through (averaged over three wavelengths) bare POFs S3, S4 and S5 under the exposure climate 100 °C / low humidity after the subtraction of the linear loss from 100 %.

Moreover, an expansion of the volume by temperature can account for a change of the refractive index of the polymer [96,97] and therefore it could lead to a transmission loss due to scattering. Another process that could take place in POFs is the polymerization of active oligomers, which can be trapped unreacted in the polymer matrix during the manufacturing process. Such a reaction can cause material inhomogeneities in POFs promoting the transmission loss to a higher extent. But the amount of oligomers depends on polymer manufacturing conditions and fiber processing history of POFs.

It is assumed that once the physical imperfections are set-in at the initial stages (i.e. an initial drop-off of the optical transmission), the loss of transmission of POFs becomes non-linear behavior as the temperature becomes stable. The non-linear behavior of the optical loss results mainly from chemical changes due to occurrence of chemical reactions such oxidative degradation, in addition to the loss due to physical defects. Therefore, it is most likely that the loss of transmission (non-linear) mainly derives from the thermo-oxidative stability of POFs. Under the exposure climate 100 °C / low

humidity, almost equal optical stability of POFs S3 and S4 and a least optical stability of S5 can be identified (see Fig. 8.27).

On the other hand, the thermo-oxidative stability investigation of these unexposed POF samples by CL reveals that POF S5 was better than that of the other two POFs (see Section 8.3.2.2) and it seems to be in contradiction to the optical results. Nevertheless, as it is discussed above, the initial drop-off (linear behavior) is attributed mainly to physical changes and therefore it can be subtracted from 100 % transmission of POFs. The resultant optical transmission loss of the same POFs appears as shown in Fig. 8.27 and it is believed to be due to chemicals changes by thermo-oxidative degradation of POFs. These results show that the optical stability exhibits by the POF S5 is higher than that of POF S3 and S4. It is in good agreement to the CL results.

The optical measurement results of the exposure of POF samples to the climate 90 °C / low humidity are displayed in Fig. 8.28. The curves show noise probably due to a change in the humidity during the exposure in the chamber. No considerable drop-off (linear behavior) of the transmission at the initial stages of the exposure can be seen. It suggests less physical changes occurrence in these POFs. Furthermore, the POFs exhibited a good optical stability with a loss of about 11 % (89 % transmission), 12 % (88 % transmission) and 18 % (82 % transmission) at the end of 3290 hours, registered for S5, S4 and S3 respectively. This result seems to be in accordance with the CL results that the sample S5 exhibited higher thermo-oxidative stability compared to other samples. Therefore, these results may indicate that the observed loss of transmission was mainly governed by thermo-oxidative stability of POFs.

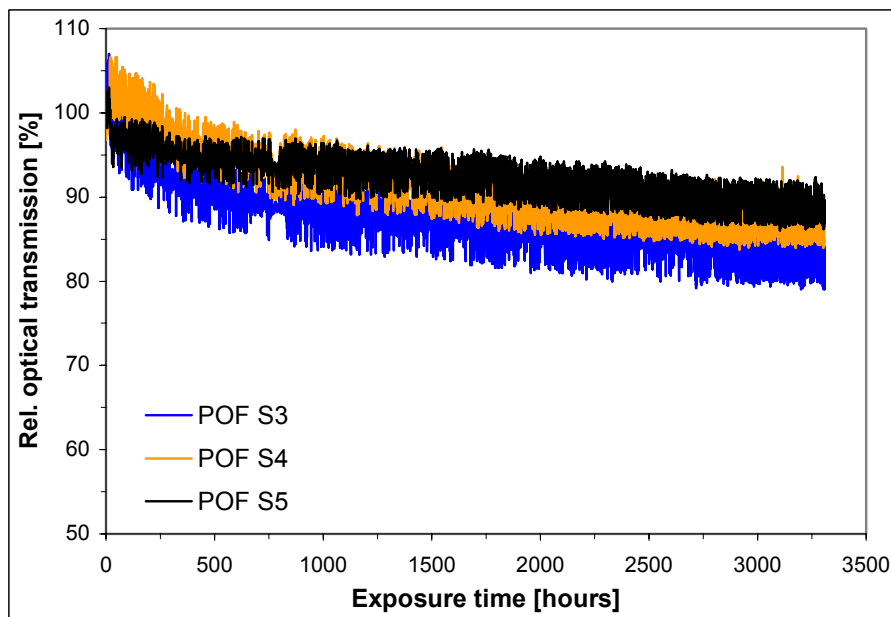


**Figure 8.28:** *Optical transmission (averaged over three wavelengths) through bare POF sample S3, S4 and S5, measured as function of time during the exposure to the climate 90 °C / low humidity.*

### 8.3.2 Investigation of thermo-oxidative stability/degradation using CL

The thermo-oxidative stability in the temperature range 77 °C to 177 °C is investigated for the POF samples S3 and S4 and S5. For the interpretation of results, it is assumed that the CL emission is proportional to the oxidation reaction rate, which generally means that the higher the CL emission the lower is the oxidative stability of the sample under test.

#### 8.3.2.1 Comparison of the unexposed bare POF with, core and cladding

The unexposed bare POF, core fiber and cladding of samples S3 and S4, and PMMA (S6) are investigated for their thermo-oxidative stability (in this Section, “PMMA” or “bulk PMMA” stands for “PMMA granules with a diameter in the order of 2 mm”). Since similar results with respect to CL behavior of core and cladding were found in both the samples S3 and S4, here the results of the sample S4 only are discussed, which can serve as a model for other POF samples of similar kind. CL of the POF

sample S5 was not recorded as its cladding and fiber core could not be separated by the method used for S3 and S4 samples.

CL of the individual components of POF S4 and PMMA are given in Fig. 8.29.

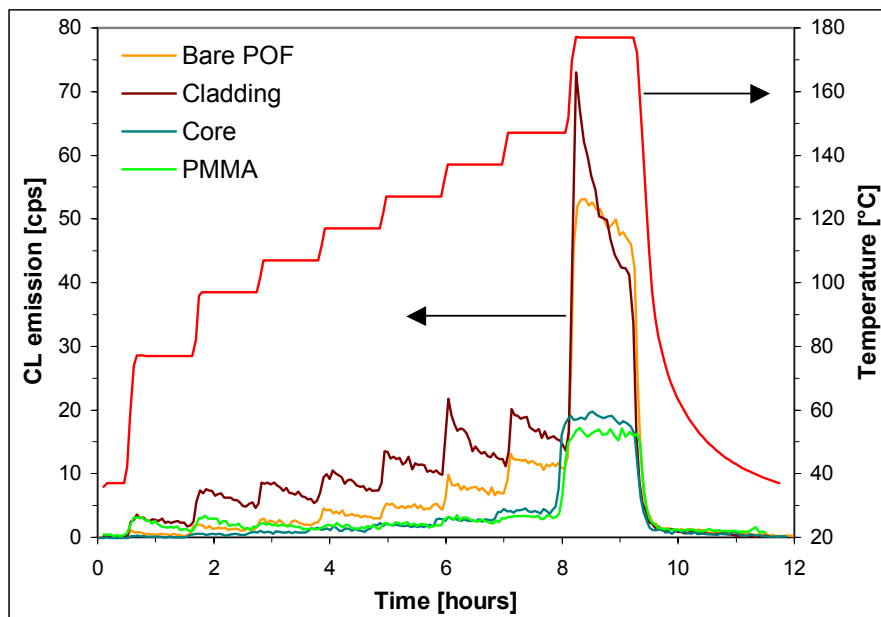


**Figure 8.29:** CL curves for the unexposed bare POF, core fiber, cladding (all sample S4) and PMMA (S6).

A comparison of the CL emission shows that cladding delivered much higher CL emission than that of bare POF, core fiber, and PMMA. A similar result with respect to CL emission from the bare POF and cladding was observed in the case of POFs S1 and S2 (see Section 8.2). However, the CL emission from the bare POF was much greater than that of core fiber and PMMA but the later ones behaved similarly with respect to their CL emission. Therefore, the cladding appeared as more liable to oxidative degradation compared to bare POF, core fiber and PMMA. From these results an importance of individual components of the bare POF in its thermo-oxidative degradation can be realized.

The bare POF is composed of two materials since it consists of the core and cladding. Therefore core, cladding and an interaction between both can accomplish the total CL emission from the bare POF. Yet, it is known that the larger part of the bare POF is the core (950  $\mu\text{m}$  to 980  $\mu\text{m}$  in diameter), major emission by the core can be foreseen. But the cladding, having a thickness of 20  $\mu\text{m}$  to 50  $\mu\text{m}$  coated on top of the core, is

not only acting as a rarer medium (to guide light in the fiber by total internal reflection) but also as a protective coating for the oxidative degradation of the core. Therefore, thermo-oxidative degradation of the core is most likely dependent on the oxygen diffusion coefficient of the cladding. The larger contribution from the cladding to the total CL emission from the bare POF compared to that of the core (see Fig. 8.29) suggests higher thermo-oxidative stability of the core than of the cladding. It is confirmed by nearly consistent CL of the core (which is PMMA) and the bulk PMMA sample.

Of course many factors are involved in the relatively high CL emission from the cladding. For instance, physical geometry and chemical compositions of samples play an important role. As already quoted, cladding samples appeared as hollow cylinders when the core was removed (see Section 7.4). This cylindrical structure makes it possible for oxygen to diffuse from all directions. As a result, a large part of the polymer is available to the oxidation scheme. In contrary, the core has a closed cylindrical fiber structure resulting in a decreasing diffusion of oxygen from the periphery towards the center of the fiber. Consequently, the relative amount of polymer available for oxidation will be less compared to the one of the cladding and the core may have a depth dependent oxidative degradation profile, at least at temperatures below its  $T_g$ . The same mechanism may be applicable to bulk PMMA since the size of the granules was comparable to the diameter of the core.

It seems that chemical compositions also would create differences in CL emission from the core and cladding. Because the core material of the present POFs was PMMA and it is different from cladding materials that were found to be polyfluoroolefins and PFMA (see Section 8.1.3). Therefore, it is possible that differences in chemical compositions of claddings and cores would additionally responsible for differences in their CL emission (particularly the respective quantum efficiencies may be different).

From the above results the following may be condensed:

- CL suggests that thermo-oxidative degradation of the bare POF is predominantly of the cladding and minor of the core.
- The thermo-oxidative stability of the cladding was found to be lower than that of the core and PMMA.

- Thermo-oxidative degradation of the core, in practice, may follow the cladding and may have a depth dependent degradation profile.

### 8.3.2.2 Comparison of the unexposed bare POFs

The thermo-oxidative stability of the unexposed bare POFs (S3, S4 and S5) and PMMA is investigated in comparison; Fig. 8.30 shows their CL curves.

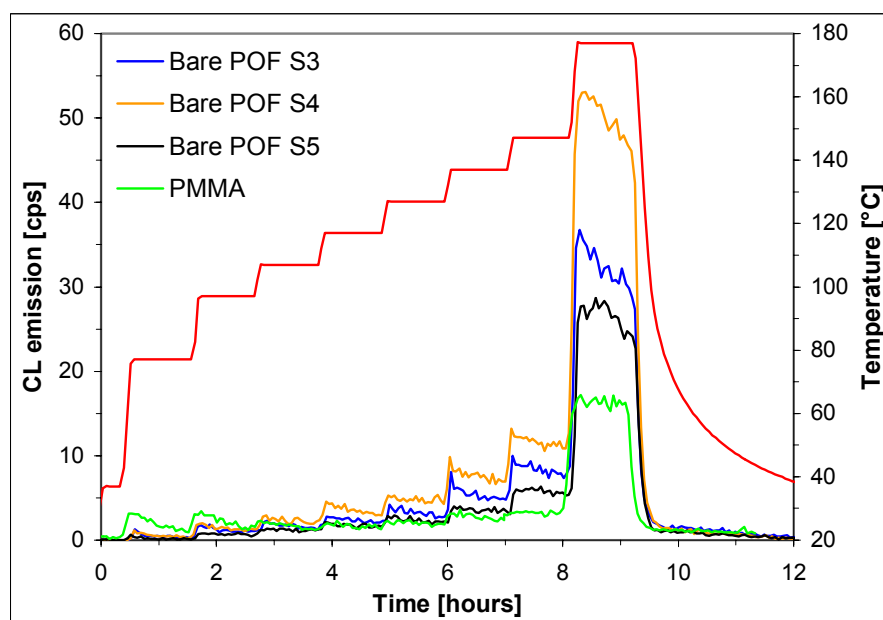


Figure 8.30: CL curves for the unexposed bare POFs.

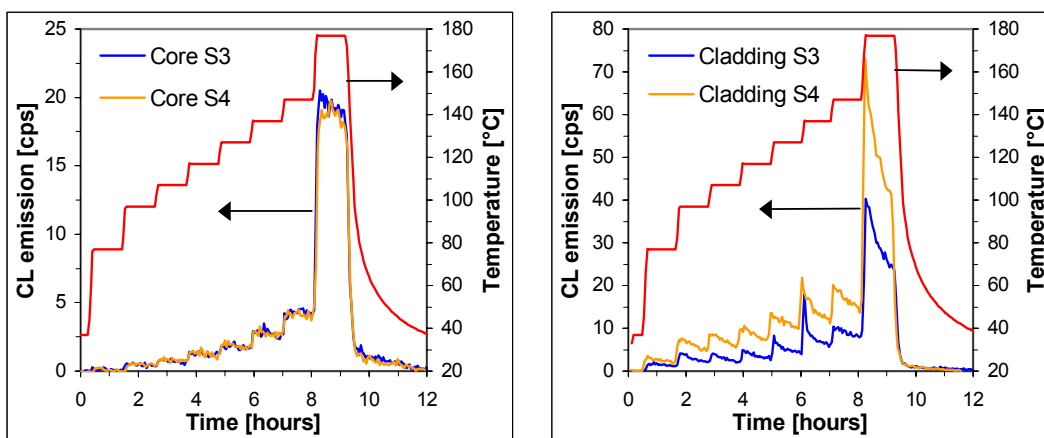


Figure 8.31: CL curves for the unexposed core and cladding of samples S3 and S4.

The CL emission difference between bare POF samples was observed. It shows a difference in their thermo-oxidative stability although they possessed the same core material PMMA. The thermo-oxidative stability of the investigated samples was found to be in the order of  $S4 < S3 < S5 < \text{bulk PMMA}$ , as they exhibited CL emission in the reverse order (see Fig. 8.30).

In order to realize the observed difference in their stability, CL of the core and cladding of samples S3 and S4 was separately recorded and compared; their CL curves are shown in Fig. 8.31. CL of the same of the sample S5 was not recorded, as they could not be separated by the method found for S3 and S4 (see Section 7.4). The comparison of CL of core samples clearly suggests almost equal thermo-oxidative stability as they displayed almost equal height in their CL emission. It also shows the CL consistency in displaying material uniformity of core samples. In contrast, cladding samples displayed a marked difference in their stability, as the height of their CL emission was different. The sample S4 exhibited higher CL emission compared to that of the sample S3 indicating its lower thermo-oxidative stability. The same was observed with CL of their respective bare POF samples. Therefore, from these results it can be understood that the observed difference in the stability of bare POFs might be due to a difference in the stability of claddings. It confirms higher stability of the bare POF S5 compared to S3 and S4 is probably due to its cladding, which was experimentally found to be an PFMA (see Section 8.1.3). If this assumption is true, the cladding of the type sample S5 shows higher stability than the polyfluoroolefin cladding of the type S3 and S4 (see Section 8.1.3).

Nevertheless, both the claddings as well as core samples behaved similarly in their CL emission. Core samples exhibited a plateau emission behavior, which could be related to thermally activated degradation processes controlled by the diffusion rate of oxygen [51,52,74,86]. The claddings also displayed the plateau emission behavior, however, seemed to exhibit the peak emission behavior in the temperature range 127 °C to 177 °C (see Fig. 8.31). A similar behavior of plateau and peak emission can also be found in their respective unexposed bare POF samples (see Fig. 8.30), which additionally supports the result that CL emission from the bare POF was mainly from the cladding and minor the core (see Section. 8.3.2.1). Nevertheless, the peak emission of both may be related to their melting since they exhibited melting

temperature ( $T_m$ ) in the range 124 °C to 137 °C. Owing to melting of polymer crystallites, homogenization of low molecular weight products from the oxidation of the polymer at the preceding temperature steps [98], an increase in the rate of oxygen dissolution and an increase of the polymer chain mobility to access for the large participation in the oxidation, could result in the CL peak emission.

It is seen that the chemical composition of the cladding of S3 and S4 was found to be similar, as detected by FTIR (see Section 8.1.3). But CL experiments showed some differences in their thermo-oxidative stability indicating a difference probably in their chemical compositions (could be either a small difference in their chemical structure or in formulation of additives). These results may indicate the superiority of the CL method in differentiating thermo-oxidative stability of samples having small differences in their chemical nature that could not be detected by techniques like FTIR.

From the above results and the discussion the following may be stated:

- The thermo-oxidative stability of bare POFs can be different although composed of the same core material PMMA.
- The observed difference in the thermo-oxidative stability among bare POFs seemed to be mainly derived by differences could be in the chemical nature of claddings.

### **8.3.2.3 CL peak emission behavior versus initial transmission loss**

In order to understand the relation between the extent of initial transmission loss (for instance, under the exposure 100 °C / low humidity, see Section 8.3.1.2) and chemical changes by oxidation reactions in bare POFs, CL under an isothermal (at 100 °C,  $\pm$  0.1 K) condition was performed for the unexposed samples, CL curves are as shown in Fig. 8.32.

CL experiments reveal a peak emission behavior followed by a constant emission-plateau behavior for all the three samples. The peak behavior could be proposed to an irreversible process that involves the consumption of one or more reactants. Such a process is discussed in little more detail in the Section 8.2.2. The plateau behavior could be interpreted as diffusion-controlled process and its rate is determined by the rate of oxygen diffusion in to the sample. Schartel et al. [51,52] have related the peak

CL emission to the transmission loss that occurs at the early stages of climatic exposure of POFs.

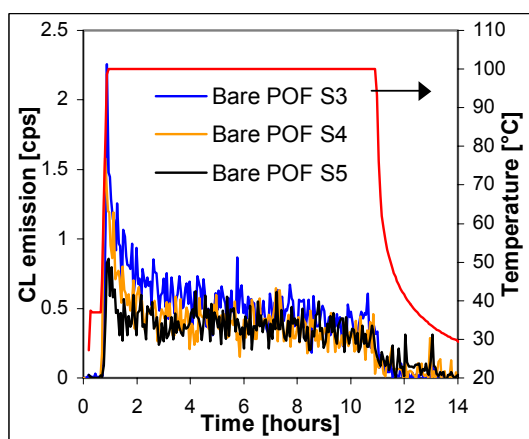


**Figure 8.32:** *CL curves for the unexposed bare POFs, recorded at 100 °C.*

Here, too, a similar consequence was encountered (see Section 8.3.1.2 for the transmission results of 100 °C / low humidity exposure). Unfortunately, the relation between the extent of the initial transmission loss and the height of the CL peak emission does not hold, at least for the observed initial transmission loss under the exposure 100 °C / low humidity. It was found that POF S5 exhibited much higher transmission loss than that of the other two POFs (see Fig. 8.26 in Section 8.3.1.2). But CL experiments performed at 100 °C reveal that sample S5 exhibited lower peak CL emission compared to the other two samples (see Fig. 8.32). These results suggest that physical changes by temperature and humidity are most likely to contribute significantly to the initial transmission loss that occurs at the early stages of the exposure. Nonetheless, the peak emission can be a clear indication of the occurrence of chemical reactions, which could result in a transmission loss by light absorption.

#### **8.3.2.4 CL of samples exposed to 92 °C / 50 %RH**

Bare POF samples S3, S4 and S5 exposed to the climate 92 °C / 50 %RH are investigated for their thermo-oxidative degradation/stability in comparison with their unexposed one's.

In order to understand causes for the observed differences in thermo-oxidative stability of the exposed bare POF samples, CL experiments to the exposed claddings S3 and S4 were performed, too, and the results were compared with their unexposed candidates.

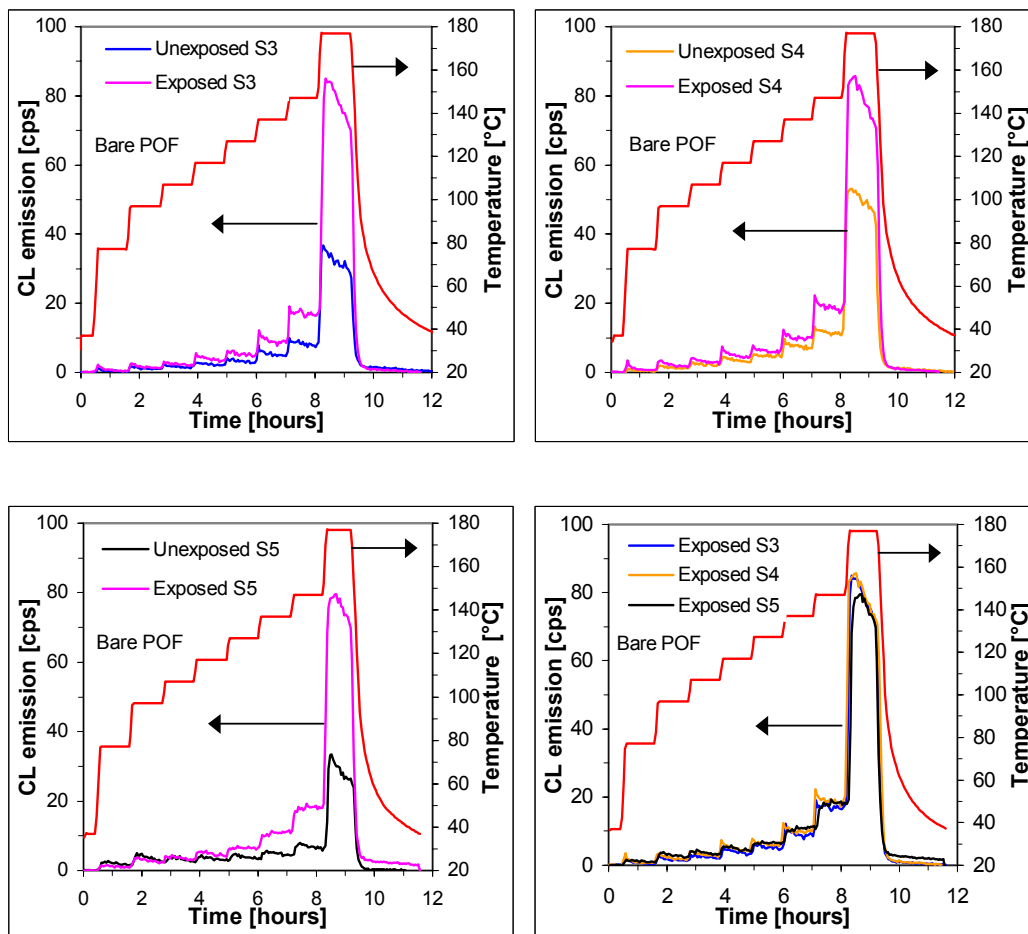


**Figure 8.33:** CL curves for the unexposed and exposed bare POF samples S3, S4 and S5. The exposure condition was 92 °C / 50 %RH.

CL curves for the unexposed and exposed bare POF samples are presented in Fig. 8.33. In general, all the exposed bare POF samples exhibited higher CL emission compared to their unexposed candidates. The lower stability of the exposed samples could be expected as a result of climatic exposure. This outcome may be a clear indication of the oxidative degradation in POFs. The higher CL emission also could result from the presence of chemisorbed water in the polymer generated by humidity [88].

However, the CL emission from the exposed samples was found almost equal at the lower temperature steps (77 °C and 97 °C) but higher at the higher temperature steps (from 107 °C to 177 °C) compared to the unexposed samples (see Fig. 8.33). These characteristics could be due to different stability of degradation products (oxidized

moieties) that form as a result of oxidative degradation due to climatic exposure. It also could be possible that the dissolution of oxygen in the sample at temperatures below their  $T_g$  may not be adequate to decompose all oxidized moieties but be sufficient or enough, at least for those which accumulated at the surface of the sample.

The ranking of the exposed samples concerning the oxidative degradation was found difficult to assign as the comparison shows almost a similar rate of the CL emission from all the samples (see Fig. 8.33).

In view of the fact that the CL emission from the bare POF is the combined emission from both the core and cladding, CL of the exposed claddings were compared with their unexposed one's, which is shown in Fig. 8.34. Both the exposed claddings S3 and S4 exhibited a considerable decrease in the CL emission in the whole investigated temperature range in comparison with the unexposed samples. The significant decrease in the CL emission indicates an increased stability, which could be caused by processes like crosslinking varying diffusion properties of the polymer [99]. It could also result from quenching of the excited state products by molecules that form due to oxidation as a result of climatic exposure.

However, CL emission comparison between the exposed claddings S3 and S4 yields no significant changes (see Fig 8.34), which indicates that no ranking could be made easily with respect to their degradation changes.

Nevertheless, in general, in result to the relative lower thermo-oxidative stability exhibited by the exposed bare POFs, the exposed claddings did not show such result. Therefore, it might be possible that the observed relative lower stability of the exposed bare POFs could be caused by the core. That means the relative stability of the core appears to be decreased due to its thermo-oxidative degradation owing to climatic exposure.

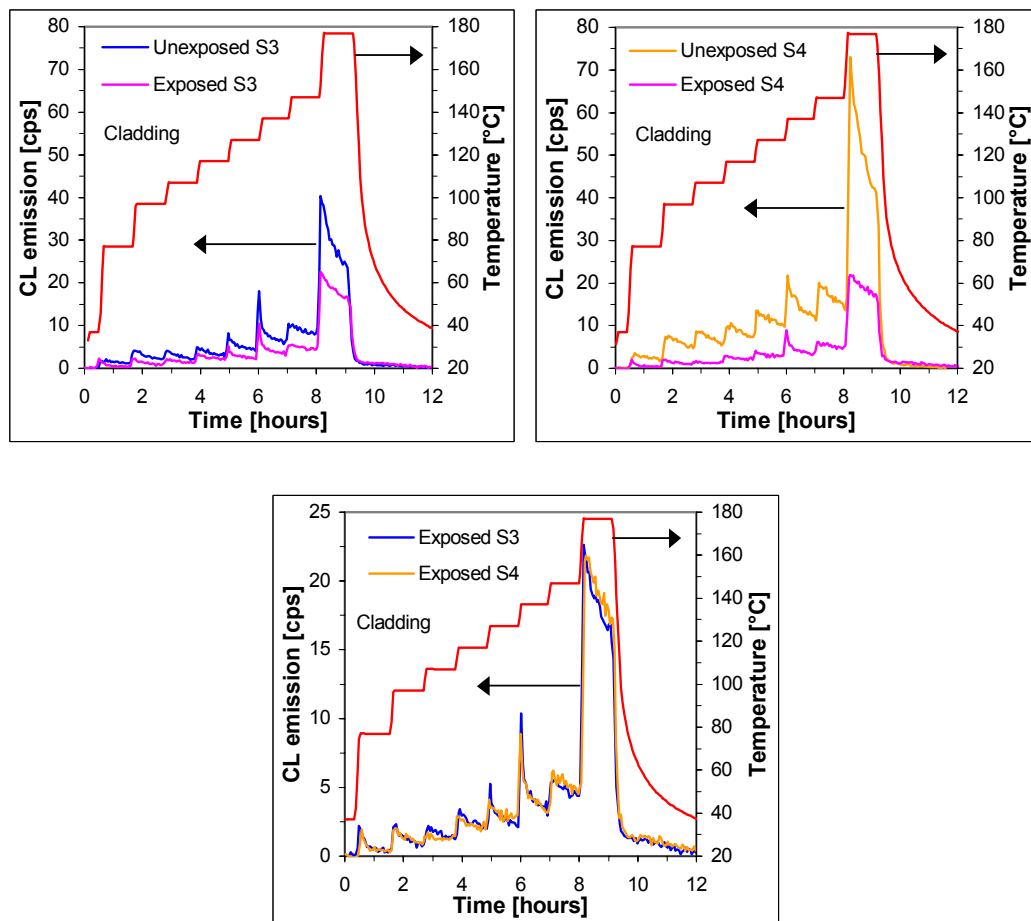


**Figure 8.34:** CL curves for the unexposed and exposed cladding samples S3 and S4. The exposure condition was 92 °C / 50 %RH

Since the exposure condition was temperature in combination of humidity, thermo-oxidative degradation of the polymer could be influenced by the presence of water. Influences of water can be both physical and chemical. As a chemical influence, the presence of water in polymers does not lead to significant chain scission occurring in degradation processes, as reported by Strlic et al. [88]. However, it could participate in chemical reactions with the functional groups of the polymer and the resultant products then may have an influence on oxidative degradation processes. As a physical influence, the presence of water in polymers can act as a polar plasticizer [60,61] that influences the degradation rate. Further on, the presence of water in oriented amorphous polymer substances like the core fiber of POFs could decrease the crystalline phase by which the oxidation-spreading rate increases as the amorphous phase becomes more available.

Similarly, in the present case of climatic exposure of POFs, too, such processes due to water can be expected. However, they most likely take place in the core of POFs, because the PMMA core is hydrophilic, whereas claddings were found to be fluoropolymers that are hydrophobic. Therefore, it may be claimed that humidity could increase the thermo-oxidative degradation rate in POFs particularly the fiber core. Consequently, climatic exposure leads to decrease in thermo-oxidative stability of POFs.

The optical results indicate a clear difference in the optical transmission stability between the three POF samples (see Section 8.3.1.1). But the CL results show no clear demarcation of the thermo-oxidation stability between the exposed bare POF samples. Therefore, the direct interpretation of the relative optical stability with the relative thermo-oxidative stability of the exposed POF samples was found difficult. On the other hand, it suggests that the optical loss could arise not only by chemical changes but also by physical changes due to temperature-humid condition as discussed in the Section 8.3.1.1. Nevertheless, CL results in the occurrence of degradation in all the exposed POFs, which suggests the loss due to absorption of light contributed to the observed transmission loss in POFs exposed to 92 °C / 50 %RH.

#### **8.3.2.5 CL of samples exposed to 100 °C / low humidity**

CL experiments to bare POF samples S3, S4 and S5 exposed to the climate 100 °C / low humidity were performed, their CL was compared with their unexposed one's and are shown in Fig. 8.35.

In comparison with CL of the unexposed bare POF samples, all the three exposed samples exhibited higher CL emission in the whole investigated temperature range. Therefore, in common, the higher CL emission from all the exposed samples suggests lower stability, which could be a clear indication of the occurrence of degradation owing to climatic exposure.

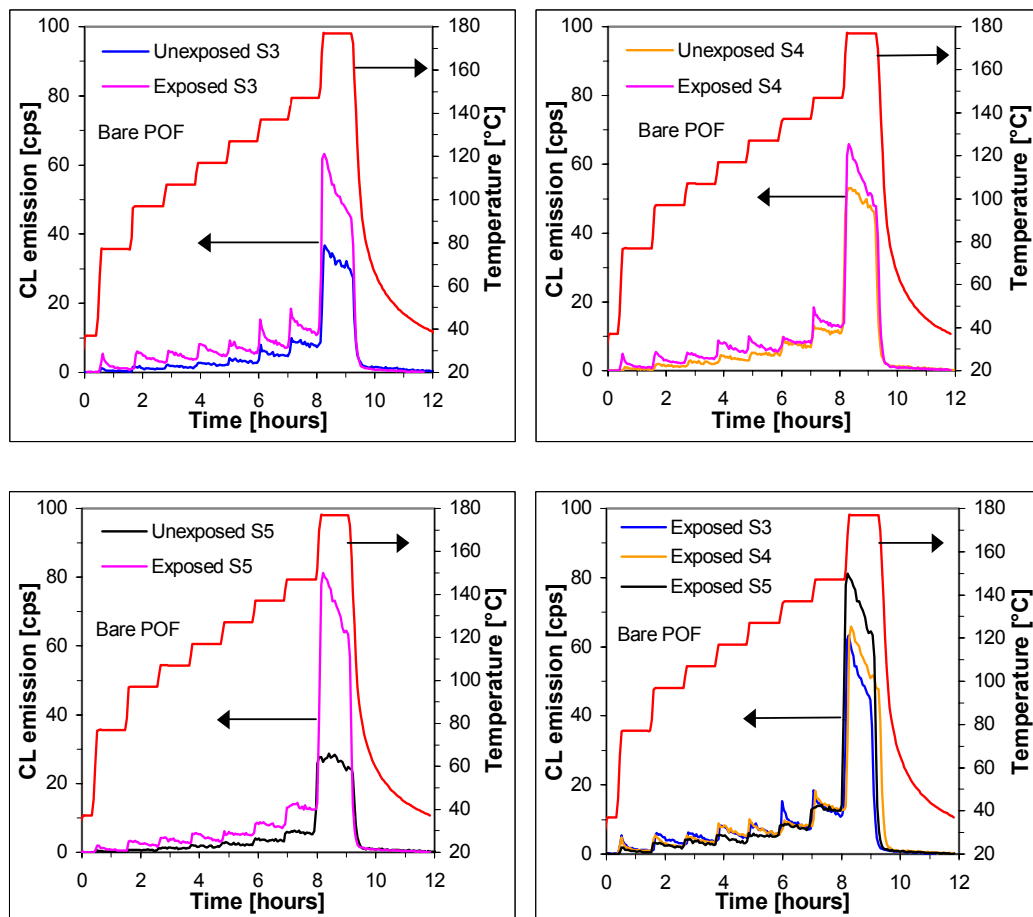


**Figure 8.35:** CL curves for the unexposed and exposed bare POF samples S3, S4 and S5. The exposure condition was 100 °C / low humidity.

The comparison of CL between the exposed samples indicates higher stability of the sample S5 compared to the sample S3 and S4 as they exhibited CL emission in the reverse sequence, at least in the temperature range 77 °C to 147 °C (see Fig.8.35). However, a stability difference between the sample S3 and S4 was found to be difficult to establish as they exhibited almost a similar rate of the CL emission except in range 127 °C to 137 °C, where the sample S3 showed higher CL emission.

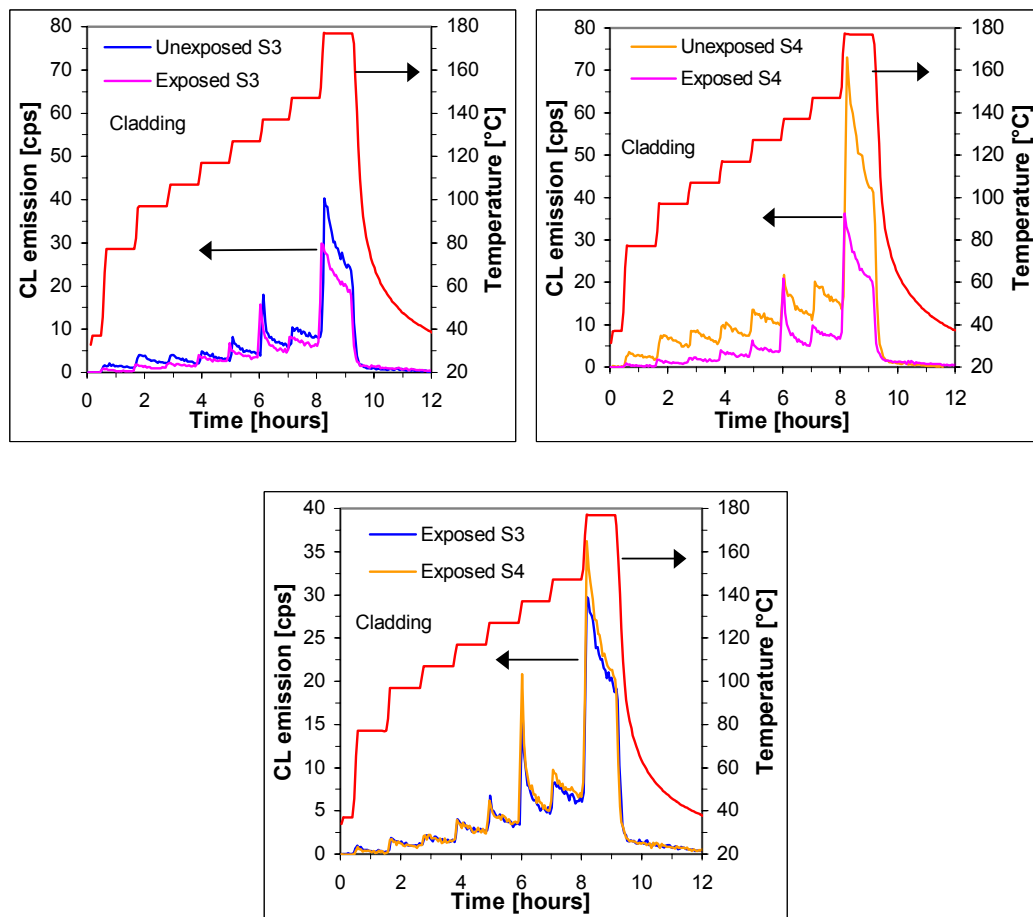


**Figure 8.36:** CL curves for the unexposed and exposed cladding samples S3 and S4. The exposure condition was 100 °C / low humidity.

CL emission curves for the unexposed and exposed claddings S3 and S4 are shown in Fig. 8.36. The results, in overall, show similar consequences as observed in CL of claddings exposed to 92 °C / 50 %RH. Both the exposed claddings, especially S4, displayed significant lower CL emission suggesting their higher stability compared to their unexposed candidates. However, CL emission at their  $T_m$  (137 °C) was found different, because both the exposed samples exhibited almost equal peak emission. This result indicates a decomposition of oxidized products that become homogenized due to melting (of the polymer) and therefore largely participate in oxidation and an increase in the diffusion rate of oxygen. Nevertheless, a decrease of the CL emission exhibited by both the claddings, may be attributed to crosslinking and/or to quenching of excited state products by molecules produced from oxidation. In order of rating the above effects with respect to the exposed claddings both their CL was compared

(Fig.8.36). The comparison shows no marked difference between their CL emission in the temperature range 77 °C to 127 °C but the sample S4 exhibited higher CL emission indicating its lower stability in the temperature range 137 °C to 177 °C. Therefore, it may be stated that the cladding S4 appears to be more affected than the cladding S3 by climatic exposure.

Overall, CL results suggest lower stability of the exposed bare POF samples but the higher stability of the exposed claddings compared to their unexposed ones. Therefore, it is possible that the core caused the lower stability of bare POFs. Consequently, a similar mechanism as described above (see the discussion of CL of POF samples exposed to 92 °C / 95 %RH) can be proposed, here too. However, the main parameter that plays a role in this case is high temperature.

In recalling the optical results of POF samples S3, S4 and S5 exposed to the climate 100 °C / low humidity, it is seen that POF S5 exhibited lower optical stability compared to POF samples S3 and S4 (see Fig.8.26 in Section 8.3.1.2). But CL experiments to the exposed bare POF samples suggest the higher thermo-oxidative stability of the sample S5 compared to the other samples. This may be a contradiction to the optical results, if the optical loss is caused by only chemical changes due to deterioration and oxidation reactions of the polymer. However, the assumption of the transmission loss at the early stages of the exposure results by mainly physical changes in POFs yields the higher optical stability of the sample S5 compared to the other two POF samples (see Fig. 8.27 in Section 8.3.1.2). This result is in excellent agreement with the CL results stated above. However, the correlation of the optical stability with thermo-oxidative stability between the samples S3 and S4 was found difficult to establish because they exhibited a very small difference in the thermo-oxidative stability according to their CL emission. Nevertheless, these consequences support two important points, that the loss of transmission occurring at the early stages of the exposure should be caused mainly by physical changes and the optical consistency of POFs is most likely be governed by their thermo-oxidative degradation, under the exposure condition 100 °C / low humidity.

As the CL results show degradation in the exposed bare POFs, the transmission loss owing to light absorption can be expected as a major part of the observed transmission loss. However, changes due to degradation of the cladding could cause also core-

cladding interface imperfections as described in Section 8.2.6. This hypothesis was supported by the results of optical simulations on the unexposed and exposed (100 °C / low humidity) bare POFs, investigated by Mr. Jankowski (a PhD student of BAM) [100].

### 8.3.2.6 CL of samples exposed to 90 °C / low humidity

CL of bare POF samples S3, S4 and S5 exposed to the climate 90 °C / low humidity was compared with that of unexposed samples; Fig. 8.37 shows their CL curves.

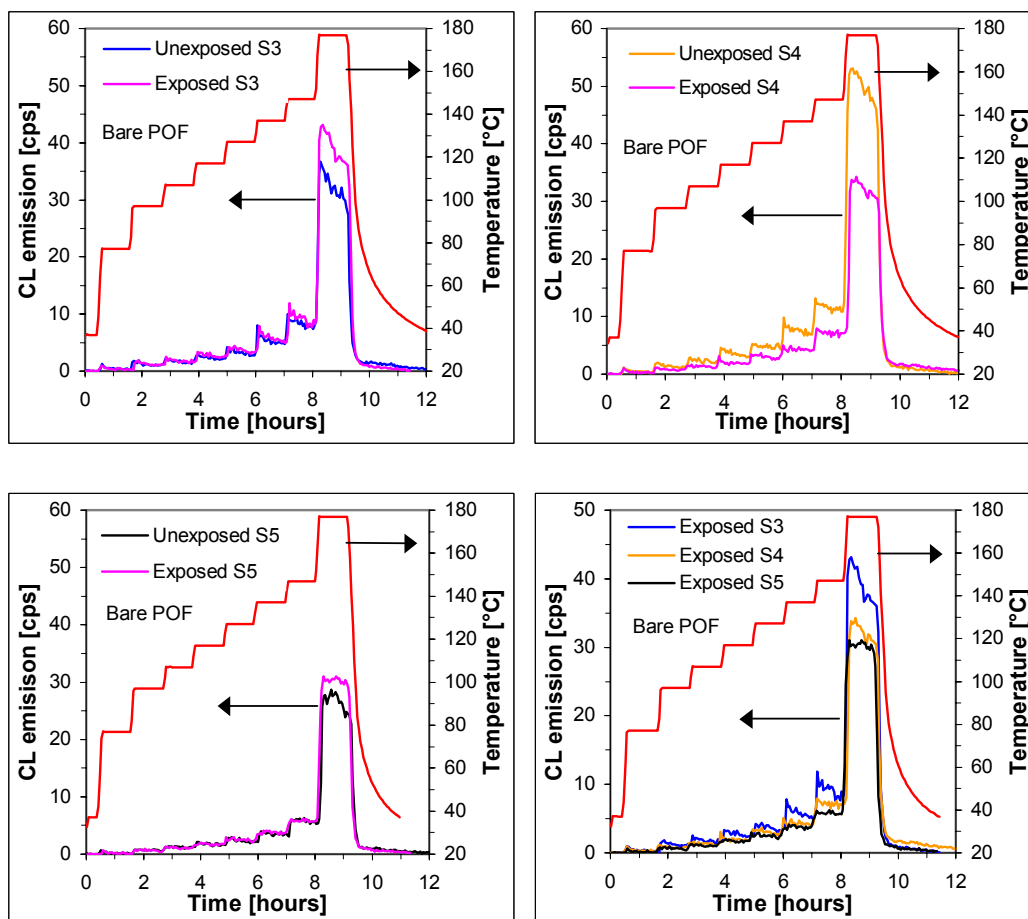


**Figure 8.37:** CL curves for the unexposed and exposed bare POF samples S3, S4 and S5. The exposure condition was 90 °C / low humidity.

In general, CL of 90 °C / low humidity exposed bare POF samples was quite different from that of the same exposed to 92 °C / 50 %RH and 100 °C / low humidity.

CL of bare POF samples S3 and S5 was found to be similar as they delivered almost equal emission implying equal stability but higher emission in the temperature range 147 °C to 177 °C suggesting its lower stability (see Fig. 8.37). While the sample S4 displayed a decrease in CL emission suggesting its increased stability compared to the unexposed sample as a result of climatic exposure (see Fig. 8.37).

The decrease of the CL emission may be explained in two ways.

(A): It could result from a decrease of the concentration of one or more participating reactants of the oxidation process. The participating reactants most likely are pre-dissolved oxygen and low molecular weight species like monomer present in the polymer. These reactants appear to be substantially consumed in the oxidation process during the course of climatic exposure. The spreading of the degradation process from these preceding steps to polymer molecules seems to be only thermally activated, as the content of pre-dissolved oxygen had already consumed. However, the exposure temperature was relatively low (90 °C) by which the thermally activated degradation is very less likely to occur. Consequently, in parallel, the oxidative degradation of the polymer could slowly begin to take place with the availability of new oxygen, but it appears to be needed a longer period than the present exposure time (see Fig. 8.28 in Section 8.3.1.2) for oxygen to effectively reach the polymer.

(B): Another possible explanation could be the taking place of crosslinking of polymer chains could lead to a slow rate of oxidative degradation by hindering the diffusion rate of oxygen. This process appears to be dominating in the whole exposure time resulting in a very less oxidation of the polymer as indicated by CL with respect to lower emission.

In either case, the exposure time seemed to be not long enough to oxidize polymer molecules, as the sample S4 exhibited the lower CL emission. But it appears to be just enough for the sample S3 and S5, as they demonstrated higher CL emission in the temperature range 147 to 177 °C (see Fig. 8.37).

In some cases, stabilization effects of oxygen are discussed for the oxidative degradation of PMMA with respect to weight loss [94]. Therefore, it is also possible that oxygen could induce such effects in POFs during the climatic exposure. As a result, a decrease of the CL emission from the exposed samples (S4) may be the case.

CL of the exposed bare POF samples was compared (see Fig. 8.37); the results suggest the thermo-oxidative stability of these exposed samples ranks in the following order:  $S4 > S5 > S3$  as their CL emission was found to be in the reverse order. These outcomes on the other hand seem to be in good correspondence with the above-discussed results that samples S3 and S5 were found to be more oxidized than the sample S4.

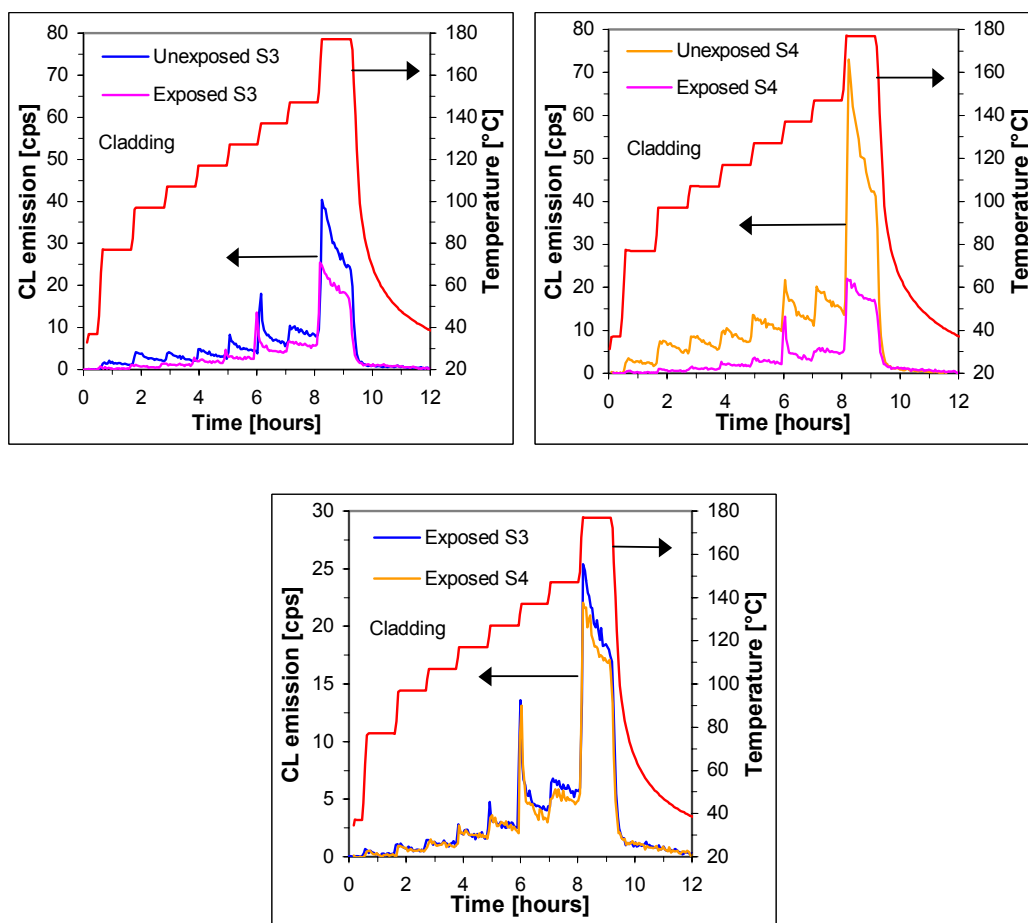


**Figure 8.38:** CL curves for the unexposed and exposed cladding samples S3 and S4. The exposure condition was 90 °C / low humidity.

The comparison of CL of the exposed claddings with the unexposed one's shows a decrease in CL emission indicating the higher stability is similar to the result observed from the same exposed to 92 °C / 50 %RH and 100 °C / low humidity (see Fig. 8.34 and 8.36). Therefore, similar processes like crosslinking and/or quenching of the excited state products might be the case, here too. By comparing CL of the exposed claddings, sample S4 appeared more stable than the sample S3 in the temperature

range 127 °C to 177 °C (see Fig. 8.38). Therefore, it may be claimed that the cladding S3 was more susceptible than the cladding S4 to degradation by climatic exposure.

CL of the exposed bare POFs and claddings show as a similar consequence an increase of the stability due to climatic exposure. However, it is seen from CL of samples exposed to 92 °C / 50 %RH and 100 °C / low humidity that, though claddings exhibited an increased stability, bare POFs displayed lower stability, indicating the cause mainly by the core. With this knowledge, it can be here claimed that the observed increase or decrease of the stability of POFs causing mainly by the core.

In comparing the optical stability with thermo-oxidative stability of bare POFs, the results are seemed to be in good agreement. However, coming to the point of loss mechanism, it is believed that the thermal-oxidation of POFs mainly causes the absorption loss. But it is seen that the increased thermo-oxidative stability of POFs as a consequence of climatic exposure could result by the (possible) mechanisms discussed above. Therefore, in view of the two proposed mechanisms, it appears that degradation products from the decomposition of low molecular weight species like monomer and crosslinking as well could increase the optical loss by significant light absorption.

### 8.3.2.7 Summary

From these results and the discussion the following may be summarized:

- The thermo-oxidative stability of POFs exposed to the climate 92 °C / 50 %RH and 100 °C / low humidity was found to be lower than that of unexposed one's indicating the occurrence of degradation.
- The thermo-oxidative stability of POF S4 exposed to the climate 90 °C / low humidity was found higher than that of the unexposed one indicating some stabilization effects by climatic exposure.
- All the exposed claddings exhibited a consistent result higher stability compared to the unexposed ones owing to climatic exposure.
- The optical transmission stability of POFs seemed to be mainly governed by their thermo-oxidative stability.

## 8.4 Short-term climatic exposures of bare POFs

In order to realize influences of individual climatic parameters on the optical transmission of POFs, they were exposed to three different conditions by varying temperature and humidity. These parameters were programmed in such a way that one was held constant throughout the test and another was varied step-wise from room condition to a desired value. After reaching this desired value it was held constant for a known period of time and then brought back to the room condition and held constant. This was repeated for different values of either temperature or humidity. During the exposure, the optical transmission of POFs was recorded as a function of time using the multiplexer device.

With these types of measurements, relative optical transmission stability of POFs also may be approximated within a short period of exposure time, assuming that they would display similar results during their long-term exposure in the temperature or humidity range of intended use.

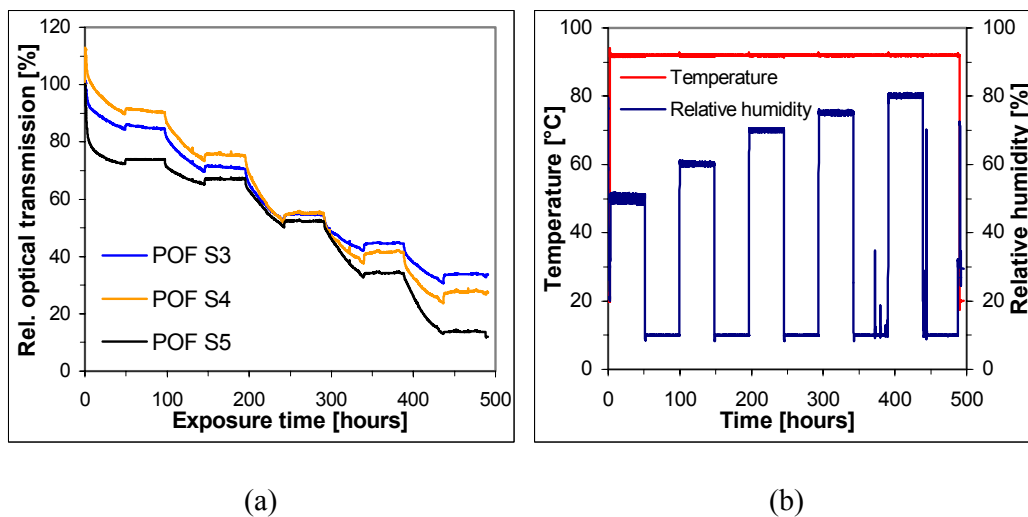


**Figure: 8.39:** (a) Relative optical transmission through bare POFs, measured during the exposure to climates of steady temperature with varying humidity; (b) Applied temperature and humidity scheme recorded during the exposure.

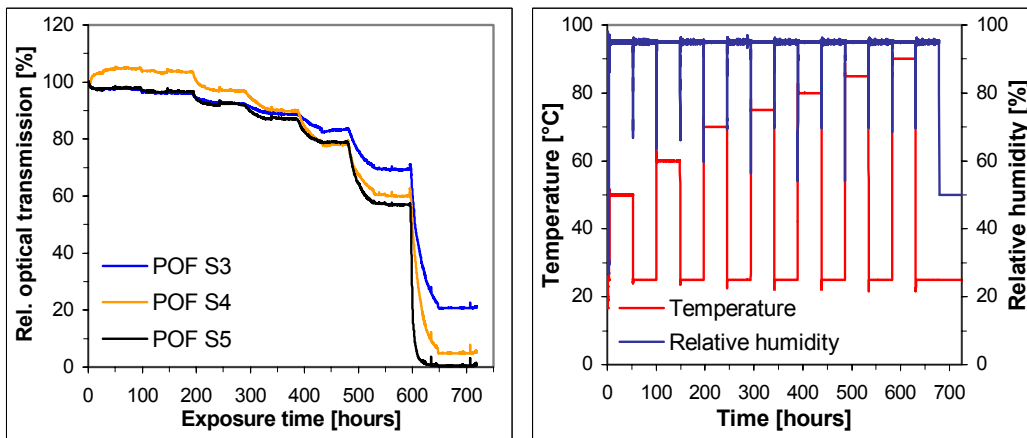
POFs were exposed to various levels of humidity from 50 %RH up to 80 %RH with a stationary temperature of 92 °C, the optical results are as shown Fig. 8.39a. The applied program of temperature and humidity was as shown in Fig. 8.39b. It was actually recorded during the exposure, with the help of an in-built software of climatic chamber.

The experiments demonstrate that the optical transmission stability of POFs under high temperature with humidity condition would follow the extent of imposed humidity. Small reversible and large irreversible transmission changes can be seen (see Fig. 8.39a). The reversible changes of the transmission happened when the humidity turned to its lowest value and was followed by a constant transmission when the humidity stayed at this low value. The irreversible change of the transmission could be caused by both physical and chemical structural changes of POFs, some of them are discussed in the earlier Section 8.3.1. However, a reversible increase of the transmission after brought down the humidity to as low as 10 %RH (temperature was always 92 °C), suggests the evaporation (desorption) of physically absorbed water from the polymer. This water could be situated either in the core-cladding interface or in the polymer. In any case, it indicates that physically absorbed water in POFs reduces the transmission to a certain extent with the ability to recover.

The experimental results, at the first glance, do not seem to match the observed transmission results of long-term exposure of POFs. For instance, the optical transmission stability of POFs was found to be in the order of S5 > S3 > S4 (optical results of the long-term exposure of POFs to 92 °C / 50 %RH, see Section 8.3.1.1). But short-term exposure test under similar condition POFs displayed the opposite results. However, by careful observation of the transmission loss behavior, the results appeared to be in the similar order. The transmission loss displayed by the sample S5 was found to be constant, whereas the samples S3 and S4 demonstrated to be decreasing at the end of the humidity stress (Fig. 8.39a). If the extrapolation is made by assuming the transmission variation following the end point, the transmission stability appears to be in the order as found in the results of long-term exposure to 92 °C / 50 %RH. However, the loss exhibited at the initial stages of the short-term exposure was different from the long-term exposure, which could be due to sampling history of POFs before exposing to stresses in the climatic chamber.

Likewise, transmission stability that exhibits by these POFs could be estimated for the other conditions 92 °C / 60 %RH, 70 %RH and so on, too. Another observation made was, the transmission stability of the sample S4 turned out to be in between the optical stability of S3 and S5 at and above the climate 92 °C / 70 %RH (see Fig. 8.39a). This seemed to be in good agreement with the results found in the long-term exposure of POFs to 92 °C / 95 %RH, where the transmission stability was found to be in the order of S3 > S4 > S5 and a similar result could be guessed in the short-exposure test although it was conducted till the exposure to 80 %RH (see Fig. 8.39a).

The results of optical transmission measurements to POFs (S3, S4 and S5) exposed to stationary humidity 95 %RH and varying temperature from 50 °C to 90 °C are shown in Fig. 7.40a. The temperature and humidity program, which was recorded during the exposure of POFs is shown in Fig. 8.40b.



(a)

(b)

**Figure: 8.40:** (a) Relative optical transmission through bare POFs, measured during the exposure to climates of steady humidity and variable temperature; (b) Applied temperature and humidity scheme recorded during the exposure<sup>1</sup>.

<sup>1</sup> The humidity variation at each step was undesired due to a short fall of humidity control by the chamber.

POFs exhibited almost an irreversible transmission variation in the investigated temperature-humid range. It suggests that under constant high humidity, temperature most probably induces permanent physical and chemical changes in POFs.

The observed optical results seemed to be in accordance with the results obtained by the long-term exposure of POFs. For instance, during the long-term exposure of POFs under 50 °C / 95 %RH the transmission stability was characterized to be in the order of  $S4 > S3 > S5$  (see Fig. 8.24 in Section 8.3.1.1). A very similar result was observed from the short-term exposure test, too (see Fig. 8.40a). An instance can be the optical stability results of long-term and short exposure of POFs to 92 °C / 95 %RH (see Fig. 8.21 in Section 8.3.1.1 and see Fig. 8.40a).

At the first two temperature levels (50 °C and 60 °C) the sample S4 displayed an increase of the transmission (the same was found in the long-term exposure), which could be brought by healing of defects like core-clad boundary imperfections in POFs.

POFs exposed to room temperature (stationary) and varying humidity from 50 %RH to 90 %RH exhibited the optical transmission as shown in Fig. 8.41a. The temperature

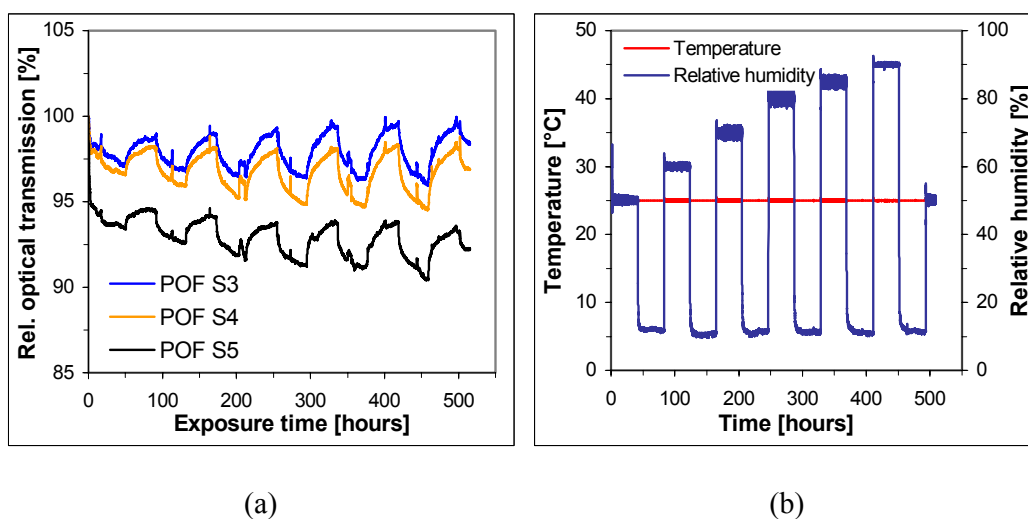


**Figure 8.41:** (a) Relative optical transmission through bare POFs, measured during the exposure to climates of steady room temperature with variable humidity; (b) Applied temperature and humidity scheme recorded during the exposure.

and humidity plan was as shown in Fig. 8.41b.

Consequences show that at room temperature condition the optical transmission stability of POFs mainly derives from the degree of water absorption. It appears mostly as a physical absorption because POFs exhibited almost an equal comeback of the transmission from the point where the humidity reduced to as low as 10 %RH (see 7.39a). The rate of transmission loss seemed to depend on humidity imposed on POFs. Furthermore, the results suggest that the rate of water absorption by POFs highly depends on the chemical composition of the cladding as the sample S5 appeared to show more transmission loss than the other two samples.

With this short-term exposure test, the optical transmission stability of POFs could be estimated as follows, the sample S5 exhibited lower stability than the other two samples S3 and S4 in the investigated temperature-humid conditions.

Although the short-term exposure tests were emerged as reasonable for approximating the relative optical transmission stability of POFs, the absolute finding (in a short exposure period) of the optical transmission stability is very difficult since the optical transmission of POFs depends on several parameters, which could influence the optical transmission stability to a different extent during the exposure.

## 9 Conclusions and Outlook

The present PhD work has performed the experimental work in the direction of the climatic reliability of POFs for long-term applications. Most of the interest has been paid to mechanisms involved in the loss of optical transmission due to climatic exposures. Also, an effort has been put to explore sensitive analytical methods such as chemiluminescence (CL) for the investigation of degradation in POFs.

In the contemporary work step-index, multimode and poly(methyl methacrylate) (PMMA) based POFs were utilized as a model. The optical performance of three POFs under seven different temperature and humid climates was investigated. With the help of the known loss mechanisms, the causes for a loss of transmission due to climatic exposures were researched by means of analytical methods such as CL and Fourier transform infrared (FTIR) spectroscopy. As a new effort, influences of climatic parameters on individual POF components bare POF (core with clad only), cladding and core were studied. By employing CL, the thermo-oxidative stability of individual components was modeled.

With the experiments, results and discussion of the present work, the following are summarized as conclusions:

- One fundamental requirement for carrying out the experiments, to encounter the difficulty in receiving the individual POF components (core and cladding) from manufacturers, was resolved by a solvent method found, as the best way of

extracting the cladding and core for the chemical analysis. It is assumed that the solvent does not significantly affect the polymer due to the separation process. Because all the investigated samples were separated in similar conditions, possible residual influences of this effect on the results should be neglectable. Therefore obtained results are at least comparable.

- As a primary task, the unexposed components of POFs were investigated for their physical constants and chemical compositions. The glass transition temperature ( $T_g$ ) of the fiber core, produced from PMMA, was found higher than that of the normal amorphous PMMA polymer suggesting an orientation influence of polymer chains. Cladding samples were found to exhibit both  $T_g$  and melting temperature ( $T_m$ ), indicating both amorphous and crystalline polymers as cladding materials.

With molecular weight findings, no considerable difference between POF cores was found though they were received from different manufacturers.

Chemical compositions investigations revealed similar core material, PMMA, but three different chemical sorts of cladding material: polyfluoroolefins, poly(fluoroalkyl acrylates) (PFA) and poly(fluoroalkyl methacrylates) (PFMA). Therefore, POFs can be distinguished by cladding materials but not by the core.

- The climatic exposure (92 °C / 95 %RH) of two POF cables (core, cladding and jacket) showed a different optical performance although both had the same core material PMMA. It suggests that the optical performance of POFs is not only confined to the core material. The transmission performance behavior of both the samples was correlated with physical and chemical changes of POFs. Physical changes (e.g.: fiber diameter fluctuations and refractive index variations) appear to cause loss of transmission at the early stages and chemical changes due to mainly thermo-oxidative degradation to cause loss in the later stages of the exposure.

CL investigation of the relative thermo-oxidative stability of the unexposed bare POFs revealed a difference in their stability. Because investigations of their cladding samples found a similar result it is confirmed that differences in cladding materials were responsible for the observed difference in thermo-oxidative stability of bare POFs, an important practical result. CL investigations of the exposed bare POFs and claddings revealed clearly degradation in both the

samples. Their relative degradation was according to the stability of the unexposed samples. These results show the consistency of the CL method.

The occurrence of degradation more in the cladding and less in the core was confirmed by complementary methods FTIR, TG, UV/visible transmittance and GPC. The observed loss of transmission was correlated with increased light absorption and imperfections at the core-cladding interface, mainly due to degradation of the cladding. The imperfections were most likely arising due to substantial decrease in the adhesion strength of the cladding as a result of degradation. Therefore, it can be stated that the optical transmission stability of POFs is mainly governed by their thermo-oxidative stability (largely of the cladding).

- Three bare POFs (core with cladding only) were exposed to seven different combinations of temperature and humidity. The optical performance of these POFs was different and poor under 92 °C / 95 %RH, 100 °C / low humidity, 110 °C / low humidity and 120 °C / low humidity, mainly according to the chemical nature of their claddings. Hence, the role of cladding is realized for their responsibility for long-term optical stability. However, in searching causes for the loss of transmission at the early stages of exposures, physical changes due to high temperature and high humidity were found, e.g.: volume expansion (believed to cause core-cladding boundary imperfections).

The bare POFs exposed 50 °C / 95 %RH, 90 °C / 50 %RH, 90 °C / low humidity displayed better optical stability compared to other exposures. At the early stages, some small changes in the transmission were observed and are related to physical changes. The changes at the later stages of exposures are related chemical changes, mainly thermo-oxidative degradation of POFs.

Using CL, for the first time, the relative thermo-oxidative stability of bare POF, core and cladding was investigated. It was found that the cladding was more prone to the oxidative degradation (than the core) and the stability of the bare POF was mainly depending on the stability of the cladding. Further on a difference in the thermo-oxidative stability of the three bare POFs was found, mainly due to claddings as confirmed by CL experiments to core and claddings.

- The degradation detection in bare POFs exposed to 90 °C / 50 %RH, 100 °C / low humidity and 90 °C / low humidity indicated a higher CL emission than for the unexposed samples. But, in contrary CL of the exposed claddings showed a decrease in the CL emission compared to the unexposed ones. Therefore, reactions like crosslinking or stable oxidized molecules or less oxidation are proposed to take place as a result of oxidation. Causes for the observed loss of transmission seemed to arise by increased light absorption in the core owing to degradation but also in the cladding. This degradation may induce imperfections (e.g.: core-cladding interface) and/or inhomogeneities (e.g.: refractive index variations).

The hypothesis of the formation of such imperfections was supported by the PhD work of Mr. Jankowski (BAM), who found by optical simulations an increased attenuation mainly due to core-clad interface imperfections in the exposed POFs (100 °C / low humidity).

- Some short-term exposure tests to realize the transmission reversibility by temperature and humidity effects on bare POFs were performed by varying one parameter and leaving other constant. POFs displayed reversible transmission changes due to physically absorbed water. Temperature effects were found to be irreversible indicating permanent changes in POFs. With these types of measurements, reasonable results in predicting long-term optical stability of POFs were obtained.
- CL was found to be sensitive method for detecting small degradation of POFs, which could not be detected by a method like FTIR. Therefore, it can be recommended as a possible sensitive tool to test the thermo-oxidative stability of POFs.

Up to now climatic exposure effects on POF core and POF cladding are researched to some extent. The causes for the loss of transmission due to climatic exposures are investigated to some scope. However, further research activities can be planned in the direction of the following:

- Mechanisms proposed for the loss of transmission are proved to some level and therefore can be taken as basis for further research.
- The general extent of the contribution of each loss factor (e.g.: absorption and scattering) to the total attenuation of POFs is overlooked in this work and therefore it further should be studied more in detail.
- By knowing more of the chemical compositions of claddings, their chemical degradation mechanism can be refined.
- A better understanding of the interaction between jacket materials and thermo-oxidative stability of the core and the cladding will improve the aging forecast.
- The until-now neglected mechanical constraints on the oxidative stability and thereby optical stability of POFs can be included.

## References

- [1] Ghatak, A.K., and Shenoy, M.R. (Editors), *Fiber Optics Through Experiments*, Viva Books Private Ltd., New Delhi, 1994.
- [2] Dutton, H.R., *Understanding Optical Communications*, IBM International Technical Support Organization, USA, 1<sup>st</sup> Edition, 1998.
- [3] Daum, W., Krauser, J., Zamzow, P.E., and Ziemann, O., *POF-Polymer Optical Fibers for Data Communication*, Springer-Verlag, Berlin Heidelberg, ISBN 3-540-42009-6, 2002.
- [4] Emslie, C., *J. Materials Sci.*, 23, 1988, pp. 2281-2293.
- [5] Kaino, T., *Polymer Optical Fibers - Polymers for Lightwave and Integrated Optics*, Editor: Hornak, L.A., Marcel Dekker, Inc., New York, ISBN 0-8247-8697-1, 1992, pp. 1-38.
- [6] Groh, W., *Macromolecular Chemistry*, 189, 1988, pp. 2861-2874.
- [7] Zubia, J., Arrue, J., *Optical Fiber Technology*, 7, 2001, pp. 101-140.
- [8] Koike, Y., Ishigure, T., *IEICE Trans. Electron.* E82-C, 8, 1999, pp. 1553-1559.
- [9] Onishi, T., Murofushi, H., Watanabe, Y., Takano, Y., Yoshida, R., Naritomi, M., *Proceedings of the Polymer Optical Fibers (POF) Conference*, 1998, pp. 39-42.
- [10] Hulme-Lowe, A., Stacey, N., *Polymer Glasses: Ultratransparency*, Encyclopedia of Materials, Editors: Buschow, K.H.J., Chan, R.W., Flemings,

- M.C., Ilschner, B., Mahajan, S., Elsevier Scientific Publishing Co., Amsterdam, 2001, pp. 7351-7354.
- [11] Weinert, A., *Plastic Optical Fibers: Principles, Components, Installations*, Publicis MCD Verlag, ISBN 3-89578-135-5, 1999.
- [12] Ohtsuka, Y., Koike, Y., Yamazaki, H., *Applied Optics*, 20, 280, 1981, pp. 2319.
- [13] Koike, Y., Nihei, E., Tanio, N., Ohtsuka, Y., *Applied Optics*, 29, 18, 1990, pp. 2686-2691.
- [14] Koike, Y., *Graded index materials and components - Polymers for Lightwave and Integrated Optics*, Editor: Hornak, L.A., Marcel Dekker, Inc., New York, ISBN 0-8247-8697-1, 1992, pp. 71-104.
- [15] Murofushi, H., *Proceedings of the POF Conference*, 1996, pp. 17-23.
- [16] Blyler, Jr., L.L., Ronaghan, C.A., Koeppen, C.S., Salamon, T., *Proceedings of the POF Conference*, 1997, pp. 42-43.
- [17] Duijnhoven, F.G.H., *Gradient refractive index polymers produced in a centrifugal field: preparation, characterization and properties*, Technical University, Eindhoven, The Netherlands, ISBN 90-386-2581-2, 1999.
- [18] Takahashi, H., Kanazawa, T., *Proceedings of the POF Conference*, 1998, pp. 50-54.
- [19] Jaquet, P., *SPIE, Plastic Optical Fibers*, 1592, 1991, pp. 165-171.
- [20] Thesis, J., Brockmeyer, A., Groh, W., Stehlin, T.F., *Polymer optical fibers in data communications and sensors applications - Polymers for lightwave and integrated optics*, Editor: Hornak, L.A., Marcel Dekker, Inc., New York, ISBN 0-8247-8697-1, 1992, pp. 39-70.
- [21] Chu, P.L., Peng, G.D., *Proceedings of the POF Conference*, 1997, pp. 76-77.
- [22] Rousseau, A., Boutevin, B., Bosc, D., *Proceedings of the POF Conference*, 1992, pp. 33-37.
- [23] Imai, H., *Proceedings of the POF Conference*, 1997, pp. 25-26.

- [24] Sakane, Y., Ono, M., Sato, H., Yabumoto, H., Kuwana, Y., Matsukura, I., Kobayashi, J., Kawakami, N., Hikita, M., Yamamoto, F. *Proceedings of the POF Conference*, 2003, pp. 187-190.
- [25] Okamoto, Y., Yang, Y., Mikes, F., Koike, Y., *Proceedings of the POF Conference*, 2003, pp. 204-207.
- [26] Flipsen, T., *Design, synthesis and properties of new materials based on densely cross-linked polymers for POF and amplifier applications*, University of Groningen, The Netherlands, ISBN 90-367-1206-8, 2000.
- [27] Ishiharada, M., Kaneda, H., Chikaraishi, T., Tomita, S., Tanimi, I., Naito, K., *Proceedings of the POF Conference*, 1992, pp. 38-42.
- [28] Stickler, M., Rhein, T., *Polymethacrylates*, Ullmann's Encyclopedia of Industrial Chemistry, Editors: Elvers, B., Hawkins, S., G. Schultz, 5<sup>th</sup> Edition, VCH Publishers, Inc., A.21, 1992.
- [29] Van Krevelen, D.W., and Hoftyzer, P.J., *Properties of Polymers*, 2<sup>nd</sup> Edition, Elsevier Scientific Publishing Co., Amsterdam, ISBN 0-444-41467-3, 1976.
- [30] Odian, G., *Principles of Polymerization*, 3<sup>rd</sup> Edition, John Wiley and Sons, Inc., New York, ISBN 0-47161-0208, 1991.
- [31] Wunderlich, W., *Physical Constants of PMMA*, Polymer Handbook, Editors: Brandrup, J., Immergut, E.H., 3<sup>rd</sup> Edition, John Wiley and Sons, Inc., 1989.
- [32] Kaino, T., *J. Polymer Sci., Part A*, 25, 1987, pp. 37-46.
- [33] Koike, Y., Ishigure, T., Nehei, *J. Lightwave Technology*, 13, 1995, pp. 1475-1489.
- [34] Baran, A.M., Levin, V.M., Radushkevich, B.V., Tarasova, T.D., *Proceedings of the POF Conference*, 1995, pp. 86-91.
- [35] [http://www.sigmaaldrich.com/img/assets/3900/Fluoromonomers\\_and\\_fluoropolymers\\_for\\_optapp.pdf](http://www.sigmaaldrich.com/img/assets/3900/Fluoromonomers_and_fluoropolymers_for_optapp.pdf)
- [36] Schleinitz, H.M., Stephan, P.G., *US Patent*, # 4,161,500, 1979.
- [37] Kaino, T., Fujiki, M., Shigeo, N., Oikawa, S., *US Patent*, # 4,381,269, 1983.

- [38] Hulme-Lowe, A.G., Doods, A.S., Babirad, S.A., Savu, P.M., *US Patent*, # 4,968,116, 1990.
- [39] Savu, P.M., McAllister, J.W., *US Patent*, # 5,148,511, 1992.
- [40] Nakamura, K., Okumura, J., Irie, K., Muro, M., Kamo, J., Shimada, K., *US Patent*, # 5,963,701, 1999.
- [41] Ballato, J., Smith, D., Ellison, M., Gregory, R., *National Textile Center Annual Report*, Clemson University, USA, 2001.
- [42] Takezawa, Y., Tanno, S., Taketani, N., Ohara, S., Asano, H., *J. Applied Polymer Sci.*, 42, 1991, pp. 2811-2817.
- [43] Groh, W., Kudler, J.E., Thesis, J., *SPIE-Plastic Optical Fiber*, 1592, 1991, pp. 20-30.
- [44] Banwell, C.N., and McCash, E.M., *Fundamentals of Molecular Spectroscopy*, 4<sup>th</sup> Edition, Tata McGraw-Hill Publishing Co. Ltd., New Delhi, ISBN 0-07-462025-8, 1995.
- [45] Kurik, M.V., *Physica Status Solidi A*, 8, 1971, pp. 9-45.
- [46] Judd, R.E., Crist, B., *J. Polymer Sci., Polymer Lett. Edn.*, 18, 1980, pp. 719.
- [47] Kaino, T., *Applied Optics*, 24, 23, 1985, pp. 4192-4195.
- [48] Pierrejean, I., Dugas, J., and Maurel, G., *Proceedings of the POF Conference*, 1992, pp. 96-100.
- [49] Dugas, J., Maurel, G., *Applied Optics*, 31, 24, 1992, pp. 5069-5079.
- [50] Daum, W., Brockmeyer, A., Goehlich, L., *Proceedings of the POF Conference*, 1992, pp. 91-95.
- [51] Schartel, B., Krüger, S., Wachtendorf, W., Hennecke, M., *Proceedings of the POF Conference*, 1998, pp. 248-249.
- [52] Schartel, B., Krüger, S., Wachtendorf, W., Hennecke, M., *J. Lightwave Technology*, 17, 11, 1999, pp. 2291-2296.
- [53] Irie, S., Nishiguchi, *Proceedings of the POF Conference*, 1994, pp. 88-91.

- [54] Ziemann, O., Daum, W., Bräuer, A., Schlick, J., Frank, W., *Proceedings of the POF Conference*, 2000, pp. 173-177.
- [55] Schnabel, W., *Polymer Degradation: Principle and Practical Applications*, Hanser Gardner, Berlin, 1981.
- [56] Feller, R.L., *Accelerated Aging: Photochemical and Thermal Aspects*, The J. Paul Getty Trust, USA, ISBN 0-89236-125-5, 1994.
- [57] Bolland, J.L., Gee, G., *Trans Faraday Soc.*, 42, 1946, pp. 236.
- [58] Jellinek, H.H.G., *Degradation of Vinyl Polymers*, Academic Press Inc. Publishers, New York, 1955.
- [59] (a): Moore, W.J., *Physical Chemistry*, 5<sup>th</sup> Edition, Longman Group Ltd., London, ISBN 0-582-44234-6, 1972; (b): Crank, J. and Park, G.S., *Diffusion in Polymers*, 2<sup>nd</sup> edition, Academic Press inc., New York, 1968.
- [60] Startsev, O.V., Krotov, A.S., Perov, B.V., Vapirov, Y.M., *Proceedings of the 4<sup>th</sup> European Conference of Advanced Materials and Processes - EUROMAT 95*, 1, 1995, pp. 245-254.
- [61] Turner, D.T., *Polymer*, 23, 1982, pp. 197-202.
- [62] Startsev, O.V., Rudnev, V.P., Perov, B.V., *Polymer Degradation and Stability*, 39, 1993, pp. 373-379.
- [63] Ichikawa, K., Mori, T., Kitano, H., Fukuda M., and Mochizuki, A., *J. Polymer Science: Part B*, 39, 2001, pp. 2175-2182.
- [64] Lakowicz, J.R., *Principles of Fluorescence Spectroscopy*, Plenum Publishing Corp., New York, ISBN 0-306-41285-3, 1983.
- [65] Campbell, A.K., *Chemiluminescence: Principles and Applications in Biology and Medicine*, Ellis Horwood Ltd., Chichester, England, ISSN 0930-3367, 1988.
- [66] Ashby, G.E., *J. Polymer Sci.*, L, 1961, pp. 99-106.
- [67] Schard, M.P., Russell, C.A., *J. Applied Polymer Sci.*, 8, 1964, pp. 985-995.
- [68] Schard, M.P., *Polymer Engineering and Sci.*, 1965, pp. 246-253.

- [69] Zlatkevich, L., *Luminescence Techniques in Solid-State Polymer Research*, Editor: Zlatkevich, L., Marcel Decker, Inc., New York, ISBN 0-8247-8045-0, 1989.
- [70] Billingham, N.C., Then, E.T.H., Gijsman, P.J., *Polymer Degradation and Stability*, 34, 1991, pp. 263-277.
- [71] Blakey I., George, G.A., *Macromolecules* 34, 2001, pp. 1873-1880.
- [72] George, G.A., *Developments in Polymer Degradation-3*, Editors: Grassie, N., Applied Science Publishers, London, 1981.
- [73] Kron, A., Stenberg, B., Reitberger, T., Billingham, N.C., *Polymer Degradation and Stability*, 53, 1996, pp. 119-127.
- [74] Wachtendorf, V., *Untersuchung thermooxidativer Veränderungen an Polymeren durch Chemilumineszenz*, Verlag Dr. Köster, Berlin, ISBN 3-89574-241-4, 1996.
- [75] George, G.A., *Luminescence Techniques in Solid-State Polymer Research*, Editor: Zlatkevich, L., Marcel Decker, Inc., New York, ISBN 0-8247-8045-0, 1989.
- [76] Kohler, D.R., Kröhnke, C., *Polymer Degradation and Stability*, 62, 1998, pp. 385-393, and in the same journal, 63, 1999, pp. 165-173.
- [77] Martin, J.W., Dickens, B., Waksman, D., Bentz, D.P., Byrd, W.E., Embree, E., Roberts, W.E., *J. Applied Polymer Sci.*, 34, 1987, pp. 377-393
- [78] Günther, B., Czepluch, W., Mäder, K., Zedler, S., *Proceedings of the POF Conference*, 2000, pp. 209-213.
- [79] Wachtendorf, V., Jansen, K., Schulz, U., Tjandraatmadja, G., *9<sup>th</sup> Intl. Conf. on Durability of Building and Construction Materials*, Australia, 2002, pp. 239-249.
- [80] Gijsman, P., Verdun, F., *Polymer Degradation and Stability*, 74, 2001, pp. 533-542.
- [81] Smith, A.L., *Applied Infrared Spectroscopy - Chemical Analysis 54*, Editors: Elving, P.J., Winefordner, J.D., John Wiley & Sons Inc., New York, ISBN 0-471-04378-8, 1979.

- [82] Bodor, G., *Structural Investigation of Polymers*, Editors: Hodgkinson, J., Ellis Horwood Ltd., Chichester, England, ISBN 0-13-852989-2, 1991.
- [83] Buckles, J.M., Garay, J.C., Kaufmann, D.J., Layson, A.R., Columbia, M.R., *The Chemical Educator*, (Springer-Verlag New York Inc.), 3, 3, 1998, pp. 1-11.
- [84] Bellamy, L.J., *The Infrared Spectra of Complex Molecules*, 2<sup>nd</sup> Edition, Methuen & Co. Ltd., London, 1958.
- [85] Ciardelli, F., Aglietto, M., Montagnini di Mirabello, L., Passaglia, E., Giancristoforo, S., Castelvetro, V., Ruggeri, G., *Progress in Organic Coatings*, 32, 1197, pp. 43-50.
- [86] Rychly, J., M-Rychla, L., Lanska, B., *Polymer Degradation and Stability*, 72, 2001, pp. 249-258.
- [87] Schartel, B., Hennecke, M., *Polymer Degradation and Stability*, 67, 2000, pp. 249-253.
- [88] Strlic, M., Kolar, J., Pihlar, B., Rychly, J., M-Rychla, L., *Polymer Degradation and Stability*, 72, 2001, pp. 157-162.
- [89] Broska, R., M-Rychla, L., Rychly, J., Mendenhall G.D., *J. Photochemistry and Photobiology A: Chem.*, 109, 1997, pp. 101-107.
- [90] Pauly, S., *Permeability and Diffusion Data – Polymer Handbook*, Editors: Brandrup, J., Immergut, E.H., 3<sup>rd</sup> Edition, John Wiley and Sons, Inc., 1989.
- [91] Holland, B.J., Hay, J.N., *Polymer*, 42, 2001, pp. 4825-4835.
- [92] Forsythe, J.S., Hill, D.J.T., *Progress in Polymer Science*, 25, 2000, pp. 101-136.
- [93] Nasef, M.M., Dhalan, K.Z.M., *Nuclear Instruments and Methods in Physics Research (NIM) B*, 201, 2003, pp. 604-614.
- [94] Hirata, T., Kashiwagi, T., Brown, *Macromolecules*, 18, 1985, pp.1410-1418.
- [95] Manring, L.E., *Macromolecules*, 22, 1989, pp. 2673-2677.
- [96] Kang, E-S., Bae, J.Y., Bae, B-S., *J. Sol-Gel Sci. & Tech.* 26, 2003, pp 981-984.
- [97] Jewell, J.M., *J. Non-crystalline Solids*, 146, 1992, pp 145-153.

- [98] Rychly, J., M- Rychla, L., Jurcak, D., *Polymer Degradation and Stability*, 68, 2000, pp 239-246.
- [99] Ahlblad, G., Reitberger, T., Terselius, B., Stenberg, B., *Polymer Degradation and Stability*, 65, 1999, pp 179-184.
- [100] Jankowski, L., Bunge, C-A., Zubia, J., Appajaiah, A., *Proceedings of the POF Conference*, 2003, pp. 148-151.